Title

Connections to the deep sea: an interdisciplinary approach to ocean change past, present, and future

Permalink

Author

Fish, Carina R.

Publication Date

2022

Peer reviewed|Thesis/dissertation

Connections to the Deep Sea: An Interdisciplinary Approach to Ocean Change Past, Present, and Future

By

CARINA RAQUEL FISH
DISSERTATION

Submitted in partial satisfaction of the requirements for the degree of

DOCTOR OF PHILOSOPHY

in

Earth and Planetary Sciences

in the

OFFICE OF GRADUATE STUDIES

of the

UNIVERSITY OF CALIFORNIA

DAVIS

Approved:

_____
Tessa M. Hill, Chair

_____
John Largier

_____
Dawn Sumner

Committee in Charge

2022

Table of Contents

Chapter 1: Twentieth-century California Current System biogeochemical variability

Chapter 2: Carbonate chemistry over the shelf in the central California Current during and after the 2014-2016 Northeast Pacific Marine Heatwave

Chapter 3: Climate justice: the ethics of deep sea mining for green futures

Acknowledgments

I thank my many communities who have been instrumental in supporting me throughout my academic journey, and without whom this dissertation would not exist. I am grateful to my primary advisor, Tessa Hill, who demonstrated and encouraged public engagement and scholarship. I thank my dissertation committee members John Largier and Dawn Sumner who enabled my oceanographic research and interdisciplinary approaches to encompass more than I could have initially dreamt. To my friends and family who kept me grounded and inspired, thank you for your support over the years. A big thank you to my partner, Alex, for keeping me sane. Special thanks to my dog, Cleo, who brought structure and joy into my graduate school days. Thanks also to my friends and housemates who have cared for Cleo and therefore me, to the many mentors who have invested in me over the years, and to the 60 pioneering Black women who earned their geosciences doctorates in the U.S. before me and thus made my journey just that much easier. Immense gratitude to my application editors extraordinaires—my sister, Nicole, and my mom, Kim—for both their writing prowess and remarkable support in many material forms over the years. This dissertation is dedicated to my mother, who patiently waited for me to also embrace her craft of writing, and laugh at my 3rd-grade-self who declared that I would pursue the sciences due to my dislike of writing.

Abstract

The deep sea is often thought of as removed from terrestrial and nearshore processes. Despite imaginaries of discontinuity, connecting seemingly separate systems informs us on how best to relate to far, or not easily accessible, regions. Such expansive views of interconnections aid in the holistic understanding of whether and how to manage areas both far and near. Toward this, I first illuminate the surface-deep connections through the biogeochemical history of deep sea coral organic skeletons off of North-Central California that reflect overlying surface water processes over the past century. I then investigate the chemical oceanographic changes of the overlying surface waters within the past decade, and attend to the accelerating geopolitical tensions of the deep sea due to demands on land. I document a shift in coral isotopic signatures over the 20th century and modified surface and subsurface waters over the past decade. I present evidence for changes in upwelling with implications for both deep water communities and surface ocean acidification during marine heatwaves. Lastly, I will show the utility of incorporating multiple perspectives to inform 1) the contextualization of deep sea mining, 2) ongoing deep sea mining discussions, and 3) the selection of the overarching goal i.e. centering climate justice rather than green futures.

Chapter 1

Twentieth-century California Current System biogeochemical variability

Abstract

Deep sea corals are unique palaeoceanographic tools for understanding the subdecadal history of surface and deep water. Here, we utilize bamboo corals (*Isidella* sp.) that span a latitudinal gradient (33.1°N–38.2°N) in an eastern boundary upwelling current system to probe the recent biogeochemical past of the highly productive California margin region. Coral skeletal gorgonin provide oceanographic archives that reflect the composition of their surface water-derived food source. We observe shifts in stable isotopic signatures, namely a depletion in $\delta^{15}N$ during the mid-20th century and a marked $\delta^{13}C$ depletion circa 1990s onward. These shifts may reflect the changes observed in equatorial Pacific wind stress over the same period, its subsequent influence on the California Undercurrent composition, and local wind intensification impacting the contribution of California Undercurrent to the euphotic zone. This work highlights the variability of the California Current System both spatially and temporally over decadal timescales, and the value of subdecadal, high-fidelity ocean archives.

1. Introduction

Deep sea or cold-water corals, residing below 50 m (Cairns, 2007), are slow growing and can live for centuries to millennia (Roark et al., 2009, 2006). Like their shallow water counterparts, they form the foundation of biodiversity hotspots (Cerrano et al., 2010; Etnoyer and Morgan, 2005; Graiff et al., 2011; Roberts and Cairns, 2014), and also provide subdecadal records of environmental data recorded in their skeletons (e.g., Sherwood et al., 2006; Williams et al., 2006). However, unlike shallow water corals, the vast majority of deep sea corals are

azooxanthellate (lacking photosynthetic symbionts) and instead rely solely on their polyps to

suspension feed marine snow (i.e., surface-derived particulate organic matter) from the water

column (e.g., Griffin and Druffel, 1989; Heikoop et al., 2002; Hill et al., 2014; Roark et al.,

2005; Sherwood et al., 2005; Williams et al., 2007).

Bamboo corals (*Isididae*) in particular have two-part skeletons, with alternating long,

rigid, low-magnesium calcite internodes and short, flexible, horn-like proteineacous gorgonin

nodes (e.g., Grant, 1976; Lamouroux, 1812; Noé and Dullo, 2006; Roark et al., 2005). While the

calcite internode records in-situ water parameters, the organic node records surface changes via

their diet (Roark et al., 2005; Sherwood et al., 2008; Sherwood and Edinger, 2009) making

bamboo corals unique dual archives. Both skeletal parts grow concentrically forming organic

layers and calcite bands that have both been previously utilized for their near-annual

geochemical environmental records (see review in Williams, 2020). Chronologies established

with the organic node use bomb-spike radiocarbon analysis that exploits the atmospheric

increase in radiocarbon due to mid-20th century nuclear weapons testing, the signal of which is

subsequently incorporated into coral gorgonin skeleton via its diet (e.g., Roark et al., 2005; Hill

et al., 2014; Frenkel et al., 2017). Importantly, over their ontogeny (up to 420 years; Sinclair et

al., 2011; Watling et al., 2011), bamboo coral nodes can be used to probe changes in surface

productivity and exported carbon in the modern (Sherwood et al., 2009). These sessile

invertebrates can therefore illuminate the past several decades to centuries of marine productivity

like that of the productive coastal waters within an eastern boundary upwelling current system.

Eastern boundary upwelling systems are highly productive regions of the ocean, covering

<1% of the ocean but supplying up to 20% of caught fish globally (Pauly and Christensen,

1995). The California Current System is one of four major eastern boundary upwelling systems;

comprised of the coastal jet, the California Current, and the California Undercurrent (CUC); and bordered by the Western United States coastline to the east and Eastern North Pacific Central Water (ENPCW) of the gyre to the west (Checkley and Barth, 2009; Fig. 2). The equatorward flowing California Current is fed by Pacific Subarctic Upper Water (Huyer, 2003; Pickard, 1964; Reid et al., 1958). The equatorward flowing coastal jet induces nearshore upwelling of the subsurface return flow, the CUC, which is fed by Pacific Equatorial Water (PEW) that is high in nutrients but low in oxygen (e.g., Castro et al., 2001; Gay and Chereskin, 2009; Hickey, 1979; Thomson and Krassovski, 2010) and reflects denitrified Eastern Tropical North Pacific source water signatures (Castro et al., 2001; Davis et al., 2019). Frequent upwelling events bring cold, nutrient rich waters to the surface, enabling blooms of phytoplankton (García-Reyes and Largier, 2012), which drive high productivity in eastern boundary upwelling systems (Wooster and Reid, 1963; Small and Menzies, 1981). Blooms not fully consumed at the surface become exported carbon—these pulses of energy to the seafloor support thriving benthic communities including deep sea coral ecosystems (e.g., Griffin and Druffel, 1989; Johnson et al., 2007; Jones et al., 2014; Smith et al., 2013). Peak upwelling season is in spring-summer, with weaker upwelling-favorable winds later during boreal summer. With weaker winds, the source of the upwelled waters is shallower in origin (Gay and Chereskin, 2009; Jacox and Edwards, 2012; Lynn and Simpson, 1987). Within the California Current System, the North-Central region is exceptionally productive primarily due in part to stronger upwelling-favorable winds (García-Reyes and Largier, 2012).

Coastal upwelling not only controls California Current System productivity but also affects regional oxygenation (Chan et al., 2008). High temporal resolution records of oxygenation in the California Current System are largely limited to the varved sediments of the

Southern California Bight. For example, Deutsch et al. (2014) found a centennial shift in the Southern California Current System oxygenation through analysis of sediment $\delta^{15}N$. The shift was interpreted to reflect the control of denitrified Eastern Tropical North Pacific waters on the oxygenation of the Southern California Current System (Davis et al., 2019), but likely also reflects plankton community and food web changes (Batista et al., 2014). The isotopic composition of deep sea corals provides a potential additional high-resolution past archive of oceanographic processes beyond regions with varved sediments.

Understanding past relationships between oceanographic processes (e.g., wind stress, upwelling, oxygenation) and productivity are particularly useful in a changing ocean where projections of upwelling strength as a function of latitude is uncertain. There are predictions of both intensification of California Current System upwelling (Bakun, 1990) and a poleward shift of upwelling in the California Current System due to continued increasing anthropogenic CO_2 and ensuing increasing temperatures (Rykaczewski et al., 2015). Records of past productivity linked to oceanographic processes (i.e. upwelling) are particularly useful in better predicting the response of productivity to changes in wind stress and upwelling. Here we present the $\delta^{15}N$ and $\delta^{13}C$ of bamboo corals from the California Current System to address the following questions:

1) How does California Current System productivity change over the 20th century?

2) What changes in physical oceanographic processes (i.e. wind stress and upwelling) can be inferred by these changes in productivity?

3) What might this mean for 21st century productivity in response to predicted changes in eastern boundary upwelling system upwelling?

2. Methodology

2.1 Coral collection

Six bamboo corals from along the California margin and within a 250 m depth range of each other were used in this study (Table 1). Three of these specimens were collected using remotely operated vehicles in 2017 on the *E/V Nautilus* (cruise NA085). The remaining three were collected via an remotely operated vehicle on the *R/V Western Flyer* in 2007 and 2004 (Hill et al., 2011). More recently collected specimens (2017) were collected within the Cordell Bank National Marine Sanctuary (38˚N, 123.5˚W) at depths between 1246 m and 1397 m (Table 1, Fig. 2) and are hereafter referred to as North-Central specimens. North-Central specimens are closest to the coastal jet (Fig. 2) where surface waters are recently upwelled south of the Point Arena upwelling center (Halle and Largier, 2011). The two specimens collected in 2007 are from within and adjacent to Monterey Bay National Marine Sanctuary's Davidson Seamount Management Zone (35.7˚N, 122.8˚W) from depths of ~1500 m and are hereafter referred to as Central specimens. Central specimens are the most offshore of the six studied herein; the surface waters above the Central specimens are a mixture of primarily California Current with entrainment of ENPCW and filaments of the coastal jet via mesoscale eddies (Huyer et al., 1998). A coral was collected (2004) on San Juan Seamount (33.1˚N, 120.9˚W) at a depth of 1295 m and is hereafter referred to as the Southern specimen. The Southern specimen sits within the larger Southern California Bight, where surface waters are a confluence of PEW, ENCPW, and PSUW (Figs. 2 and S1; Bograd et al., 2019) and mixing is driven in part by baroclinic Rossby waves propagating PEW offshore (Todd et al., 2011). All methods described here are in reference to sample preparation for the corals acquired in 2017 (NA085- corals). These protocols followed established laboratory processes that had been previously followed for corals sampled in 2004 and 2007 (Hill et al., 2011).

2.2 Coral sampling

Live-collected specimens were stripped of their polyps with a scalpel, and all specimens were rinsed with fresh water, air-dried, and archived at UC Davis Bodega Marine Laboratory. The organic nodes nearest the base of each coral were selected for both chronology and stable isotope analyses. Nodes overgrown with calcite were disregarded and the next most basal node was chosen. Skeletons were broken manually either by hand or with pliers to separate the calcite portions from the basal nodes. A stereomicroscope was used to photograph and measure the diameters of the nodes. Isolated organic nodes were then immersed in 10% HCl to dissolve any calcite residue. Once all calcite was removed, nodes were rinsed and stored in vials with MilliQ water. Organic node layers were peeled under a stereomicroscope using forceps and a scalpel. Number of layers was recorded, as well as layer thickness, which was approximated using a glass slide with micrometer subdivisions under the stereomicroscope. Distance from edge was measured by summation of layer thickness determined by stage micrometer. Layers were individually rinsed with MilliQ ultrapure water, dried at 70˚C overnight, and then stored dry in individual vials.

2.3 Radiocarbon analyses

Six to eight organic samples per specimen were analyzed for radiocarbon, distributed across the width of the organic node. Individual organic layers were weighed (~400 µg each) and combusted at 900˚C with copper oxide (~20x the coral sample weight) in sealed quartz tubes overnight to produce carbon dioxide (CO_2). The CO_2 samples were then reduced to graphite with an excess of hydrogen using iron catalysts (e.g., Vogel et al., 1984). The resulting graphite was pressed into cathodes and analyzed via accelerator mass spectrometry. Radiocarbon results were $\delta^{13}C$-normalized either with $\delta^{13}C$ values measured for the sample itself or with an appropriate average $\delta^{13}C_{coral}$ value (e.g., -16‰ for bamboo coral organic nodes in the California Current

System), and were background corrected using similarly handled ^{14}C-free coal. The resulting reported ages are in conventional non-reservoir-corrected radiocarbon years following Stuiver and Polach (1977) using the 5568 year Libby half-life, and in fraction Modern (Fm). We note that following Stuiver and Polach (1977), Fraction modern is equivalent to F^{14}C (Reimer et al., 2004).

2.4 Calcite paired light/dark band counts

Bomb-spike radiocarbon chronologies were independently verified for the three NA085-specimens by calcite internode paired light/dark band counting. Two methodologies were used. First, the standard observational methodology of mounting polished thin sections of the calcite internodes onto an inverted binocular microscope with a camera attachment. Paired light/dark bands were counted twice along two different radii by separate researchers and averaged. Second, the computer-aided methodology of counting paired measured greyscale peaks and troughs as identified by Fiji/ImageJ software. Scanned images of thin sections were converted to greyscale and the greyscale intensity of three radii for each thin section were plotted. Light/dark bands were assessed observationally from the paired peaks and troughs of the radii greyscale plots. Individual band counts from each radius were averaged for each scanned thin section.

2.5 Bulk stable isotopic analyses

Every third organic layer was subsampled (~1 mg, n = 96) and encapsulated in a 5x9 mm tin capsule. Samples were analyzed at University of California, Davis' Stable Isotope Facility for both δ^{13}C and δ^{15}N on a PDZ Europa ANCA-GSL elemental analyzer interfaced to a PDZ Europa 20-20 isotope ratio mass spectrometer (Sercon Ltd., Cheshire, UK). Samples were combusted and oxidized in a reactor with silvered copper oxide and chromium oxide at 1000˚C, and subsequently reduced in a reactor with copper at 650˚C. Any water vapor from the

combustion was removed as the CO_2 and N_2 on a helium gas carrier stream passed through a water trap of magnesium perchlorate and phosphorous pentoxide. A Carbosieve gas chromatograph column separated CO_2 and N_2 at 65°C and 65 mL/min. The gases were then introduced into the isotope ratio mass spectrometer and measured in continuous flow mode. In house references that are calibrated against international references were repeatedly interspersed with the samples. Reference material peaks are basis for a sample's provisional isotope ratio and are also used to correct the values of the entire batch. The laboratory detection limit including a long-term standard deviation is 0.2‰ for ^{13}C and 0.3‰ for ^{15}N. Corrected values are reported in delta notation and are relative to international standard (Vienna Pee Dee Belemnite) and air for $\delta^{13}C$ and $\delta^{15}N$, respectively.

3. Results

Organic layer counts for each specimen numbered 102 ± 14.74 (Table 1). The average layer thickness is 0.07 ± 0.01 mm.

3.1 Radiocarbon analyses

Radiocarbon results are reported in Table 2. The seven NA085-033 samples range in $F^{14}C$ values between 0.907 and 1.060, with the largest value occurring 6.75 mm from its center and the first four (0–5.35 mm) are indistinguishable from each other. NA085-081 radiocarbon values (n = 5) show mostly large $F^{14}C$ values ranging between 0.993 and 1.052, where the smallest value is the outermost sample (7.93 mm from center), and the largest is only 1.95 mm from its center. NA085-079 radiocarbon values (n = 6) range from 0.901 to 1.050, where its largest $F^{14}C$ value is 8.08 mm from center and the four innermost (0–6.78 mm) are all within 0.016 of the smallest $F^{14}C$ value. T1102-A10 $F^{14}C$ values (n = 5) range from 0.917 to 1.025, where its largest value is its outermost sample (5.5 mm from center), and the three innermost

samples (0–3.55 mm from center) are within 0.002 of the smallest $F^{14}C$ value. T1102-A12 $F^{14}C$ values (n = 5) range from 0.898 to 1.078, where its largest value is the penultimate sample (5.1 mm from center), and the smallest is the innermost (1 mm from center). Finally, T664-A17 (n = 6) $F^{14}C$ values range between 0.920 to 1.043 where its largest value is the outermost sample (6.5 mm from center).

3.2 Calcite paired light/dark band counts

The calcite thin section of NA085-033 shows 94.5 ± 20.5 paired light/dark bands (Table 1). NA085-081 exhibits 42 ± 8.5 light/dark bands and NA085-079 has 121.5 ± 12.0 paired bands. With the computer-aided methodology, NA085-033 and NA085-081 exhibit 96.17 ± 22.7 paired peaks/troughs and 42.67 ± 1.53 paired peaks/troughs, respectively, and NA085-079 exhibits 164.1 ± 7.47 paired peaks/troughs.

3.3 Bulk stable isotopic analyses

We observe cyclical $\delta^{13}C$ variability in the majority of specimens, most pronounced in NA085-033 and NA085-079 (Fig. 4). While NA085-079 exhibits <1‰ variability (-16.77 ± 0.30‰), NA085-033 displays a >2‰ variability (-17.40 ± 0.58‰). There is also a slight $\delta^{13}C$ enrichment across coral radii superimposed on their cyclical variability, most pronouncedly seen in specimen NA085-079. Specimen NA085-081 (-18.04 ± 0.81‰) shows a marked depletion toward the outer edge of its radius; the $\delta^{13}C$ values of its outer edge span nearly the full $\delta^{13}C$ range of all six corals. The Central specimens are on average the most depleted of the six studied herein, -18.84 ± 0.65‰ and -18.67 ± 0.51‰ for T1102-A10 and -A12, respectively. The southern coral, T664-A17, displays low $\delta^{13}C$ variability, -18.49 ± 0.55‰.

We observe ~1‰ bamboo coral $\delta^{15}N$ variability throughout each specimen (Table 3). North-Central specimen NA085-033 exhibits an average $\delta^{15}N$ of 14.9 ± 0.52‰ (n = 24).

Specimen NA085-081 exhibits an average $\delta^{15}N$ of $14.08 \pm 0.30‰$ (n = 16), and specimen NA085-079 exhibits an average $\delta^{15}N$ of $14.68 \pm 0.43‰$ (n = 29). Central coast specimens T1102-A10 and T1102-A12 show $\delta^{15}N$ averages of $14.77 \pm 0.45‰$ (n = 11) and $14.98 \pm 0.39‰$ (n = 10), respectively. The southern coral, T664-A17, exhibits a mean $\delta^{15}N$ value of $14.74 \pm 0.31‰$ (n = 10).

Carbon to nitrogen ratio (C:N) for all specimens display low variability (Table 3). The North-Central specimen NA085-033 exhibits an average C:N value of 2.63 ± 0.02, n = 21. Specimen NA085-081 exhibits a similar C:N mean and variability of 2.62 ± 0.02, n = 16. Specimen NA085-079 exhibits a C:N mean of 2.73 ± 0.04, n = 22. The Central coast coral specimens T1102-A10 (n = 9) and T1102-A12 (n = 8) show C:N means of 3.13 ± 0.07 and 3.24 ± 0.04, respectively. Lastly, the southern coral, T664-A17, exhibits a C:N mean of 3.13 ± 0.04, n = 8.

4. Discussion

4.1 Organic node chronology

The inner layers of three of the six specimens described here contain $F^{14}C$ values of 0.900 ± 0.013 (indicative of pre-bomb carbon growth; (Ingram and Southon, 1996), whereas the outer layers from all six corals are enriched in ^{14}C indicating growth after 1957 (post-bomb testing). The enrichment is consistent with the rise of ^{14}C in the atmosphere due to nuclear bomb testing (Broecker et al., 1985; Nydal and Lövseth, 1983). Prior to nuclear bomb testing, ^{14}C of CCS surface waters was $\leq -72‰$ (Ingram and Southon, 1996; Pearson et al., 2000). Regionally within the Northeast Pacific, the inflection point and peak are assigned the dates of 1957 ± 2 years and 1970, respectively (e.g., Kerr et al., 2004; 2005). Using these time constraints, we develop organic node chronologies for each coral specimen studied herein by assigning 1957 to the ^{14}C

inflection points and 1970 to the ^{14}C maxima of each specimen, and constrain chronologies further if the coral was live collected by assigning the year of collection to the outermost layer (Table 1). Due to assigning tie points, robust chronologies hinge in part on sampling frequency. We therefore acknowledge uncertainty introduced if the data density does not capture the true ^{14}C maxima. We apply the Frenkel et al. (2017) area-based chronology method to develop two growth rates per coral if all three tie points exist for the specimen. We apply the 1957-1970 growth rate to the oldest part of the coral i.e., prior to 1957, and therefore acknowledge that the chronologies are most accurate for mid-1950s onwards. This produces chronologies that range between 61 to 93 years for the six corals studied herein.

The coral radiocarbon chronologies are robust in part due to the precision of the measured atmospheric bomb-spike within ± 2 yrs (Kerr et al., 2005; Manning et al., 1990); we are therefore confident in our ability to apply tie-points of 1957 and ~1970 to the inflection points and peaks of F^{14}C. The use of bomb-spike tie points relies on benthic-pelagic coupling, which has been shown previously (Griffin and Druffel, 1989; Hill et al., 2014). Additionally, Frenkel et al. (2017) independently measured the F^{14}C composition of specimen T1102-A12 on a different accelerator mass spectrometer; we show the Frenkel et al. (2017) chronology of T1102-A12 and our independent reproduction of the same coral's chronology are within error of each other. We are thus confident in our overall interpretation of five of the six corals studied herein, given the capture of the bomb curve including the ^{14}C maxima. The only tie-point of significant concern for interpreting coral chronological age is the "1970" point for specimen T664-A17, which, due to the need of applying the 1957-1970 growth rate to pre-1957, may overestimate the age of this coral by up to 23 years. Additionally, the chronological errors for specimens NA085-033, NA085-079, and to a lesser extent T1102-A10, include uncertainty due to the inherent need

to apply the 1957-1970 growth rate to pre-1957. This may contribute to an overestimation of ages for these specimens prior to 1957 as growth rates are typically faster early in ontogeny compared to later growth rates (Noe and Dullo, 2006; Frenkel et al., 2017). We observe no signs of diagenesis/reworking as indicated by the expected $D^{14}C$ values (Fig. 3), which is consistent with previously analyzed bamboo corals (Sherwood and Edinger, 2009).

Radiocarbon-based chronologies developed using the organic node are compared to chronologies estimated by counting the growth bands of the calcite internodes as well as counting the number of organic layers. The growth band counts and number of organic layers both agree with the radiocarbon-based chronology for NA085-033, and both methods for determining calcite band counts are within error of each other for each specimen (Table 1). However, discrepancies arise in comparing band counts to number of organic layers and radiocarbon-based chronologies for both NA085-081 and -079. This could be due to human error in misidentifying organic layers, and/or misinterpreting banding as annual growth features. While previous work in the same region showed organic node extension rates agreed with calcite extension rates (Hill et al., 2014), calcite extension rates (which yield bands) varied extremely and were limited to measurements of the outer edge only of the coral cross section (Hill et al., 2011). Given that we apply the area-based radiocarbon method instead of the older linear method, we henceforth rely on the radiocarbon-based chronologies only.

The three North-Central corals span nearly a century (~93 years, 1924–2017), their individual organic layers average 75 ± 27 μm thick, their growth rates range from 155 to 205 μm yr^{-1}, and their isotope (F^{14}C, δ^{13}C, δ^{15}N) sampling resolution averages ~2.2 years. The two Central corals span six decades (~62 years, 1946–2007) with individual organic layer thickness averaging 77 ± 34 μm and growth rates of 120 to 132 μm yr^{-1}. As such, each Central coral

isotope sample ($F^{14}C$, $\delta^{13}C$, $\delta^{15}N$) integrates on average 3 ± 1.2 years. The southernmost coral, T664-A17 spans ~75 years (1929–2004) and grew an average of 200 μm yr^{-1}. The individual organic layers of the southern coral average 68 ± 24 μm thick, and each of its isotope samples ($F^{14}C$, $\delta^{13}C$, $\delta^{15}N$) integrate on average 3.9 ± 1.5 years.

4.2 Coral geochemistry

The stability of the coral organic node C:N values through time (Table S1) suggest that the dominant source of food for these corals remained constant over the study period and is marine-based rather than terrestrial. This interpretation is aligned with previous work on bamboo corals along the California margin that report zooplankton as the primary origin of food (Griffin and Druffel, 1989; Hill et al., 2014; Sherwood et al., 2005, 2009). We attribute the invariability to low terrestrial inputs to the offshore marine food webs as shown by previous work in the California Current System (Walker and McCarthy, 2012).

4.2.1 $\delta^{15}N$

In general, $\delta^{15}N$ composition is more variable in the older (innermost) sections of the coral, and less variable with more depleted $\delta^{15}N$ in the more recent portions of the record. We observe greater variability intraspecimen in North-Central specimens NA085-033 and -079 prior to 1964, in addition to a marked 0.5‰ depletion in $\delta^{15}N$ circa 1964 in all three North-Central specimens. Both Central corals display $\delta^{15}N$ depletions until the mid-1980s, followed by a rapid enrichment in $\delta^{15}N$. Depth, trophic fidelity, and distance from upwelling center are three variables that may have caused the decrease in $\delta^{15}N$ variability, mid-century depletion, and rapid enrichment post-1980s in the respective corals. We consider depth an unlikely control of $\delta^{15}N_{coral}$ as we selected specimens from within a 250 m depth bin. Furthermore, previous work demonstrated that corals selectively feed upon fresh, recently exported sinking particulate

13

organic matter (Hill et al., 2014) as opposed to suspended particulate organic matter that would have a more degraded signature (enriched $\delta^{15}N_{coral}$) due to a longer residence time and more microbial activity. Similarly, we surmise that changes in the amount of export production and therefore rate of sinking would not be reflected in these samples as seasonality of spring/summer blooms are smoothed over the temporal resolution of each layer ~2–4 years.

Bulk $\delta^{15}N_{coral}$ enrichment sometimes indicates a food chain elongation. However, we consider a discernable change in trophic position to be unlikely given that multi-decadal zooplankton $\delta^{15}N$ records in both central and southern California Current exhibit long-term stability (Ohman et al., 2012; Rau et al., 2003; Rebstock, 2001), suggesting no change in plankton food chain length. Further isotopic analysis of coral source amino acids would be able to confirm suggested stability of CCS coral trophic position through time. In addition, on shorter timescales, warm periods have been shown to increase $\delta^{15}N_{zoopl.}$ and nitrate utilization has been suggested to affect $\delta^{15}N_{zoopl.}$ (Ohman et al., 2012). Thus, rather than food chain elongation, changes in $\delta^{15}N_{coral}$ likely reflects other factors, such as the impact of sea surface temperature and nitrate utilization on $\delta^{15}N_{zoopl.}$ variability.

Lastly, source water nitrogen may have changed through time as indicated by the coral records. Specifically, different proportions of source water in which the zooplankton grew may exert a control on $\delta^{15}N_{coral}$ of these specimens, which would then record the influence and/or history of upwelling centers. The fact that we observe similarities amongst corals from the same region is compatible with the surface-derived coral food source growing in different proportions of source water. There is significant variability in source waters off the coast of California, i.e., (from most depleted to most enriched $\delta^{15}N_{nitrate}$ water): gyre ENPCW, California Current Pacific Subarctic Upper Water, and upwelled CUC PEW (Altabet et al., 1999; Kienast et al., 2002; Liu

and Kaplan, 1989; Sigman et al., 2003). North-Central corals are closest to the coastal jet (Fig. 2) and grew in an upwelling region; therefore, plankton in that region likely see the highest contribution of PEW. Whereas the plankton in the vicinity of the Central corals offshore of Point Sur likely see the highest contribution of ENPCW of the three locales. We interpret that the North-Central corals may reflect the $\delta^{15}N_{nitrate}$ signature of the CUC and/or strength of upwelling or depth of upwelled waters.

The core of the CUC is ~300 m deep (Lynn & Simpson, 1987; Bograd et al., 2015) and the typical depth of upwelled waters is ~80 m, which is dependent on wind stress and shelf slope steepness amongst other parameters (Jacox and Edwards, 2012). Depth profiles of $\delta^{15}N_{nitrate}$ in central California Current show a rapid depletion from the near-surface to 200 m (Santoro et al., 2010), indicative of the importance of wind stress strength and depth of upwelled waters. Changes in upwelling source depth may therefore change the relative contributions of water masses upwelled and subsequently alter the $\delta^{15}N_{nitrate}$ available to zooplankton. As such, greater $\delta^{15}N_{coral}$ variability of North-Central specimens prior to 1965 (Fig. 4, warm colors) suggests that either wind stress variability decreased such that the depth of upwelled waters became consistent or the source water of the CUC (i.e., PEW) became more stable in $\delta^{15}N_{nitrate}$ composition after 1965.

If wind stress variability decreased as coastal upwelling intensified (Schwing and Mendelssohn, 1997), it would have led to a greater contribution of upwelled, nitrate-rich waters over the past half century. We interpret the 0.5‰ depletion in the North-Central specimens post-1965 to be due to less complete nutrient utilization by plankton from more consistent upwelling events. Toward the end of the 20th century, we do not observe a change in North-Central $\delta^{15}N_{coral}$ and suggest that increased wind stress (García-Reyes and Largier, 2010) advected blooms

offshore (Botsford et al., 2003) during peak upwelling season such that North-Central $\delta^{15}N_{coral}$ primarily reflects $\delta^{15}N_{nitrate}$ of autumn plankton blooms. The alternative interpretation is that PEW changed in composition. North-Central $\delta^{15}N_{coral}$ became more depleted over the 20th century (Fig. 4b) consistent with PEW $\delta^{15}N_{nitrate}$ steadily became more depleted over most of the 20th century (Deutsch et al., 2014). The documented late 20th century reversal (i.e. 1990s and onward enrichment) of PEW $\delta^{15}N_{nitrate}$ (Deutsch et al., 2014), however, is not apparent in North-Central $\delta^{15}N_{coral}$ as the relatively weaker winds later in the upwelling season lead to plankton blooms grown in waters upwelled from a shallower depth in the water column than the CUC.

The depletion of $\delta^{15}N$ in Central specimens until the late 20th century followed by a sharp reversal to subsequent $\delta^{15}N_{coral}$ enrichment is consistent with the timing of previously documented $\delta^{15}N_{nitrate}$ enrichment of the denitrified PEW (Davis et al., 2019; Deutsch et al., 2014; Ohman et al., 2012). Thus, one possible explanation for the Central specimens $\delta^{15}N$ trends is that Central $\delta^{15}N_{coral}$ record also reflects PEW. However, both Central specimens are farther from the nearest upwelling center (Point Sur) than the North-Central specimens (i.e., Point Arena), so we therefore consider a second explanation where the influence of CUC to the total plankton biomass exported to the Central specimens is reduced. Specifically, we posit that it is unlikely for mesoscale eddies to be delivering the only source of exported productivity to this site because of local production derived from offshore wind stress curl-induced upwelling (Macías et al., 2012; Pickett and Paduan, 2003). Thus, we consider the probability that Central $\delta^{15}N_{coral}$ in part reflect the $\delta^{15}N_{nitrate}$ history of ENPCW.

The role of ENPCW is supported by Station M2 (~72 km offshore) and Station M1 (~26 km from shore) $\delta^{15}N$ histories. Station M2 is often stratified and not influenced by upwelling (Kudela and Chavez, 2002, 2000; Pennington and Chavez, 2000; Wankel et al., 2007), and

$\delta^{15}N_{nitrate}$ ranged from 6.91–7.68‰ in 2003–2004. In contrast, the more nearshore Station M1 was consistently more ^{15}N enriched (Wankel et al., 2007). The offshore Central coral specimen (T1102-A10) is also consistently more depleted than the coastal Central specimen (T1102-A12). This offshore-onshore $\delta^{15}N_{nitrate}$ gradient is also documented further north in the subarctic northeast Pacific where the California Current source waters bifurcate (Wu et al., 1997). Further, without contribution of ENPCW, we would expect the Central specimens to be more enriched than the North-Central corals following the documented nearshore trend of enriched $\delta^{15}N$ in Southern California Current System and depleted $\delta^{15}N$ northward (Vokhshoori and McCarthy, 2014), which is not the case.

Extrapolating the average open ocean $\delta^{15}N_{nitrate}$ value of 4.6‰ (Sigman, 1997) and Station ALOHA subsurface $\delta^{15}N_{nitrate}$ values of 4.5–7‰ (Sigman et al., 2009) to the ENPCW, we attribute the enrichment of both specimens relative to ENPCW to the trophic position of the corals and partial influence of upwelled PEW waters that are advected offshore. Given that the two Central corals show similar temporal trends, one possibility is that the ENPCW underwent a regime shift of phytoplankton community structure [i.e., trophic lengthening and/or shift in dominate species (Alexander et al., 2015; Karl et al., 2001)], and another is that stronger upwelling favorable winds beginning mid-20th century (Schwing and Mendelssohn, 1997) induced positive wind stress curl offshore thus bringing more ENPCW water to the surface, reducing nitrate utilization and increasing plankton biomass. With even greater wind stress toward the end of the 20th century (García-Reyes and Largier, 2010), we posit that increased wind stress induced more coastal upwelled water to advect offshore, increasing the contribution of enriched $\delta^{15}N$ sub-euphotic zone nitrate to offshore benthic communities.

We attribute the lack of any discernable change in isotopic composition of the Southern coral to the confluence of water masses in the Southern California Bight (Bograd et al., 2019). Together the variable influence of each end member—PEW (δ^{15}N >15‰, Cline and Kaplan, 1975; Liu and Kaplan, 1989; Sigman et al., 2003), ENCPW (δ^{15}N=4.5–7‰; Sigman et al., 2009), and Pacific Subarctic Upper Water (δ^{15}N=8.1‰ for both δ^{15}N$_{nitrate}$ and δ^{15}N$_{zooplankton}$; Wu et al., 1997)—likely mix and dampen any specific isotopic change within a water source.

4.2.2 δ^{13}C

All three North-Central specimens are more nearshore, and their organic nodes are more δ^{13}C enriched than the Central and Southern corals further offshore. Given that nearshore locations receive more marine snow due to coastal upwelling (Rykaczewski and Checkley, 2008), the nearshore δ^{13}C$_{coral}$ enrichment we observe here is consistent with both δ^{13}C enrichment due to high benthic-pelagic coupling nearshore (e.g., Miller et al., 2008; Perry et al., 1999; Kline, 1999; Hill et al., 2014) and the rough correlation between carbon flux and δ^{13}C$_{coral}$ (Heikoop et al., 2002; Shen et al., 2021). To further support the nearshore/offshore trends, we compare our six δ^{13}C records to a bamboo coral collected in Monterey Canyon (Schiff et al. 2014). The Monterey Canyon coral is the most nearshore of all seven specimens and significantly more ^{13}C enriched than any of our corals (on average 2‰ more enriched).

Specimens NA085-033 and NA085-079 from the North-Central region have similar cyclical δ^{13}C trends that track each other. However, NA085-079 exhibits ~1‰ δ^{13}C variability, while NA085-033 exhibits >2‰ δ^{13}C variability. We thus explore why the cyclical variability of NA085-033 exhibits a greater range. The two corals might reflect differences in stability versus fluctuations between low carbon flux periods (more depleted δ^{13}C) and high carbon flux periods (more enriched δ^{13}C). For example, the bathymetry near specimen NA085-079 may induce

persistent upwelling of nutrients such that it regularly receives high carbon flux and thus records a smaller range in $\delta^{13}C$. We note a long-term stability of $\delta^{13}C$ over much of the 20th century (Fig. 5), and explore possible explanations below.

The $\delta^{13}C$ of phytoplankton (and more generally particulate organic carbon) is controlled by taxon-specific fractionation, sea surface temperature, $\delta^{13}C_{DIC}$, and CO_2 (aq.) concentration (Rau et al., 1996; Young et al., 2013). We consider a taxon-specific (i.e. a change in plankton community composition) explanation controlling for the long-term stability to be unlikely even though diatoms remain dominate, specifically *Chaetoceros* and *Corethron*, in the California Current System (Lassiter et al., 2006; Rodgers et al., 2020; Venrick, 2002; Wu et al., 1997). Specifically, all four phytoplankton assemblage studies are from the turn of the century onward, yet the consistency of phytoplankton assemblage during this period does not coincide with a stable $\delta^{13}C_{coral}$ signature and therefore suggests that phytoplankton assemblage does not control $\delta^{13}C_{coral}$ long-term stability.

Rather, we interpret this long-term stability to more likely reflect a combination of sea surface temperature, $\delta^{13}C_{DIC}$, and CO_2 (aq.) concentration likely through upwelling. This long-term stability could contain a combined signal of both carbon export to the deep sea and $\delta^{13}C$ signature of upwelled waters. Toward the end of the century, there is a pronounced $\delta^{13}C$ depletion of specimen NA085-081 (-2.13‰), and to a lesser extent specimen NA085-079 (-0.30‰), a marked change from the stability over much of the 20th century. Stronger upwelling favorable winds from the 1980s onward (García-Reyes and Largier, 2010) may have deepened the source of upwelled waters, pulling more consistently and closer to the ~300 m depth core of the CUC (Reed and Halpern, 1976). We suggest the increased upwelling brought to the surface depleted $\delta^{13}C_{DIC}$ values that led to the depletion of $\delta^{13}C_{coral}$ via plankton.

While a range of potential interpretations are possible for these observed changes the one that is most consistent between both $\delta^{13}C$ and $\delta^{15}N$ interpretations are changes in source water dynamics and wind stress. Altogether, we posit that the changes in coral $\delta^{13}C$ and $\delta^{15}N$ likely reflect a combination of source water dynamics (i.e. PEW history), their relative contributions to the upwelled water, and wind stress more generally. Specifically, we posit that increased wind stress over the 20th century induced stronger and more frequent upwelling favorable winds that deepened the upwelled water source and subsequently advected blooms offshore shifting the dominate marine snow signature nearshore to that of shallower source waters (i.e. PSUW).

5. Conclusions

We present $\delta^{15}N$ and $\delta^{13}C$ records from six deep sea bamboo corals from along the California margin. We determined the growth rates of each coral and showed that together they spanned most of the 20th century and the beginning of the 21st century. This study documents the $\delta^{15}N$ and $\delta^{13}C$ variability of exported productivity on subdecadal to decadal timescales in an eastern boundary upwelling system. From the initial questions:

1) How does California Current System productivity change over the 20th century? The $\delta^{15}N$ records reveal a mid-20th century 0.5‰ depletion. Additionally, our records indicate a $\delta^{13}C$ stability over much of the 20th century followed by a reversal just before the turn of the century. While these records show changes in the biogeochemistry of the California Current System, future work could constrain food web dynamics to better ascertain mechanism(s) for the biogeochemical changes.

2) What changes in physical oceanographic processes (i.e. wind stress and upwelling) can be inferred by these changes in productivity? We hypothesize that the mid-century $\delta^{15}N$ depletion may be due to source water nitrogen history, specifically that of PEW, and

changing contributions of CUC to different regions of the photic zone due to increased wind stress during the second half of the century. We suggest this reflects the same increase in wind stress that not only upwells more CUC/PEW but also advects blooms offshore.

3) What might this mean for 21st century productivity in response to predicted changes in eastern boundary upwelling system upwelling? This work highlights the complexity of coastal upwelling systems, the interconnectedness of different water masses, and value of deep sea corals as oceanic archives. Given location-specific 21st century wind stress predictions and continued ocean warming, deoxygenation, and ocean acidification, the response of eastern boundary current system productivity may be difficult to ascertain due to complexity of how the drivers manifest together in coral geochemistry.

6. Acknowledgments

7. Tables

Specimen	NA085–081	NA085–079	NA085–033	T1102–A10	T1102–A12	T664–A17
Region	North–central	North–central	North–central	Central	Central	Southern
Latitude	38.2294	38.2293	38.2278	35.7311	35.7306	33.1320
Longitude	–123.6046	–123.6042	–123.6385	–123.7250	–122.7261	–120.9070
Depth (m)	1246	1254	1397	1521	1500	1295
Year collected	2017	2017	2017	2007	2007	2004
Alive/dead	Live	Dead	Live	Live	Live	Live
^{14}C–derived age (yrs)	25	81	93	61	51	68
Organic layer counts	118	122	95	86	91	100
Calcite band counts	42 ± 8.5	121.5 ± 12.0	94.5 ± 20.5	*NaN*	*NaN*	*NaN*
Computer–aided calcite band counts	42.67 ± 1.53	164.1 ± 7.47	96.17 ± 22.7	*NaN*	*NaN*	*NaN*
Diameter (mm)	11	32.7	29	15	14	30
Water ˚C	3.193	3.202	2.835	*NaN*	*NaN*	*NaN*
[O$_2$]	21.729	21.606	33.573	*NaN*	*NaN*	*NaN*

Table 1. Coral specimens from along the California margin. All specimens were collected by remotely operated vehicles and were identified visually as *Keratoisis* sp.. The most basal node of each coral was used to develop ^{14}C radiocarbon chronologies and analyzed for δ^{13}C and δ^{15}N via accelerator mass spectrometer and elemental analyzer isotope ratio mass spectrometer, respectively. Alternative chronologies for NA085 specimens only were done on calcite thin sections also near the base of the coral.

Sample ID	radial distance from center (mm)	fraction modern	fraction modern uncertainty	CAMS #	C-14 age	C-14 age uncertainty
NA085–033w–2	7.25	1.0260	0.0031	182114	>Modern	NA
NA085–033w–6	6.75	1.0596	0.0031	182757	>Modern	NA
NA085–033w–12	6.05	0.9340	0.0028	182756	550	25
NA085–033w–18	5.35	0.9067	0.0026	182115	785	25
NA085–033w–33	3.35	0.9105	0.0026	182116	755	25
NA085–033w–46	2.00	0.9108	0.0024	182117	750	25
NA085–033w–56	0.75	0.9073	0.0026	182118	780	25
NA085–81–8	0.95	1.0490	0.0031	182119	>Modern	NA
NA085–81–18	1.95	1.0515	0.0031	182120	>Modern	NA
NA085–81–34	3.46	1.0477	0.0028	182121	>Modern	NA
NA085–81–50	5.40	1.0275	0.0029	182122	>Modern	NA
NA085–81–67	7.83	0.9934	0.0028	182123	Modern	NA
NA085–079–02	0.45	0.9009	0.0025	182124	840	25
NA085–079–13	3.00	0.9087	0.0023	182125	770	25
NA085–079–25	5.09	0.9133	0.0023	182126	730	25
NA085–079–37	6.78	0.9170	0.0021	182127	695	20
NA085–079–49	8.08	1.0503	0.0027	182128	>Modern	NA
NA085–079–63	9.75	1.0162	0.0027	182129	>Modern	NA
T1102–A10–1	0.80	0.9188	0.0030	182790	680	30
T1102–A10–6	2.40	0.9173	0.0027	182791	695	25
T1102–A10–10	3.55	0.9185	0.0027	182792	685	25
T1102–A10–14	4.50	0.9395	0.0031	182793	500	30
T1102–A10–18	5.50	1.0252	0.0040	182771	>Modern	NA
T1102–A12–2	1.00	0.8984	0.0029	182770	860	30
T1102–A12–6	2.05	0.9175	0.0028	182769	690	25
T1102–A12–10	3.45	1.0325	0.0032	182768	>Modern	NA
T1102–A12–14	5.10	1.0781	0.0032	182767	>Modern	NA
T1102–A12–18	6.75	1.0337	0.0031	182766	>Modern	NA
T664 A17–1	0.45	0.9218	0.0033	182763	655	30
T664 A17–7	1.80	0.9212	0.0030	182762	660	30
T664 A17–12	3.05	0.9278	0.0028	182761	600	25
T664 A17–16	3.95	0.9196	0.0028	182760	675	25
T664 A17–19	5.25	1.0117	0.0033	182759	>Modern	NA
T664 A17–22	6.50	1.0427	0.0031	182758	>Modern	NA

Table 2. Radiocarbon values for bamboo corals sampled herein as a function of radial distance of a coral basal organic node. Fraction modern follows the strict definition of Stuiver and Polach (1977) including both a background and stable carbon isotope correction and is synonymous with F14C (Reimer et al., 2004).
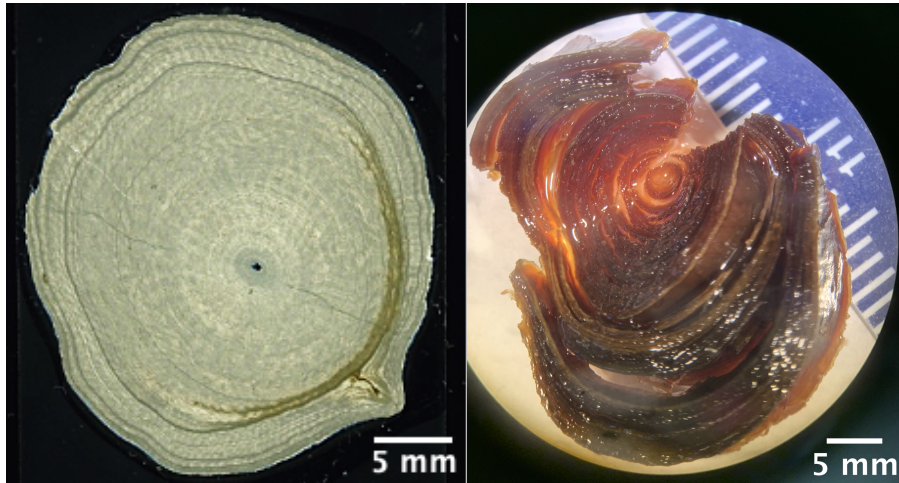
8. Figures

Figure 1. Bamboo coral skeleton cross sections. Left: scanned thin section of calcitic internode (NA085-033). Right: layers of black scleroprotein in a cross section of a gorgonian node under a light microscope (NA085-079).
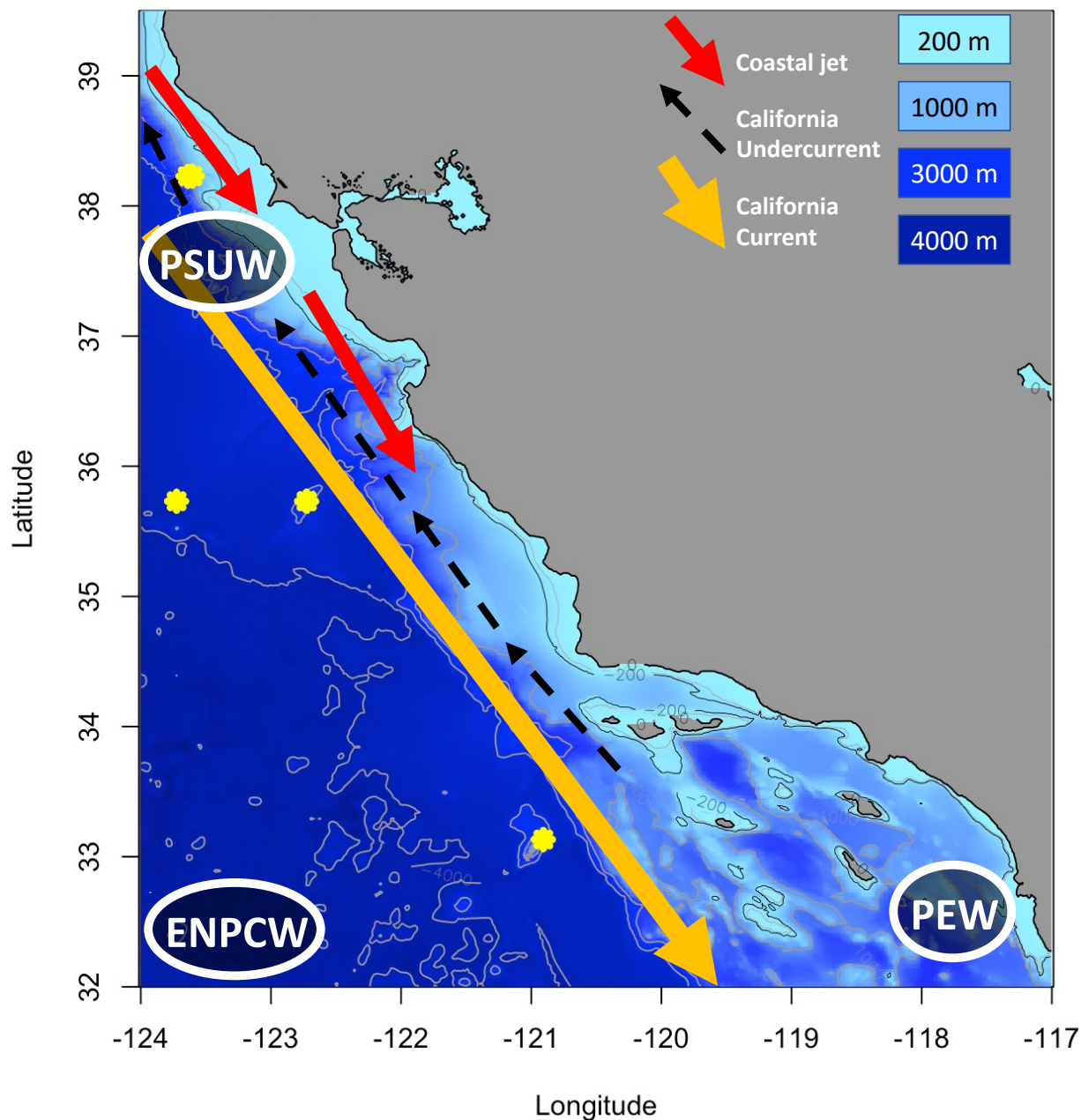
Figure 2. Map of study system and coral collection sites. Yellow symbols denote coral specimens studied herein, note the three North-Central specimens plot as one given their proximity to each other. Map and bathymetric data are from Marmap package in R that pulls from NOAA bathymetry data. Contour lines for 4000–500 in 500 m increments in addition to 200 m contour line as well. Water masses are indicated by their three abbreviations which are circled. Arrows denote the different currents in the region. Readers are referred to Bograd et al. (2019) for water masses and Checkley and Barth (2009) for the currents.
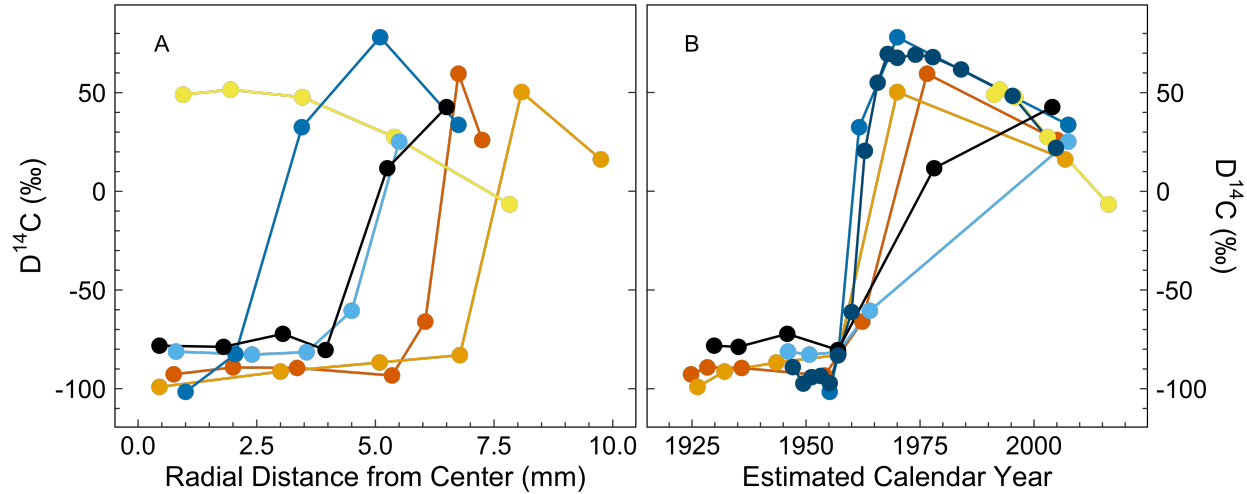
Figure 3. Radiocarbon values (A) as a function of radial distance of a coral basal organic node, and (B) as a function of years. North-Central corals (warm colors) and Southern coral (black color) reflect new data collected as a part of this study. The Central corals (blue colors) reflect two specimens both of which were analyzed for radiocarbon as a part of this study. Additionally, previously published data for one of the two specimens (T1102-A12) is also shown on (B), denoted in the darkest blue (Frenkel et al., 2017).
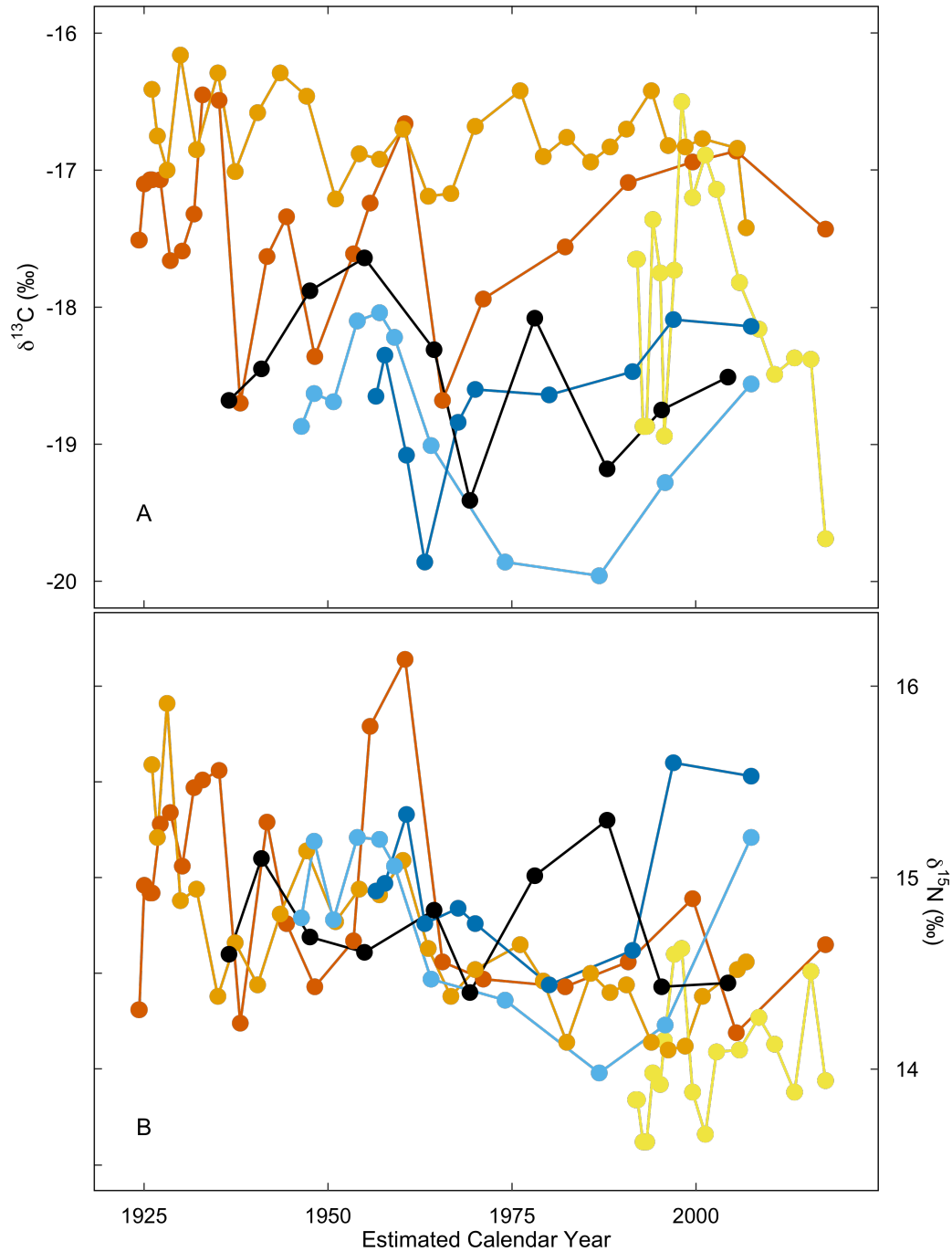
Figure 4. All six specimens a) $\delta^{13}C$ and b) $\delta^{15}N$ through time. Warm colors are North-Central specimens, blues are Central specimens off of Point Sur (dark blue is T1102-A12, and light blue is T1102-A10), and black specimen (T664-A17) is from within the CalCOFI grid near the Southern California Bight. North-Central specimens NA085-033 (red), NA085-079 (orange), and NA085-081 (yellow) show a 0.5‰ $\delta^{15}N$ depletion circa 1965.
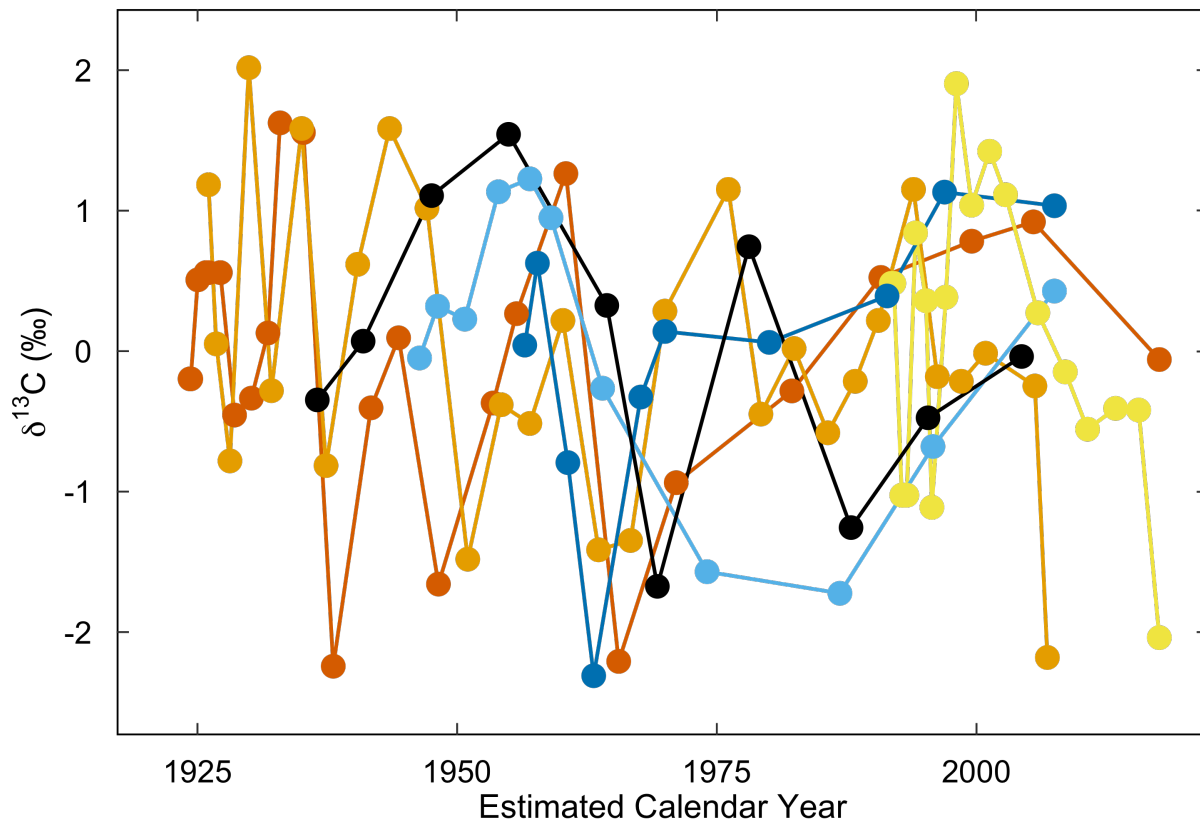
Figure. 5. Standardized $\delta^{13}C$ records of all six specimens through time. Same colors as in Fig. 4, warm colors are North-Central specimens, blues are Central specimens off of Point Sur, and black specimen is from within the CalCOFI grid near the Southern California Bight. Enrichment of $\delta^{13}C$ is evident until the turn of the century (most clearly in specimens NA085-033 and -079), where a reversal occurs marked by a sharp $\delta^{13}C$ depletion (most clearly in NA085-079 and -081).

9. Supplemental material

Sample ID	δ13C	δ15N	C:N
NA085–033w–1	−17.43	14.65	2.701
NA085–033w–4	−17.09	14.56	2.648
NA085–033w–7	−17.94	14.47	2.634
NA085–033w–10	−18.68	14.56	2.614
NA085–033w–13	−16.66	16.14	2.651
NA085–033w–16	−17.24	15.79	2.637
NA085–033w–19	−17.61	14.67	2.628
NA085–033w–22	−18.36	14.43	2.636
NA085–033w–25	−17.34	14.76	2.627
NA085–033w–28	−17.63	15.29	2.632
NA085–033w–31	−18.7	14.24	2.642
NA085–033w–34	−16.49	15.56	2.624
NA085–033w–37	−16.45	15.51	2.622
NA085–033w–39	−17.32	15.47	2.617
NA085–033w–42	−17.59	15.06	2.622
NA085–033w–45	−17.66	15.34	2.616
NA085–033w–49	−17.07	15.28	2.610
NA085–033w–51	−17.07	14.92	2.608
NA085–033w–52	−17.07	14.92	2.608
NA085–033w–55	−17.1	14.96	2.600
NA085–033w–58	−17.51	14.31	2.613
NA085–81–13–15	−17.65	13.84	2.609
NA085–81–20–23	−18.87	13.62	2.616
NA085–81–26	−17.36	13.98	2.603
NA085–81–30	−17.75	13.92	2.603
NA085–81–33	−18.94	14.15	2.593
NA085–81–37	−17.73	14.6	2.616
NA085–81–40	−16.5	14.63	2.615
NA085–81–43	−17.2	13.88	2.617
NA085–81–46	−16.89	13.66	2.634
NA085–81–49	−17.14	14.09	2.623
NA085–81–53	−17.82	14.1	2.637
NA085–81–56	−18.16	14.27	2.625
NA085–81–59	−18.49	14.13	2.626
NA085–81–62	−18.37	13.88	2.639
NA085–81–65	−18.38	14.51	2.649
NA085–81–68	−19.69	13.94	2.685
NA085–079–01	−16.41	15.59	2.731
NA085–079–04	−16.75	15.21	2.739
NA085–079–07	−17	15.91	2.716
NA085–079–10	−16.16	14.88	2.713
NA085–079–13	−16.85	14.94	2.742
NA085–079–16	−16.29	14.38	2.692
NA085–079–19	−17.01	14.66	2.703
NA085–079–22	−16.58	14.44	2.697
NA085–079–25	−16.29	14.81	2.681
NA085–079–28	−16.46	15.14	2.693
NA085–079–31	−17.21	14.77	2.727
NA085–079–34	−16.88	14.94	2.721
NA085–079–37	−16.92	14.91	2.727
NA085–079–40	−16.7	15.09	2.732
NA085–079–43	−17.19	14.63	2.742
NA085–079–46	−17.17	14.38	2.723
NA085–079–49	−16.68	14.52	2.716
NA085–079–52	−16.42	14.65	2.736
NA085–079–55	−16.94	14.5	2.746
NA085–079–58	−16.42	14.14	2.744
NA085–079–61	−16.77	14.38	2.746
NA085–079–63	−17.42	14.56	2.885
T1102–A10–2	−18.87	14.79	3.103
T1102–A10–4	−18.63	15.19	3.097
T1102–A10–6	−18.69	14.78	3.079
T1102–A10–8	−18.1	15.21	3.081
T1102–A10–10	−18.04	15.2	3.068
T1102–A10–12	−18.22	15.06	3.092
T1102–A10–14	−19.01	14.47	3.205
T1102–A10–16	−19.96	13.98	3.189
T1102–A10–18	−18.56	15.21	3.275
T1102–A12–5	−18.65	14.93	3.179
T1102–A12–7	−18.35	14.97	3.198
T1102–A12–9	−19.08	15.33	3.252
T1102–A12–11	−19.86	14.76	3.279
T1102–A12–13	−18.84	14.84	3.209
T1102–A12–15	−18.64	14.44	3.229
T1102–A12–17	−18.09	15.6	3.312
T1102–A12–18	−18.14	15.53	3.266
T664 A17–8	−18.68	14.6	3.216
T664 A17–11	−18.45	15.1	3.140
T664 A17–13	−17.88	14.69	3.108
T664 A17–15	−17.64	14.61	3.109
T664 A17–17	−18.31	14.83	3.141
T664 A17–19	−18.08	15.01	3.100
T664 A17–21	−18.75	14.43	3.117
T664 A17–22	−18.51	14.45	3.140

Table S1. C:N of all specimens studied herein. Bulk $\delta^{13}C$ and $\delta^{15}N$ values for all samples of the six specimens studied herein.
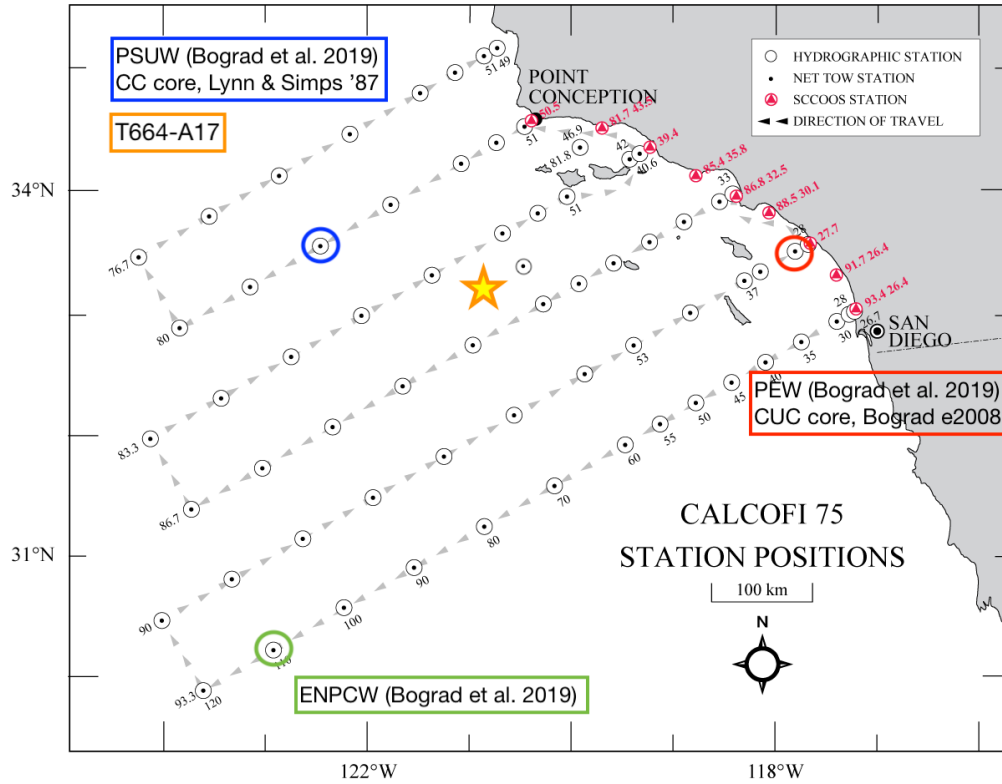
Figure S1. Map of Southern California Bight including the 75-station CalCOFI grid, Bograd et al. (2019) water mass end member locations (blue, green, and red circles for Pacific Subarctic Upper Water, ENCPW, and PEW, respectively), and location of Southern coral T664-A17 studied herein (gold star).

10. References

Alexander, H., Rouco, M., Haley, S.T., Wilson, S.T., Karl, D.M., Dyhrman, S.T., 2015. Functional group-specific traits drive phytoplankton dynamics in the oligotrophic ocean. Proc. Natl. Acad. Sci. 112, E5972–E5979. https://doi.org/10.1073/pnas.1518165112

Altabet, M.A., Pilskaln, C., Thunell, R., Pride, C., Sigman, D., Chavez, F., Francois, R., 1999. The nitrogen isotope biogeochemistry of sinking particles from the margin of the Eastern North Pacific. Deep Sea Res. Part Oceanogr. Res. Pap. 46, 655–679. https://doi.org/10.1016/S0967-0637(98)00084-3

Bakun, A., 1990. Global Climate Change and Intensification of Coastal Ocean Upwelling. Science 247, 198–201. https://doi.org/10.1126/science.247.4939.198

Batista, F.C., Ravelo, A.C., Crusius, J., Casso, M.A., McCarthy, M.D., 2014. Compound specific amino acid δ 15 N in marine sediments: A new approach for studies of the marine nitrogen cycle. Geochim. Cosmochim. Acta 142, 553–569. https://doi.org/10.1016/j.gca.2014.08.002

Bograd, S.J., Schroeder, I.D., Jacox, M.G., 2019. A water mass history of the Southern California current system. Geophys. Res. Lett. 46, 6690–6698. https://doi.org/10.1029/2019GL082685

Botsford, L.W., Lawrence, C.A., Dever, E.P., Hastings, A., Largier, J., 2003. Wind strength and biological productivity in upwelling systems: an idealized study: *Wind and productivity in upwelling systems*. Fish. Oceanogr. 12, 245–259. https://doi.org/10.1046/j.1365-2419.2003.00265.x

Broecker, W.S., Peng, T.-H., Ostlund, G., Stuiver, M., 1985. The distribution of bomb radiocarbon in the ocean. J. Geophys. Res. 90, 6953. https://doi.org/10.1029/JC090iC04p06953

Cairns, S.D., 2007. Deep-water corals: an overview with special reference to diversity and distribution of deep-water scleractinian corals. Bull. Mar. Sci. 81, 311–322.

Castro, C.G., Chavez, F.P., Collins, C.A., 2001. Role of the California Undercurrent in the export of denitrified waters from the eastern tropical North Pacific. Glob. Biogeochem. Cycles 15, 819–830. https://doi.org/10.1029/2000GB001324

Cerrano, C., Danovaro, R., Gambi, C., Pusceddu, A., Riva, A., Schiaparelli, S., 2010. Gold coral (Savalia savaglia) and gorgonian forests enhance benthic biodiversity and ecosystem functioning in the mesophotic zone. Biodivers. Conserv. 19, 153–167. https://doi.org/10.1007/s10531-009-9712-5

Chan, F., Barth, J.A., Lubchenco, J., Kirincich, A., Weeks, H., Peterson, W.T., Menge, B.A., 2008. Emergence of Anoxia in the California Current Large Marine Ecosystem. Science 319, 920–920. https://doi.org/10.1126/science.1149016

Cline, J.D., Kaplan, I.R., 1975. Isotopic fractionation of dissolved nitrate during denitrification in the eastern tropical north pacific ocean. Mar. Chem. 3, 271–299. https://doi.org/10.1016/0304-4203(75)90009-2

Davis, C.V., Ontiveros-Cuadras, J.F., Benitez-Nelson, C., Schmittner, A., Tappa, E.J., Osborne, E., Thunell, R.C., 2019. Ongoing Increase in Eastern Tropical North Pacific Denitrification as Interpreted Through the Santa Barbara Basin Sedimentary δ 15 N Record. Paleoceanogr. Paleoclimatology 34, 1554–1567. https://doi.org/10.1029/2019PA003578

Deutsch, C., Berelson, W., Thunell, R., Weber, T., Tems, C., McManus, J., Crusius, J., Ito, T., Baumgartner, T., Ferreira, V., Mey, J., van Geen, A., 2014. Centennial changes in North Pacific

anoxia linked to tropical trade winds. Science 345, 665–668. https://doi.org/10.1126/science.1252332

Etnoyer, P., Morgan, L.E., 2005. Habitat-forming deep-sea corals in the Northeast Pacific Ocean, in: Freiwald, A., Roberts, J.M. (Eds.), Cold-Water Corals and Ecosystems, Erlangen Earth Conference Series. Springer-Verlag, Berlin/Heidelberg, pp. 331–343. https://doi.org/10.1007/3-540-27673-4_16

Frenkel, M.M., LaVigne, M., Miller, H.R., Hill, T.M., McNichol, A., Gaylord, M.L., 2017. Quantifying bamboo coral growth rate nonlinearity with the radiocarbon bomb spike: A new model for paleoceanographic chronology development. Deep Sea Res. Part Oceanogr. Res. Pap. 125, 26–39. https://doi.org/10.1016/j.dsr.2017.04.006

García-Reyes, M., Largier, J., 2010. Observations of increased wind-driven coastal upwelling off central California. J. Geophys. Res. 115, C04011. https://doi.org/10.1029/2009JC005576

García-Reyes, M., Largier, J.L., 2012. Seasonality of coastal upwelling off central and northern California: New insights, including temporal and spatial variability: Upwelling Seasonality off California. J. Geophys. Res. Oceans 117, n/a-n/a. https://doi.org/10.1029/2011JC007629

Gay, P.S., Chereskin, T.K., 2009. Mean structure and seasonal variability of the poleward undercurrent off southern California. J. Geophys. Res. 114, C02007. https://doi.org/10.1029/2008JC004886

Graiff, K., Roberts, D.C., Howard, D., Etnoyer, P., Cochrane, G., Hyland, J., Roletto, J., 2011. A characterization of deep-sea coral and sponge communities on the continental slope west of Cordell Bank, Northern California using a remotely operated vehicle, DSC Res. Tech. NOAA, Silver Spring, MD.

Grant, R., 1976. The marine fauna of New Zealand: isididae (Octocorallia: gogonacea) from New Zealand and the Antarctic. NZ Ocean. Inst Mem 66, 5–54.

Griffin, S., Druffel, E.R.M., 1989. Sources of Carbon to Deep-Sea Corals. Radiocarbon 31, 533–543. https://doi.org/10.1017/S0033822200012121

Heikoop, J.M., Hickmott, D.D., Risk, M.J., Shearer, C.K., Atudorei, V., 2002. Potential climate signals from the deep-sea gorgonian coral Primnoa resedaeformis. Hydrobiologia 471, 117–124. https://doi.org/10.1023/A:1016505421115

Hickey, B.M., 1979. The California current system—hypotheses and facts. Prog. Oceanogr. 8, 191–279. https://doi.org/10.1016/0079-6611(79)90002-8

Hill, T.M., Myrvold, C.R., Spero, H.J., Guilderson, T.P., 2014. Evidence for benthic–pelagic food web coupling and carbon export from California margin bamboo coral archives. Biogeosciences 11, 3845–3854. https://doi.org/10.5194/bg-11-3845-2014

Hill, T.M., Spero, H.J., Guilderson, T., LaVigne, M., Clague, D., Macalello, S., Jang, N., 2011. Temperature and vital effect controls on bamboo coral (*Isididae*) isotope geochemistry: A test of the "lines method": Bamboo coral isotope geochemistry. Geochem. Geophys. Geosystems 12, n/a-n/a. https://doi.org/10.1029/2010GC003443

Huyer, A., Barth, J.A., Kosro, P.M., Shearman, R.K., Smith, R.L., 1998. Upper-ocean water mass characteristics of the California current, Summer 1993. Deep Sea Res. Part II Top. Stud. Oceanogr. 45, 1411–1442. https://doi.org/10.1016/S0967-0645(98)80002-7

Ingram, B.L., Southon, J.R., 1996. Reservoir Ages in Eastern Pacific Coastal and Estuarine Waters. Radiocarbon 38, 573–582. https://doi.org/10.1017/S0033822200030101

Jacox, M.G., Edwards, C.A., 2012. Upwelling source depth in the presence of nearshore wind stress curl: CURL-DRIVEN UPWELLING. J. Geophys. Res. Oceans 117, n/a-n/a. https://doi.org/10.1029/2011JC007856

Jones, D.O.B., Yool, A., Wei, C., Henson, S.A., Ruhl, H.A., Watson, R.A., Gehlen, M., 2014. Global reductions in seafloor biomass in response to climate change. Glob. Change Biol. 20, 1861–1872. https://doi.org/10.1111/gcb.12480

Karl, D.M., Bidigare, R.R., Letelier, R.M., 2001. Long-term changes in plankton community structure and productivity in the North Pacific Subtropical Gyre: The domain shift hypothesis. Deep Sea Res. Part II Top. Stud. Oceanogr. 48, 1449–1470. https://doi.org/10.1016/S0967-0645(00)00149-1

Kerr, L.A., Andrews, A.H., Munk, K., Coale, K.H., Frantz, B.R., Cailliet, G.M., Brown, T.A., 2005. Age validation of quillback rockfish (Sebastes maliger) using bomb radiocarbon. Fish. Bull. 103, 97–107.

Kienast, S.S., Calvert, S.E., Pedersen, T.F., 2002. Nitrogen isotope and productivity variations along the northeast Pacific margin over the last 120 kyr: Surface and subsurface paleoceanography: $\Delta ^{15}$ N Isotope in the NE Pacific. Paleoceanography 17, 7-1-7–17. https://doi.org/10.1029/2001PA000650

Kudela, R.M., Chavez, F.P., 2002. Multi-platform remote sensing of new production in central California during the 1997–1998 El Niño. Prog. Oceanogr. 54, 233–249. https://doi.org/10.1016/S0079-6611(02)00051-4

Kudela, R.M., Chavez, F.P., 2000. Modeling the impact of the 1992 El Niño on new production in Monterey Bay, California. Deep Sea Res. Part II Top. Stud. Oceanogr. 47, 1055–1076. https://doi.org/10.1016/S0967-0645(99)00136-8

Lamouroux, J.V.F., 1812. Extrait d'un mémoire sur la classification des Polypiers coralligènes non entièrement pierreux. Nouv. Bull. Sci. Société Philos. 3, 181–188.

Lassiter, A.M., Wilkerson, F.P., Dugdale, R.C., Hogue, V.E., 2006. Phytoplankton assemblages in the CoOP-WEST coastal upwelling area. Deep Sea Res. Part II Top. Stud. Oceanogr. 53, 3063–3077. https://doi.org/10.1016/j.dsr2.2006.07.013

Liu, K.-K., Kaplan, I.R., 1989. The eastern tropical Pacific as a source of 15N-enriched nitrate in seawater off southern California: Origin of 15N-rich nitrate. Limnol. Oceanogr. 34, 820–830. https://doi.org/10.4319/lo.1989.34.5.0820

Lynn, R.J., Simpson, J.J., 1987. The California Current system: The seasonal variability of its physical characteristics. J. Geophys. Res. 92, 12947. https://doi.org/10.1029/JC092iC12p12947

Macías, D., Franks, P.J.S., Ohman, M.D., Landry, M.R., 2012. Modeling the effects of coastal wind- and wind–stress curl-driven upwellings on plankton dynamics in the Southern California current system. J. Mar. Syst. 94, 107–119. https://doi.org/10.1016/j.jmarsys.2011.11.011

Manning, M.R., Lowe, D.C., Melhuish, W.H., Sparks, R.J., Wallace, G., Brenninkmeijer, C.A.M., McGill, R.C., 1990. The Use of Radiocarbon Measurements in Atmospheric Studies. Radiocarbon 32, 37–58. https://doi.org/10.1017/S0033822200039941

Noé, S.U., Dullo, W.-Chr., 2006. Skeletal morphogenesis and growth mode of modern and fossil deep-water isidid gorgonians (Octocorallia) in the West Pacific (New Zealand and Sea of Okhotsk). Coral Reefs 25, 303–320. https://doi.org/10.1007/s00338-006-0095-8

Nydal, R., Lövseth, K., 1983. Tracing bomb [14] C in the atmosphere 1962–1980. J. Geophys. Res. 88, 3621. https://doi.org/10.1029/JC088iC06p03621

Ohman, M.D., Rau, G.H., Hull, P.M., 2012. Multi-decadal variations in stable N isotopes of California Current zooplankton. Deep Sea Res. Part Oceanogr. Res. Pap. 60, 46–55. https://doi.org/10.1016/j.dsr.2011.11.003

Pauly, D., Christensen, V., 1995. Primary production required to sustain global fisheries. Nature 374, 255–257. https://doi.org/10.1038/374255a0

Pearson, A., Eglinton, T.I., McNichol, A.P., 2000. An organic tracer for surface ocean radiocarbon. Paleoceanography 15, 541–550. https://doi.org/10.1029/1999PA000476

Pennington, J.T., Chavez, F.P., 2000. Seasonal fluctuations of temperature, salinity, nitrate, chlorophyll and primary production at station H3/M1 over 1989–1996 in Monterey Bay, California. Deep Sea Res. Part II Top. Stud. Oceanogr. 47, 947–973. https://doi.org/10.1016/S0967-0645(99)00132-0

Pickett, M.H., Paduan, J.D., 2003. Ekman transport and pumping in the California Current based on the U.S. Navy's high-resolution atmospheric model (COAMPS). J. Geophys. Res. 108, 3327. https://doi.org/10.1029/2003JC001902

Rau, G., Riebesell, U., Wolf-Gladrow, D., 1996. A model of photosynthetic 13C fractionation by marine phytoplankton based on diffusive molecular CO2 uptake. Mar. Ecol. Prog. Ser. 133, 275–285. https://doi.org/10.3354/meps133275

Rau, G.H., Ohman, M.D., Pierrot-Bults, A., 2003. Linking nitrogen dynamics to climate variability off central California: a 51 year record based on 15N/14N in CalCOFI zooplankton. Deep Sea Res. Part II Top. Stud. Oceanogr. 50, 2431–2447. https://doi.org/10.1016/S0967-0645(03)00128-0

Rebstock, G.A., 2001. Long-term stability of species composition in calanoid copepods off southern California. Mar Ecol Prog Ser 215, 213–224.

Reed, R.K., Halpern, D., 1976. Observations of the California Undercurrent off Washington and Vancouver Island: Circulation off Washington. Limnol. Oceanogr. 21, 389–398. https://doi.org/10.4319/lo.1976.21.3.0389

Reimer, P.J., Brown, T., Reimer, R., 2004. Discussion: Reporting and calibration of post-bomb 14C data. Radiocarbon 46, 1299–1304.

Roark, E.B., Guilderson, T.P., Dunbar, R.B., Fallon, S.J., Mucciarone, D.A., 2009. Extreme longevity in proteinaceous deep-sea corals. Proc. Natl. Acad. Sci. 106, 5204–5208. https://doi.org/10.1073/pnas.0810875106

Roark, E.B., Guilderson, T.P., Dunbar, R.B., Ingram, B.L., 2006. Radiocarbon based ages and growth rates: Hawaiian deep sea corals. Mar. Ecol. Prog. Ser. 327, 1–14.

Roark, E.B., Guilderson, T.P., Flood-Page, S., Dunbar, R.B., Ingram, B.L., Fallon, S.J., McCulloch, M., 2005. Radiocarbon-based ages and growth rates of bamboo corals from the Gulf of Alaska: [14] C ages/growth rates of bamboo corals. Geophys. Res. Lett. 32. https://doi.org/10.1029/2004GL021919

Roberts, J.M., Cairns, S.D., 2014. Cold-water corals in a changing ocean. Curr. Opin. Environ. Sustain. 7, 118–126. https://doi.org/10.1016/j.cosust.2014.01.004

Rodgers, L., Fish, C., Hill, T.M., Vines, C., Guilderson, T.P., 2020. Tracing isotopic signatures of a deep-sea coral from the North-Central California margin. Presented at the Ocean Sciences Meeting 2020, San Diego, CA.

Rykaczewski, R.R., Dunne, J.P., Sydeman, W.J., García-Reyes, M., Black, B.A., Bograd, S.J., 2015. Poleward displacement of coastal upwelling-favorable winds in the ocean's eastern boundary currents through the 21st century: Upwelling responses to climate change. Geophys. Res. Lett. 42, 6424–6431. https://doi.org/10.1002/2015GL064694

Santoro, A.E., Casciotti, K.L., Francis, C.A., 2010. Activity, abundance and diversity of nitrifying archaea and bacteria in the central California Current: Nitrification in the central California Current. Environ. Microbiol. 12, 1989–2006. https://doi.org/10.1111/j.1462-2920.2010.02205.x

Schwing, F.B., Mendelssohn, R., 1997. Increased coastal upwelling in the California Current System. J. Geophys. Res. Oceans 102, 3421–3438. https://doi.org/10.1029/96JC03591

Shen, Y., Guilderson, T.P., Sherwood, O.A., Castro, C.G., Chavez, F.P., McCarthy, M.D., 2021. Amino acid δ13C and δ15N patterns from sediment trap time series and deep-sea corals: Implications for biogeochemical and ecological reconstructions in paleoarchives. Geochim. Cosmochim. Acta 297, 288–307. https://doi.org/10.1016/j.gca.2020.12.012

Sherwood, O., Scott, D., Risk, M., Guilderson, T., 2005. Radiocarbon evidence for annual growth rings in the deep-sea octocoral Primnoa resedaeformis. Mar. Ecol. Prog. Ser. 301, 129–134. https://doi.org/10.3354/meps301129

Sherwood, O.A., Edinger, E.N., 2009. Ages and growth rates of some deep-sea gorgonian and antipatharian corals of Newfoundland and Labrador. Can. J. Fish. Aquat. Sci. 66, 142–152. https://doi.org/10.1139/F08-195

Sherwood, O.A., Edinger, E.N., Guilderson, T.P., Ghaleb, B., Risk, M.J., Scott, D.B., 2008. Late Holocene radiocarbon variability in Northwest Atlantic slope waters. Earth Planet. Sci. Lett. 275, 146–153. https://doi.org/10.1016/j.epsl.2008.08.019

Sherwood, O.A., Scott, D.B., Risk, M.J., 2006. Late Holocene radiocarbon and aspartic acid racemization dating of deep-sea octocorals. Geochim. Cosmochim. Acta 70, 2806–2814. https://doi.org/10.1016/j.gca.2006.03.011

Sherwood, O.A., Thresher, R.E., Fallon, S.J., Davies, D.M., Trull, S.J., 2009. Multi-century time-series of 15N and 14C in bamboo corals from deep Tasmanian seamounts: evidence for stable oceanographic conditions. Mar. Ecol. Prog. Ser. 397, 209–218.

Sigman, D.M., 1997. The Role of Biological Production in Pleistocene Atmospheric Carbon Dioxide Variations and the Nitrogen Isotope Dynamics of the Southern Ocean (Doctoral thesis). Massachusetts Institute of Technology, Woods Hole Oceanographic Institution MA.

Sigman, D.M., DiFiore, P.J., Hain, M.P., Deutsch, C., Karl, D.M., 2009. Sinking organic matter spreads the nitrogen isotope signal of pelagic denitrification in the North Pacific. Geophys. Res. Lett. 36, L08605. https://doi.org/10.1029/2008GL035784

Sigman, D.M., Robinson, R., Knapp, A.N., van Geen, A., McCorkle, D.C., Brandes, J.A., Thunell, R.C., 2003. Distinguishing between water column and sedimentary denitrification in the Santa Barbara Basin using the stable isotopes of nitrate: Denitrification in Santa Barbara Basin. Geochem. Geophys. Geosystems 4, n/a-n/a. https://doi.org/10.1029/2002GC000384

Smith, K.L., Ruhl, H.A., Kahru, M., Huffard, C.L., Sherman, A.D., 2013. Deep ocean communities impacted by changing climate over 24 y in the abyssal northeast Pacific Ocean. Proc. Natl. Acad. Sci. 110, 19838–19841. https://doi.org/10.1073/pnas.1315447110

Stuiver, M., Polach, H.A., 1977. Discussion Reporting of [14]C Data. Radiocarbon 19, 355–363. https://doi.org/10.1017/S0033822200003672

Thomson, R.E., Krassovski, M.V., 2010. Poleward reach of the California Undercurrent extension. J. Geophys. Res. 115, C09027. https://doi.org/10.1029/2010JC006280

Todd, R.E., Rudnick, D.L., Mazloff, M.R., Davis, R.E., Cornuelle, B.D., 2011. Poleward flows in the southern California Current System: Glider observations and numerical simulation. J. Geophys. Res. 116, C02026. https://doi.org/10.1029/2010JC006536

Venrick, E.L., 2002. Floral patterns in the California Current System off southern California: 1990-1996. J. Mar. Res. 60, 171–189. https://doi.org/10.1357/002224002762341294

Vogel, J.S., Southon, J.R., Nelson, D.E., Brown, T.A., 1984. Performance of catalytically condensed carbon for use in accelerator mass spectrometry. Nucl. Instrum. Methods Phys. Res. Sect. B Beam Interact. Mater. At. 5, 289–293. https://doi.org/10.1016/0168-583X(84)90529-9

Vokhshoori, N.L., McCarthy, M.D., 2014. Compound-Specific δ15N Amino Acid Measurements in Littoral Mussels in the California Upwelling Ecosystem: A New Approach to Generating Baseline δ15N Isoscapes for Coastal Ecosystems. PLoS ONE 9, e98087. https://doi.org/10.1371/journal.pone.0098087

Wankel, S.D., Kendall, C., Pennington, J.T., Chavez, F.P., Paytan, A., 2007. Nitrification in the euphotic zone as evidenced by nitrate dual isotopic composition: Observations from Monterey Bay, California: Nitrate isotopes in Monterey Bay. Glob. Biogeochem. Cycles 21, n/a-n/a. https://doi.org/10.1029/2006GB002723

Williams, B., 2020. Proteinaceous corals as proxy archives of paleo-environmental change. Earth-Sci. Rev. 209, 103326. https://doi.org/10.1016/j.earscirev.2020.103326

Williams, B., Halfar, J., Steneck, R.S., Wortmann, U.G., Hetzinger, S., Adey, W., Lebednik, P., Joachimski, M., 2011. Twentieth century δ13C variability in surface water dissolved inorganic carbon recorded by coralline algae in the northern North Pacific Ocean and the Bering Sea. Biogeosciences 8, 165–174. https://doi.org/10.5194/bg-8-165-2011

Williams, B., Risk, M., Stone, R., Sinclair, D., Ghaleb, B., 2007. Oceanographic changes in the North Pacific Ocean over the past century recorded in deep-water gorgonian corals. Mar. Ecol. Prog. Ser. 335, 85–94. https://doi.org/10.3354/meps335085

Williams, B., Risk, M.J., Ross, S.W., Sulak, K.J., 2006. Deep-water antipatharians: Proxies of environmental change. Geology 34, 773. https://doi.org/10.1130/G22685.1

Wu, J., Calvert, S.E., Wong, C.S., 1997. Nitrogen isotope variations in the subarctic northeast Pacific: relationships to nitrate utilization and trophic structure. Deep Sea Res. Part Oceanogr. Res. Pap. 44, 287–314. https://doi.org/10.1016/S0967-0637(96)00099-4

Young, J.N., Bruggeman, J., Rickaby, R.E.M., Erez, J., Conte, M., 2013. Evidence for changes in carbon isotopic fractionation by phytoplankton between 1960 and 2010: 50 Year record of global surface ε_p. Glob. Biogeochem. Cycles 27, 505–515. https://doi.org/10.1002/gbc.20045

Chapter 2

Carbonate chemistry over the shelf in the central California Current during and after the 2014-2016 Northeast Pacific Marine Heatwave

Abstract

Increasing anthropogenic carbon dioxide emissions are rapidly changing coastal ocean systems through increasing surface temperature, ocean acidification, and potentially intensified upwelling. Here we investigated the strength, timing, duration, and co-occurrence of temperature, wind stress, and carbonate chemistry fluctuations over a key period of environmental change off the northern Californian coast (38˚N, 123.5˚W). This region is well studied in terms of surface water productivity, oceanographic variability, and more recently, carbon chemistry and climate impacts through the Applied California Current Ecosystem Studies (ACCESS) partnership. Oceanographic cruises sample water column hydrography and discrete water samples from 1 m and 200 m depth at five stations along three primary transects, three times annually. Here we present regional bottle carbonate chemistry from 2013-2019 and hindcast 2010-2012 that together span before, during, and after the 2014-2016 northeast Pacific marine heatwave. The 2014-2016 marine heatwave ameliorated ocean acidification in this region from the height of the marine heatwave (i.e. late 2015) onward. We also suggest that regional aragonite saturation state equations require re-evaluation given the likelihood of warm anomalies impacting local modification but also affecting upwelled source waters including the depth distribution of water masses in the California Current System.

1. Introduction

The California Current System (CCS) is the eastern limb of the North Pacific Gyre, and one of four major eastern boundary upwelling systems. Eastern boundary upwelling systems are highly productive regions of the ocean, home to nearly one-fifth of the world's fisheries despite comprising <1% of the ocean (Pauly and Christensen, 1995). The high productivity is driven by injections of cold, nutrient-rich subsurface waters upwelling to the photic zone (e.g., Thomson and Krassovski, 2010; Huyer, 1983), which enable blooms of phytoplankton. The north-central CCS from Point Arena to San Francisco, CA in particular has intense seasonal upwelling (Dorman and Winant, 1995; García-Reyes and Largier, 2010) that supports high concentrations of phytoplankton (Largier et al 2006; García-Reyes and Largier, 2014) and in turn a rich marine ecosystem (Santora et al., 2011; Yen et al., 2004).

The prevailing flow within the north-central CCS is the wind-dominated coastal jet (e.g. (Largier et al 1993; Halle and Largier, 2011; Huyer et al., 1998, 1991; Largier et al., 2006). In spring and summer, the Point Arena coastal jet is southward-moving and may bifurcate into a shelf jet and an offshore jet (Halle and Largier, 2011). The direct effect of wind stress is to drive an offshore Ekman transport, which induces upwelling that is occurs year-round but is maximum in April-June (García-Reyes and Largier, 2012). The upwelled water is a mixture of the California Undercurrent and Pacific Subarctic Water, with a stronger undercurrent contribution predicted with warming surface waters (Song et al., 2011).

Under a warming ocean, upwelling in poleward regions of eastern boundary upwelling systems is expected to intensify (e.g. (Bakun, 1990; Bakun et al., 2015; Snyder et al., 2003), and both observations off central California (García-Reyes and Largier, 2010; García-Reyes et al., 2015) and a meta-analysis support these predictions (Sydeman et al., 2014). Despite intensified

upwelling winds, the flux of upwelled waters and therefore nutrients entering the euphotic zone is uncertain due to warming surface waters also leading to the competing force of intensified stratification (García-Reyes et al., 2015). In turn, if upwelling is constrained then its ability to temporarily buffer against warming temperatures (Seabra et al., 2019) and moderate marine heatwave (MHW) occurrences (Varela et al., 2021) is reduced.

Interannual to decadal scale variability (e.g., El Niño-Southern Oscillation [ENSO] and warm anomaly conditions [e.g. Chavez et al., 2002; Di Lorenzo and Mantua, 2016; Mantua et al., 1997; Norton and McLain, 1994]) overlay the seasonal variability of regional CCS coastal upwelling. While mean sea surface temperature (SST) for the CCS showed a decreasing trend over the satellite period, i.e. since 1982 (Lima and Wethey, 2012), the 2014-2016 North Pacific MHW reversed the decadal scale trend (Seabra et al., 2019). The 2014-2016 North Pacific MHW was driven by a persistent high pressure ridge (Bond et al., 2015; Chao et al., 2017; Di Lorenzo and Mantua, 2016; Hartmann, 2015) and impacted biology across the ecosystem (e.g. Cavole et al., 2016; Lilly et al., 2019; McCabe et al., 2016; Peterson et al., 2017), delayed upwelling (Peterson et al., 2015), and increased stratification and deepened the thermocline (Chao et al., 2017). Spatial variability of the 2014-2016 North Pacific MHW manifested as different regional timings for coastal and offshore warm anomalies in part due to coastal upwelling (Gentemann et al., 2017). For coastal central CCS, SST anomalies peaked in late 2015 and extended into 2016 (Gentemann et al., 2017) and was driven mostly by the MHW but also the 2015 El Niño (Jacox et al., 2016) that propagated poleward slowly (Chao et al., 2017). Upwelling in the central CCS was strong throughout 2013, normal for 2014 with strong upwelling during June, and stronger than average in 2015 in terms of upwelling-favorable conditions (Leising et al., 2015). Despite

no weakening of upwelling winds in the central CCS during the MHW, the ecological

disturbances suggest that the upwelling source waters were atypical (Gentemann et al., 2017).

The uncertainty in a warming eastern boundary upwelling system given stratification and

upwelling also extends to the carbonate system since upwelled waters are more corrosive than

surface waters and temperature impacts the carbonate system. Marine carbonate chemistry is

governed in part by ocean pH, which has changed over the past several decades. Specifically,

average surface ocean pH has decreased by more than 0.1 units due to anthropogenic carbon

dioxide (CO_2) emissions (Feely et al., 2009; Jiang et al., 2019). Such a reduction, termed ocean

acidification (OA), is caused by excess atmospheric CO_2 rapidly dissolving into seawater,

reacting with water to form carbonic acid, and as a weak acid, carbonic acid quickly dissociating

into bicarbonate and a hydrogen ion. For shelled organisms made of calcium carbonate, oceanic

uptake of anthropogenic CO_2 can cause a myriad of problems, including decreased calcification

rates and dissolution (e.g., Feely et al., 2004; Orr et al., 2005).

Globally, the ocean has absorbed 155 PgC of anthropogenic origins (Khatiwala et al.,

2013), approximately one third of anthropogenic CO_2 emissions (e.g., Canadell et al., 2007; Le

Quéré et al., 2018; Sabine et al., 2004). While the resulting OA is a surface ocean global average

(e.g., Caldeira and Wickett, 2003; Kleypas et al., 1999; Orr et al., 2005), there is substantial

temporal and spatial variability (e.g., Alin et al., 2012; Davis et al., 2018; Feely et al., 2008;

Juranek et al., 2009). Within the CCS, surface water variability includes that driven by episodic

upwelling, photosynthesis, respiration, and the chemical signature of the upwelled water itself is

influenced by anthropogenic CO_2 (Chan et al., 2017; Feely et al., 2016, 2008; Harris et al.,

2013). Increased intensity of upwelling increases the exposure of organisms to low pH and

therefore low carbonate ion concentrations [CO_3^{2-}] too (Gruber et al., 2012; Hauri et al., 2013).

The carbonate chemistry heterogeneity combined with the effects of a warming ocean highlight the need for understanding the consequences of multiple parameters shifting simultaneously.

Davis et al. (2018) began to characterize the spatial and temporal variability of the north-central CCS carbonate chemistry leading up to and during part of the 2014-2016 MHW (i.e. 2013-2015). Specifically, Davis et al. (2018) investigated aragonite saturation (Ω_{arag}), defined as $\Omega_{arag} = [Ca^{2+}][CO_3^{2-}]/K_{sp}$, where $[Ca^{2+}]$ is the concentration of calcium cations and K_{sp} is a phase-specific, temperature-, and salinity-dependent constant. Davis et al. (2018) found a deepening of the aragonite saturation horizon and increased near-surface aragonite saturation state during the first half of the MHW. Given that MHWs will likely become more frequent and/or intense using a fixed threshold and due to a warming ocean (Solomon et al., 2007; Oliver et al., 2018), understanding regional ocean acidification in a coastal upwelling system is important for effectively managing such dynamic ecosystems. We expect carbonate chemistry to change due to temperature impacts on both upwelling and local modification (i.e. respiration). To ascertain whether expected changes in carbonate chemistry are due to changes in upwelling or local modification, we sought to assess carbonate chemistry parameters during and after the 2014-2016 MHW. As such, here we present seven years of bottle carbonate chemistry for the north-central CCS. Additionally, we report regional upwelling indices, *in situ* water column temperature and salinity, and alongshore wind stress for this 2013-2019 study period.

2. Methods

2.1 Study region

The oceanographic data and water samples for carbonate chemistry were collected through The Applied California Current Ecosystem Studies (ACCESS, www.accessoceans.org) program, a collaboration between Cordell Bank and Greater Farallones National Marine

Sanctuaries and Point Blue Conservation Science. The north-central CCS study area (Fig. 1), lies downstream of the Point Arena upwelling center. The physical dynamics of this region have been well studied (e.g., Beardsley and Lentz, 1987; Dever and Lentz, 1994; Largier et al., 1993) along with intermittent biological characterizations of the region since 1994 (e.g., Largier et al., 2006, Botsford et al., 2006; Papastephanou et al., 2006; Wilkerson et al., 2006; Wing et al., 1998), including through the ACCESS program (e.g. Fontana et al., 2016; Hameed et al., 2018; Anderson et al., 2022).

2.2 Shipboard data

Oceanographic cruises surveyed the region up to three times per year during May, July, and September from 2004 to 2019. Carbonate chemistry sampling efforts began in 2013 and were conducted onboard the R/V Fulmar along five transects, three of which were prioritized. The transects span the continental shelf and coastal jet as close as 13 km from the coastline to 65 km offshore. Depth profiles of temperature, salinity, and dissolved oxygen (DO) were collected at five stations along each of the transects (Fig. 1). Paired water column hydrography and discrete water samples were collected using a conductivity-temperature-depth (CTD) profiler (Sea-Bird Electronics [SBE] 19) equipped with a SBE 63 optical DO sensor, and 3-L Niskin bottle. Salinity values below 32.27 psu were considered erroneous and omitted from the dataset. The DO sensor was factory calibrated annually (initial accuracy $\pm$ 3 μmol/kg [~0.07 ml/L] or $\pm$ 2%). Water was collected at 1 m and 200 m depths or ~3 m above the seafloor. Water was immediately dispensed from the Niskin bottle into duplicate 125 mL borosilicate glass bottles with mercuric chloride ($HgCl_2$) to cease respiration and stabilize the sample until analysis.

Water samples were analyzed at UC Davis Bodega Marine Laboratory for pH (total scale) and total alkalinity on a spectrophotometer (Ocean Optics Jaz EL200) and an automated

Gran titrator (Metrohm 855 Robotic Titrosampler; SD $\pm$ 6.42 µmol/kg), respectively. The

spectrophotometer used *m*-cresol purple (Dickson et al., 2007), so each dye batch required a

calibration regression against TRIS (2-amino-2-hydroxymethyl-1,3-propanediol). Measured pH

values were corrected for any offsets using repeated analyses of TRIS; offsets were all within $\pm$

0.065. Acid concentrations were standardized to Dickson certified reference materials for each

set of analyses on the titrator. Aragonite saturation (Ω_{arag}) and in-situ pCO_2 were both calculated

using R software package *SeaCarb* (Gattuso et al., 2020; Proye and Gattuso, 2003) from the pH,

total alkalinity, and CTD measurements (i.e. temperature, salinity, pressure) with CO_2

equilibrium constants, K1 and K2, from Lueker et al. (2000).

2.3 Buoy observations and indices source

Alongshore wind was determined by NOAA's National Data Buoy Center buoy N46013

(38.23°N, 123.32°W), where coastal orientation angle is 310° as determined clockwise from true

north (Dorman and Winant, 1995; García-Reyes and Largier, 2012). Wind speed from wind

direction of 310° $\pm$ 40° was averaged along with wind speed set to zero for wind directions

outside of 310° $\pm$ 40°, except for wind from the opposite direction (130 $\pm$ 40°) for which the wind

speed was factored in as negative values into the mean. Wind stress was averaged for the five-

day prior to sampling. As a proxy for water column stratification, N46013 buoy sea surface

temperature data was averaged for 30 days prior to sampling. Upwelling index was determined

by the Coastal Upwelling Transport Index (CUTI; (Jacox et al., 2018) at 38°N. Daily indices

were averaged for the five days prior to sampling.

2.4 Modeled aragonite saturation state

Hindcast and full water column estimates of Ω_{arag} were approximated using the

relationship described in Davis et al. (2018) that was developed for this study region. Two

additional relationships were developed here. Our modified models used the linear regression function, lm, in R software *stats* package version 3.6.3 and the same predictor variables and interaction terms as the Davis et al. (2018) model. The first modified model was developed on bottle data from 2013-2015, similar to the Davis et al. (2018) model, but increased the original dataset by >150 % with additional samples from the same region and time period (n = 94; Fig. S1). The second modified model was developed on bottle data spanning the full 2013-2019 dataset.

3 Results

3.1 Seasonal variability

Integrated water column temperatures increased from the May cruises to September cruises (Fig. 2a). Seasonal increase in mean water column temperatures is most noticeable for May and June in comparison to September. Subsurface (i.e. below 50 m) salinity is highest during May and lowest during September, consistent with seasonal reduction in upwelling (Fig. 3b). Seasonal mean water column (i.e. averaged surface to 200 m) Ω_{arag} either stays constant within its variability or increases from upwelling season (i.e. May-July surveys) to relaxation season (i.e September surveys) with the exception of 2013, when mean Ω_{arag} was lowest in September (Fig. 2c). Similarly, September subsurface median Ω_{arag} is typically higher than of earlier in the season with the exception of 2013 and 2017 (Fig. 3d). Lastly, seasonal pH variability is also small (< 0.5, except for 2015), but pH in September is typically higher than earlier in the same year (Fig. 2d). Subsurface median pH is also highest in September with the exception of 2013 and 2017 (Fig. 3c).

3.2 Interannual variability

Seasonal temperature differences are greatest for 2014-2015, and to a lesser extent 2008 and 2017 (Fig. 2a). The year with the largest range in temperature is 2014, which along with 2015, have the highest percent of temperatures over 15˚C (21.2%, 16%, and 12% for Sept. 2014, Sept. 2015, and July 2015, respectively). Temperatures for 2014 are the warmest and the mean CUTI during the five days preceding sampling were amongst the lowest for all years. Annual thermal minima were the warmest for 2014 and 2015 (Fig. 2a). While maximum temperatures increased for both July and September of 2014-2015, subsequent annual and seasonal thermal maximums decreased (Fig. 2a). Mean September salinities show a decreasing trend from 2010 to 2015, with the lowest means for 2015 and to a lesser degree 2007, 2009, and 2014 (Fig. 2b). Precipitation events do not significantly correlate with pH and salinity (Fig. S2), and there is no significant correlation between water chemistry and approximated 5-day alongshore wind speed means and mean CUTI for the five days prior to observation (Fig. 4b & c). During the month of September, the percent of $\Omega_{arag} < 1$ observations decreased from 2017 onward relative to 2017 (Fig. S3). For the Ω_{arag} of subsurface samples, aragonite saturation state increases in September for 2015, 2016, and 2019 in descending order (Fig. 3d). All years show a difference between pH intraannual means of < 0.07 except for 2015 with a difference of 0.23 between June/July and September due to an increase mean pH during September (Fig. 3c). While mean pH increases by 0.2 over the seven-year period (Fig. 2d), subsurface pH (i.e. >50 m) shows negligible change though time except for 2015 and May 2016 (Fig. 3c).

3.3 *Ω_{arag} data model comparison*

The modified models developed on different subdatasets (i.e. 2013-2015, 2013-2015 excluding September, subsurface 2013-2015 and excluding September, subsurface 2013-2019, subsurface 2013-2019 excluding September) yield new coefficients (Table 1). The only modified

model that is significant is the subsurface 2013-2019 excluding September data model (Eqn. 5). Subsurface-only and, to a lesser degree, full water column July Ω_{arag} were both best fit by Eqn. 5 post-MHW (i.e. 2016 onward; Fig. 2c). Additionally, Eqn. 5 marginally outperformed the original Davis et al. (2018) model for May Ω_{arag} for both full water column and subsurface-only (Fig. 2c).

3.4 Carbonate chemistry and stratification indices

Local maxima of sea surface temperature as determined by *in situ* buoy data during September 2013, 2014, and 2017 cruises, align with subsurface aragonite undersaturation (Fig. 4). However, relatively warm sea surface temperatures during September 2015 and September 2019 cruises align with supersaturated subsurface medians. Similarly, periods of subsurface aragonite undersaturation and supersaturation show no clear correlation with either alongshore wind stress or coastal upwelling index (Fig. 4).

4. Discussion

We focus the discussion on the full water column studied herein (i.e. surface to 200 m where the bathymetry allowed) and subsurface only (i.e. 50 m and below) as this omits the euphotic zone and surface mixed layer. The parameters discussed hereafter pertain to the water column unless noted as subsurface.

4.1 Seasonal and interannual variability

Seasonal water column (surface to 200 m) warm anomalies are evident in September temperatures during the 2008 El Niño and during the MHW in 2014-2015. July temperatures during the MHW were also abnormally warm despite coastal upwelling, supporting the suggestion from Gentemann et al. (2017) that upwelled source water characteristics were likely atypical at this time. The complex nearshore SST phenology given the warm anomalies and

persistence of strong coastal upwelling (Gentemann et al., 2017), lead to less robust trends in carbonate chemistry (Fig. 2 and 3).

The two pre-MHW cruises in 2013 resemble early MHW (i.e. 2014) pH despite the elevated surface temperatures of September 2014 and therefore a stratified water column. While the low pH and low temperature of June 2014 may be explained by strong coastal upwelling (Leising et al., 2015), the relatively low September 2014 pH despite the warm anomaly may be indicative of biological respiration without new upwelled waters due to stratification. Similar to September 2014, July 2015 shows a clear warm anomaly yet also low pH and Ω_{arag} (Fig. 2).

However, during the peak of the MHW in September 2015, subsurface pH was highest (Fig. 3), suggesting that ocean acidification was ameliorated during the height of the MHW. Post-MHW from September 2016 onward, regional pH does not completely return to pre-MHW values. September 2017 is similar to that of September 2014 in that pH is relatively low despite warmer SSTs and stratification. Conversely, September 2019 echoes September 2015, showing strong stratification and elevated aragonite saturate although to a lesser degree.

Subsurface Ω_{arag} is relatively unchanged throughout the seven years except for during the second half of the MHW (i.e. from the peak of the MHW in September 2015 through the end of the MHW in 2016; Fig. 3d). This delayed response of subsurface waters to the MHW may be indicative of the weak influence of the concurrent 2015 El Niño (Jacox et al., 2016; Gentemann et al., 2017) that slowly propagated poleward and reached the central California coastal area in late 2015 (Chao et al., 2017). The El Niño may have caused atypical California Undercurrent contributions and the subsequent central CCS carbonate chemistry response of elevated pH and Ω_{arag}. Regardless of mechanism, subsurface Ω_{arag} during the latter half of the MHW was supersaturated, appearing to ameliorate ocean acidification through the sampling interval.

4.2 *Model comparisons*

 Aragonite saturation approximated from the regional Davis et al. (2018) empirical model largely overestimates Ω_{arag} calculated from bottle parameters, most noticeable in the offshore surface samples (Fig. S1a). For subsurface $\Omega_{arag} > 1$, years 2018 and 2019 (and to a lesser extent 2016 as well), the equation underestimates Ω_{arag} (Fig. S1a and S4b). The underestimation is most clearly seen for July 2018 and 2019 (Fig. 2c & S4b). One possible explanation for Ω_{arag} underestimation in 2018 and 2019 may be that primary productivity elevated pH given that pH is higher than expected for typical temperatures (Fig. S5b). While the modified coefficients of Eqn. 5 capture post-MHW July Ω_{arag} well, Ω_{arag} for June and July during the MHW in 2015 are noticeably overestimated but nonetheless the modified model performs better than the original model for estimating July 2015 Ω_{arag}.

 The original regional empirical model for approximating Ω_{arag} excluded September data due to less robust linear relationship (Davis et al., 2018). September cruises were largely during periods of stratification which Davis et al. (2018) posited could lead to more dissolution from carbonate sediments changing the relationship, a shift in the relative importance of productivity/respiration and/or air-sea exchange. Further, as Davis et al. (2018) notes, seasonal changes in source waters may also change the relationship between temperature, salinity, and dissolved oxygen and Ω_{arag}. During relaxation of upwelling, this may include net northward transport of San Francisco Bay outflows (e.g., Kaplan and Largier, 2006; Largier et al., 2006, 1993). Regardless of mechanism, periods of stronger stratification during more frequent warm anomalies may no longer be limited to just relaxation season such that the model may need careful evaluation sooner than 10 years from calibration.

In addition to regional Ω_{arag} equations coefficients needing revision for increased stratification from warm anomalies moderating upwelling contributions to the euphotic zone, the relationships themselves may require careful analysis to reflect changes in upwelled source waters. Specifically, given that the contribution of the California Undercurrent to upwelled waters necessitates regional equations for Ω_{arag} (Alin et al., 2012; Chhak and Di Lorenzo, 2007; Thomson and Krassovski, 2010), the assumed atypical California Undercurrent contributions to upwelled waters during the MHW suggest that the coefficients likely need revision not only due to increased contribution of anthropogenic CO_2 over time (Alin et al., 2012; Kim et al., 2010), but also due to changes in source water and upwelling characteristics. As such, future work should assess if the relationship between predictor variables and aragonite saturation state has changed.

5. Conclusions

Here we documented seven years of measured bottle carbonate chemistry from 2013-2019 paired with oceanographic parameters from 2004 onward. We observe a delayed amelioration of ocean acidification during the latter half of the 2014-2016 MHW. We posit the elevated subsurface pH and Ωarag during the latter half of the MHW were due to atypical upwelled waters caused by the 2015 El Niño. Lastly, we suggest that regional Ωarag models require re-evaluation in light of warming anomalies impacting coastal upwelling and local modification of waters. This work highlights the added variability of a warming ocean to an already variable coastal upwelling system, and the need for careful application of regional models in a system with more frequent warm anomalies.
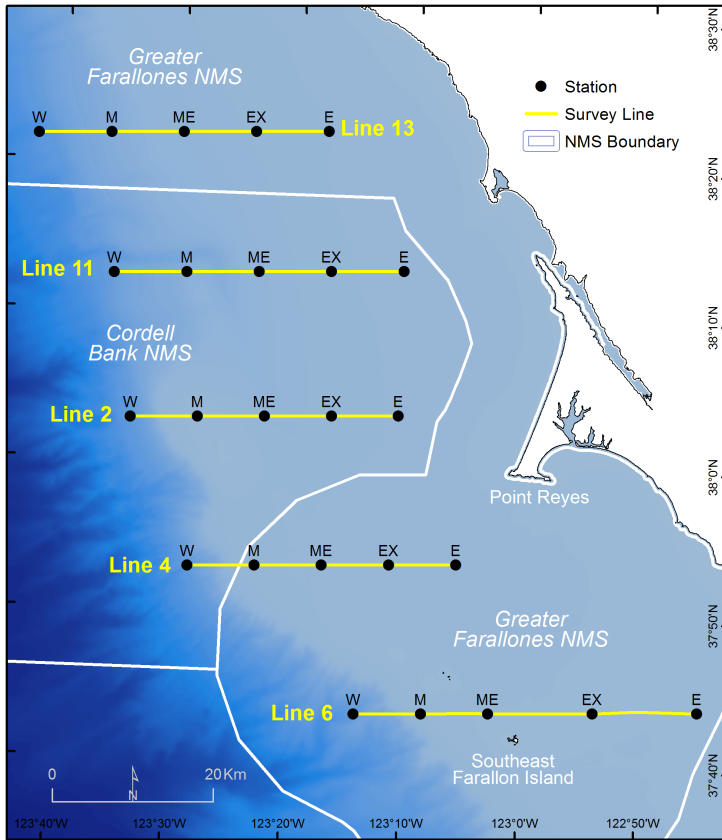
6. Acknowledgments

7. Figures

Figure 1. Map of study region, just north of San Francisco Bay within the north-central California Current System. Yellow lines are survey transects, with black dots indicating the five sampling stations per line. Core lines are 2, 4, and 6, which are surveyed routinely each cruise. Lines 11, 13, and 10 (not pictured, south of line 6) are sampled when weather and ship constraints allow. All stations are shallower then 200 m water depth except for station W of each line which are off the shelf break. Thus near-benthic samples include one sample per line at station W that is mid-water column at 200 m.
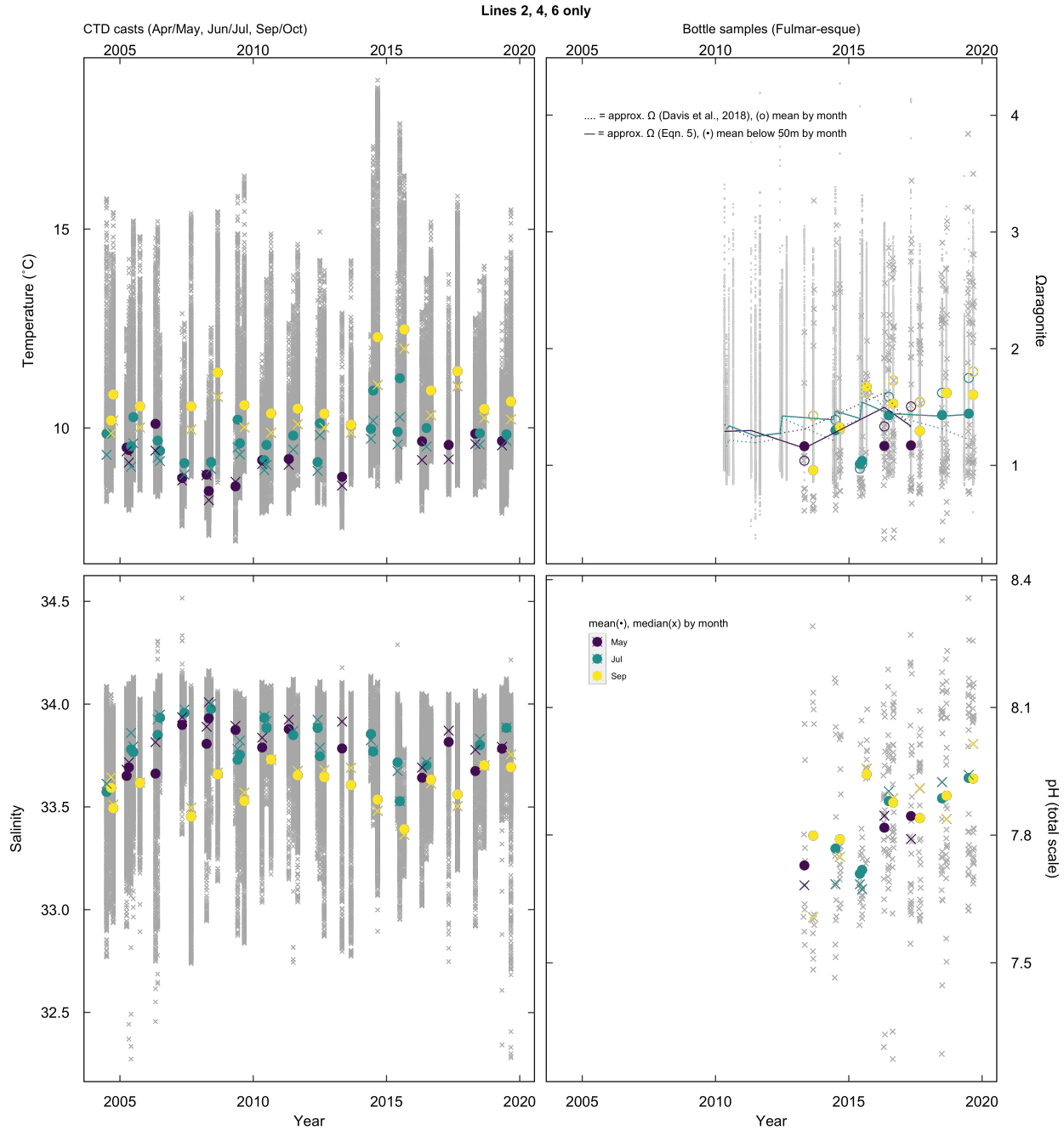
Figure 2. A) *In situ* temperature data from CTD casts at all stations along transect 2, 4, and 6 through time (grey Xs). Colors denote cruise mean (circles) and median (X) for May (purple), June/July (green), and September (yellow). Mean temperatures increase for July of 2009, 2014, and 2015, in addition to mean September temperatures for 2008, 2014, and 2015. B) *In situ* salinity data from CTD casts at all stations along transects 2, 4, and 6 through time (grey Xs) with the same colors as in (A). Salinity decreases in September, most pronounced in 2007, 2009, 2014, 2015, and 2017. C) Aragonite saturation

state calculated from bottle carbonate chemistry measurements (grey Xs) and approximated from Davis et al. (2018) equation using temperature, salinity, and dissolved oxygen measurements from CTD casts (grey points). Colors denote cruise mean Ω_{arag} for full water column (open circles) and subsurface mean (i.e. below 50 m only; filled circles). Colored solid lines correspond to approximated cruise means for subsurface using Eqn. 5, while dotted lines correspond to approximated cruise means for full water column using Davis et al. (2018) model. D) pH measured from discrete water samples at all stations along transects 2, 4, and 6 (grey Xs). Colors denote cruise means (circles) and medians (Xs) same as (A) and (B). pH increases by 0.2 over the seven-year period.
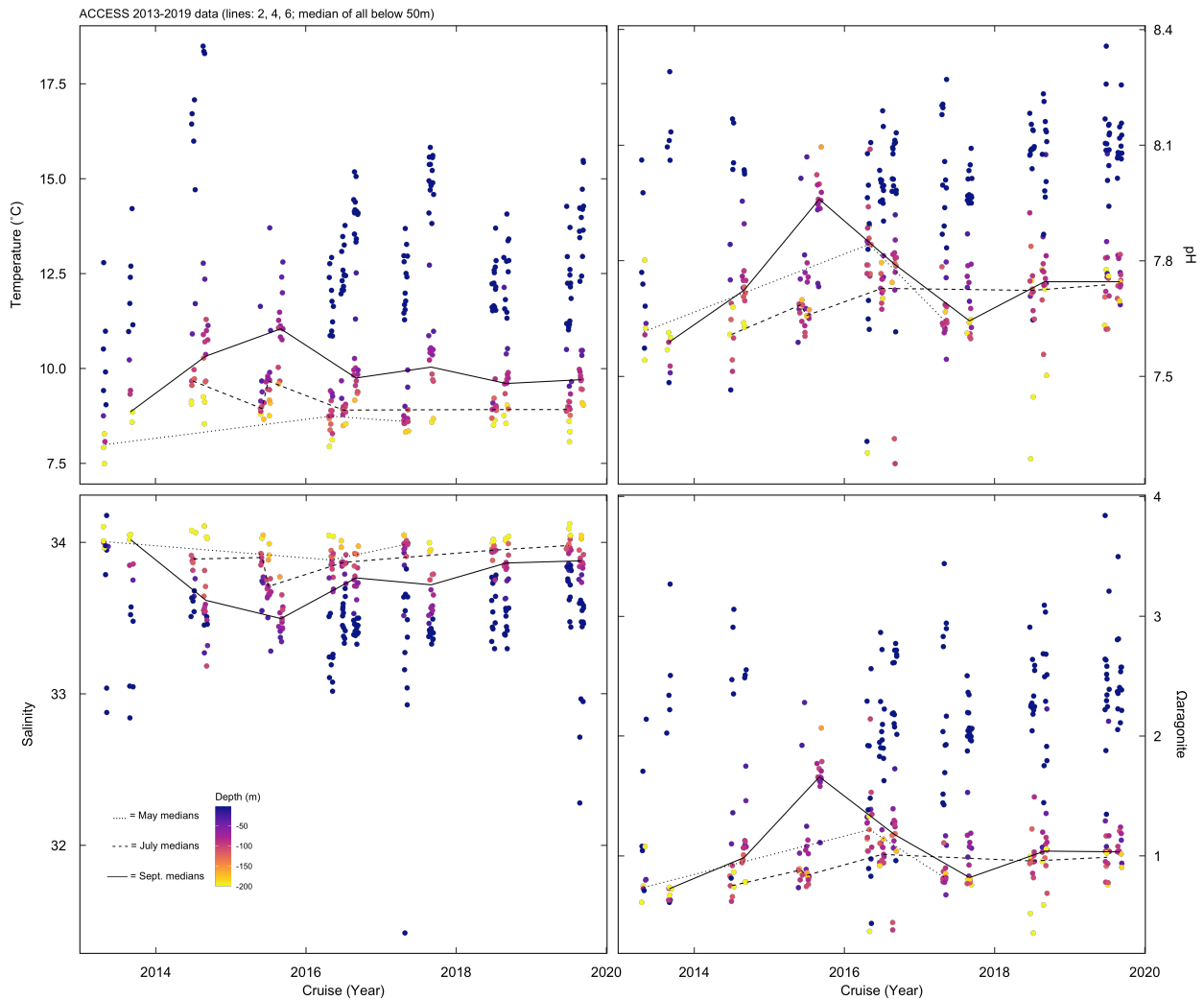
Figure 3. A) Subsurface temperature through time, colored by depth. Cruise medians for subsurface temperature denoted by dashed and solid lines. Median September temperatures from below 50 m were warmer during the heatwave (i.e. 2014 and 2015) than all other years. B) Subsurface salinity through time, colored by depth with lines denoting cruise medians. Median September salinity from below 50 m were fresher during the heatwave than other years. C) Subsurface pH through time, colored by depth with cruise medians denotes by lines. Median pH from below 50 m was elevated for September 2014 and pronouncedly in September 2015 and May 2016 too. D) Subsurface Ω_{arag} through time, colored by depth with lines denoting cruise medians. Aragonite saturation state largely mirrors temporal trends of pH (C).
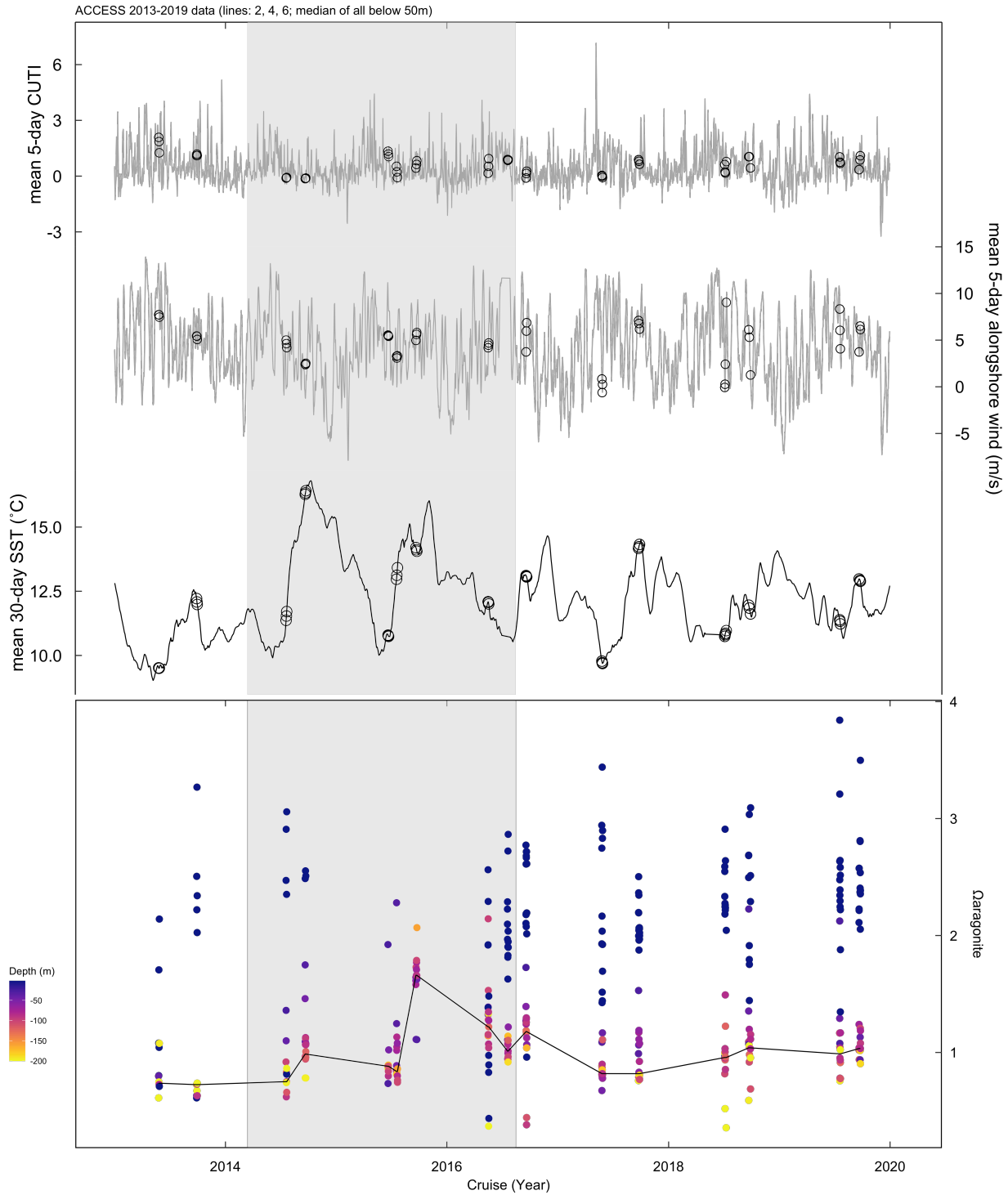
Figure 4. Stratification proxies through time, A) Coastal Upwelling Transport Index 5-day running mean (grey line) with samplings days denoted by black circles, B) same as (A) but for 5-day running mean of alongshore windstress approximation, C) 30-day running mean of sea surface temperature, D) calculated

Ω_{arag} saturation from measured discrete water carbonate chemistry, where color is depth and line denotes median of samples below 50 m. MHW start and end date for coastal California south of Cape Mendocino (Gentemann et al., 2017) denoted by grey rectangle.

8. Table

Parameters	Constants ± standard error	Trained dataset	
Eqn. 1	$\alpha 0 = -41.431 \pm 96.489$ $\alpha T = 8.026 \pm 8.882$ $\alpha S = 1.311 \pm 2.850$ $\alpha DO = 0.445 \pm 0.533$ $\alpha TS = -0.244 \pm 0.263$ $\alpha TDO = -0.049 \pm 0.046$ $\alpha DOS = -0.013 \pm 0.016$ $\alpha TSDO = 0.001 \pm 0.001$	2013-2015 inclusive of September and surface samples	
Eqn. 2	$\alpha 0 = 115.5 \pm 93.54$ $\alpha T = -14.60 \pm 9.898$ $\alpha S = -3.350 \pm 2.769$ $\alpha DO = 0.123 \pm 0.499$ $\alpha TS = 0.427 \pm 0.294$ $\alpha TDO = 0.015 \pm 0.046$ $\alpha DOS = -0.004 \pm 0.015$ $\alpha TSDO = 0.000 \pm 0.001$	2013-2015 excluding September	
Eqn. 3	$\alpha 0 = 46.681 \pm 82.499$ $\alpha T = -7.519 \pm 8.510$ $\alpha S = -1.328 \pm 2.422$ $\alpha DO = 0.320 \pm 0.356$ $\alpha TS = 0.218 \pm 0.250$ $\alpha TDO = -0.007 \pm 0.033$ $\alpha DOS = -0.010 \pm 0.010$ $\alpha TSDO = 0.000 \pm 0.001$	2013-2015 below 50 m and excluding September	
Eqn. 4	$\alpha 0 = 61.995 \pm 70.680$ $\alpha T = -7.132 \pm 7.085$ $\alpha S = -1.789 \pm 2.084$ $\alpha DO = 0.2844 \pm 0.468$ $\alpha TS = 0.208 \pm 0.210$ $\alpha TDO = -0.019 \pm 0.044$ $\alpha DOS = -0.0086 \pm 0.014$ $\alpha TSDO = 0.0006 \pm 0.001$	2013-2019 below 50 m	
Eqn. 5	$\alpha 0 = 435.114 \pm 136.697$ $\alpha T = -46.241 \pm 14.728$ $\alpha S = -12.714 \pm 4.019$ $\alpha DO = -0.871 \pm 0.582$ $\alpha TS = 1.353 \pm 0.434$ $\alpha TDO = 0.088 \pm 0.060$ $\alpha DOS = 0.025 \pm 0.017$ $\alpha TSDO = -0.0025 \pm 0.0018$	2013-2019 below 50 m and excluding September	

Table 1. New coefficients for Davis et al. (2018) north-central CCS Ω_{arag} equation. All modified models use the same parameters and interaction terms as the preferred Davis et al. (2018) equation: T, S, DO, T $*$ S, T $*$ DO, S $*$ DO, T $*$ S $*$ DO. Eqn. 1 is trained on all data from 2013-2015 including September and surface bottle data, Eqn. 2 is trained on all 2013-2015 except for September data, Eqn. 3 is trained on only subsurface 2013-2015 data and excluding September data too. Eqn 4 is trained on all 2013-2019 subsurface data from below 50 m as is Eqn. 5 with the added exclusion of September data too.

9. Supplemental Figures
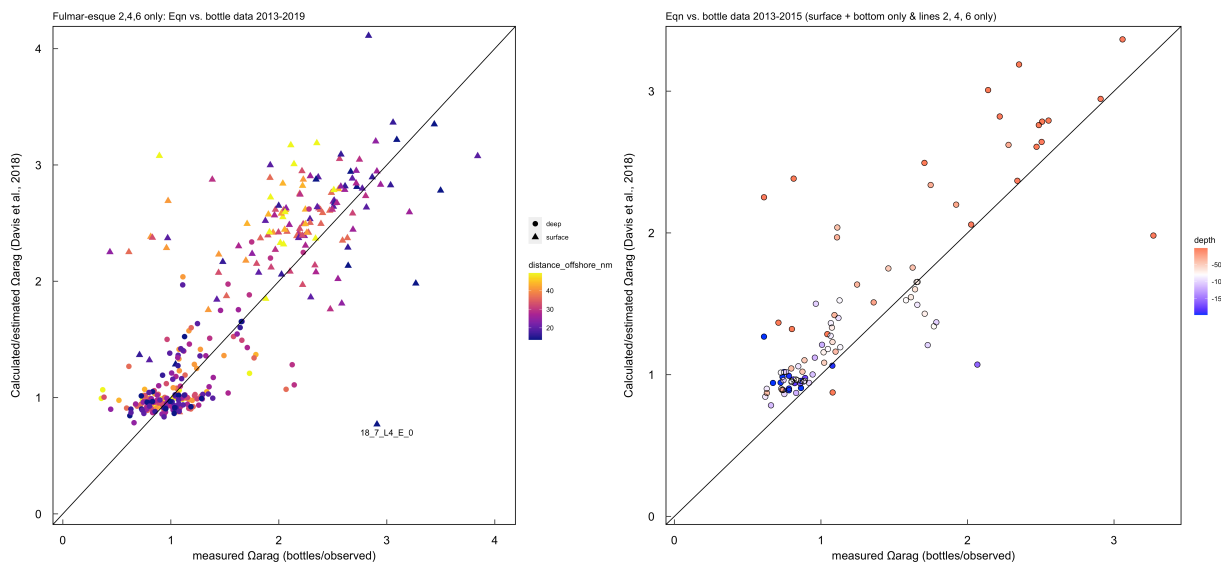
Figure S1. Correlation between calculated and estimated Ω_{arag} as determined by discrete water sample measurements and using the Davis et al. (2018) model, respectively. Ideal fit (1:1) is shown as black line. A) full carbonate chemistry dataset presented herein from 2013 to 2019 colored by distance offshore and symbols reflecting surface or subsurface water samples. The furthest offshore surface samples are routinely overestimated (yellow triangles). B) subset of carbonate chemistry data (n = 94) that were collected and measured during the same period and region for which the Davis et al. (2018) algorithm was developed (i.e. core transect lines 2, 4, and 6 from 2013 to 2015 only). The reader is referred to Fig. 2 of Davis et al. (2018) for comparison.
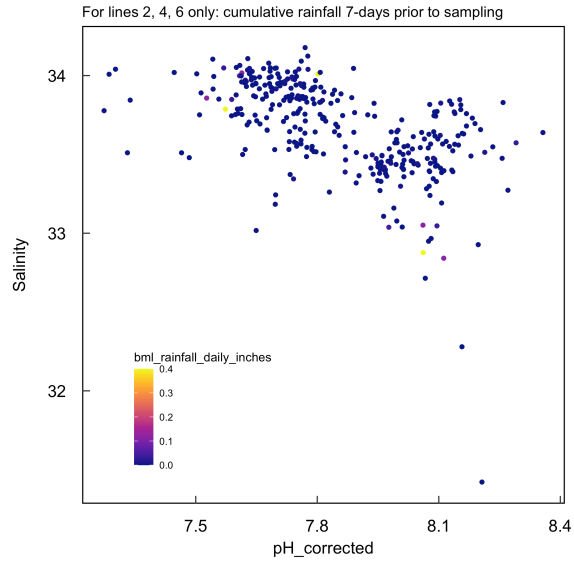
Figure S2 Salinity and pH correlation with precipitation events for one week prior to sampling (i.e. sum of all inches of rain, but does not include an precipitation on day of sampling).
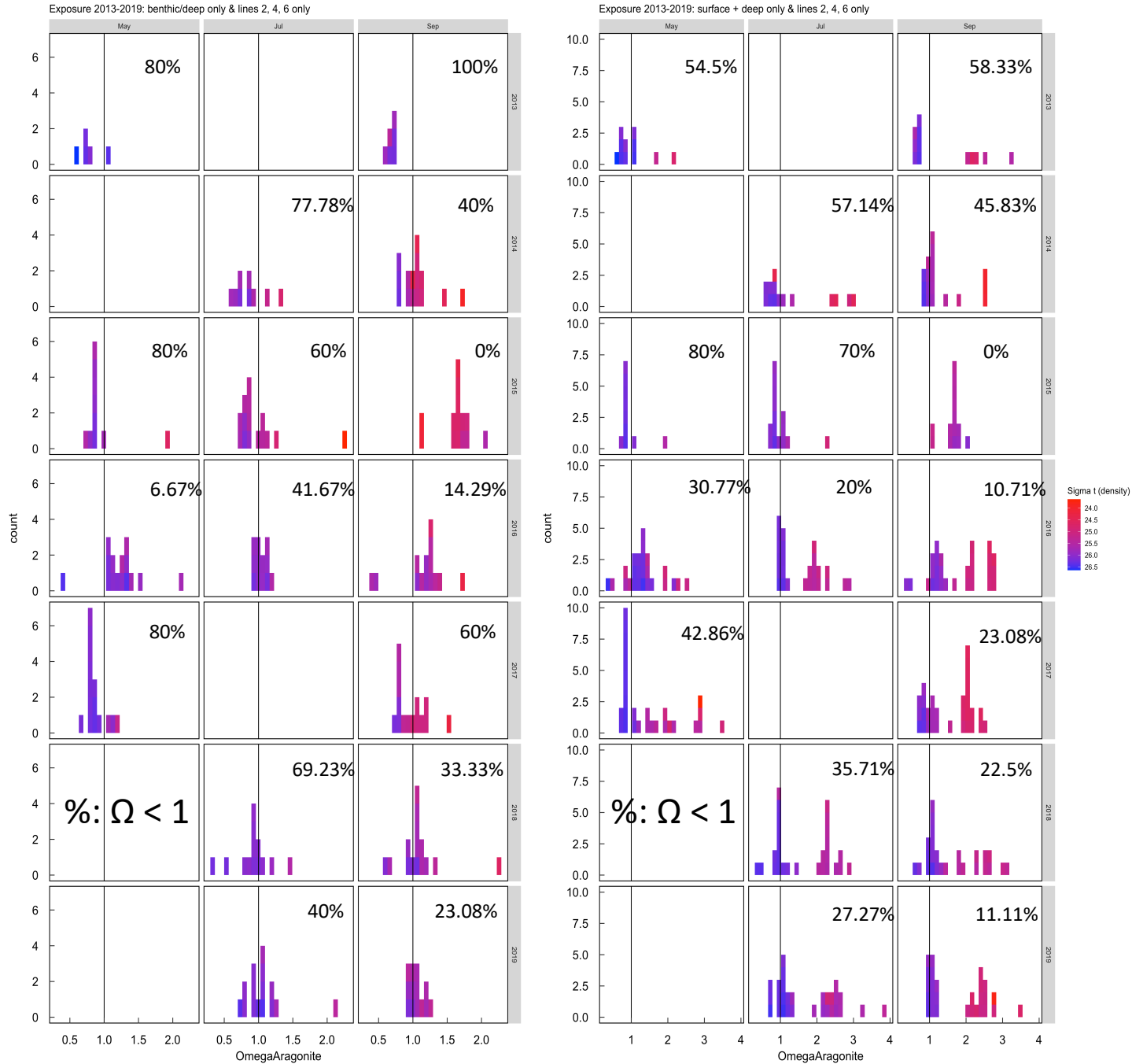
Figure S3. Histograms of aragonite saturation states by cruise, where color denotes density of the water (sigma t) and vertical line demarcates undersaturation. Percentage of observations that are undersaturated for each cruise is noted on its respective histogram. A) subsurface samples only (n=201), B) all samples (n=339)
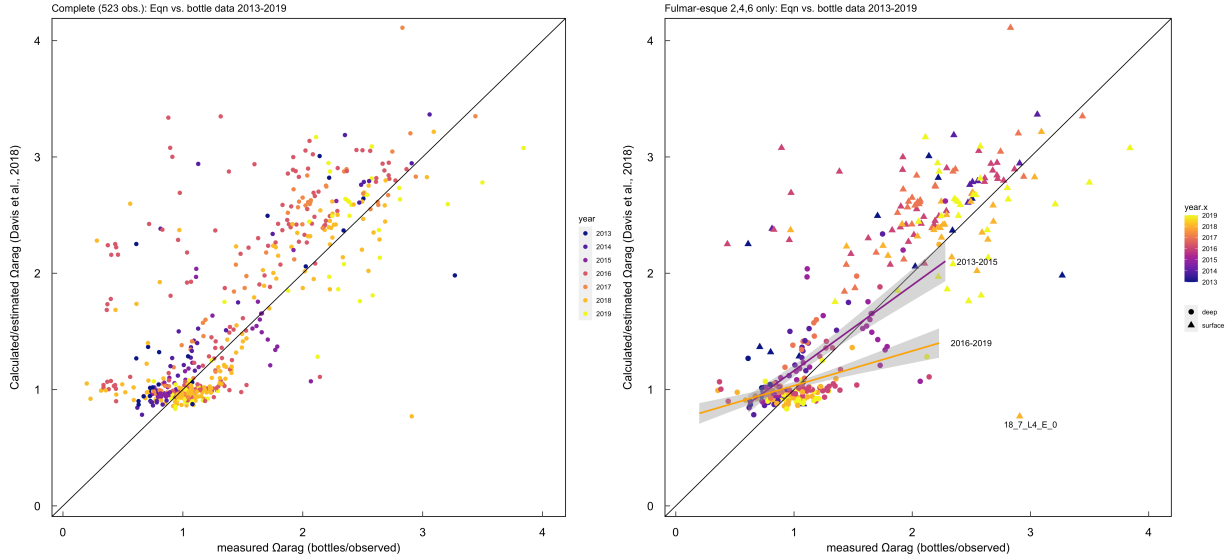
Figure S4 Aragonite saturation calculated from bottle measurements versus Ωarag approximated from Davis et al. (2018) algorithm. A) complete dataset that includes multiple water column bottle samples for May 2016 and July 2018. B) subset of data with just surface and subsurface water samples for Shimada cruises (i.e. May 2016 and July 2018) and only lines 2-6, colored by year. Purple line indicates deep/subsurface samples only relationship for 2013-2015, orange line indicates deep/subsurface observed versus approximated relationship for 2016-2019. For 2016-2019, subsurface $Ω_{arag}$ are mostly underestimated when $Ω_{arag} > 1$.
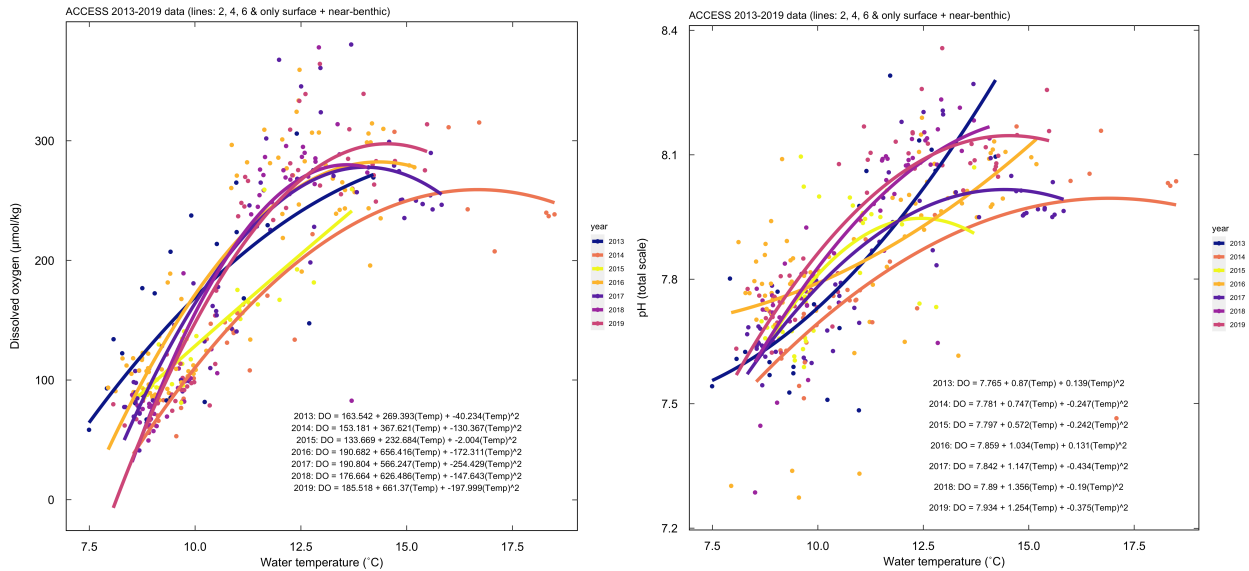
Figure S5 Temperature and A) dissolved oxygen and B) pH relationships by year. Warm colors are from the NE Pacific MHW, purples are after the MHW and blue is from prior to the MHW. Dissolved oxygen values for 2014 and 2015 are lower than other years for a given temperature. While 2015 also shows lower pH values for a given temperature, the same pattern is not as evident for 2014.

Figure S6 Same as Fig. 2 in main text, but also includes pCO_2 calculated from pH and alkalinity using *SeaCarb*, and dissolved oxygen measurements from CTD casts with a dissolved oxygen sensor. F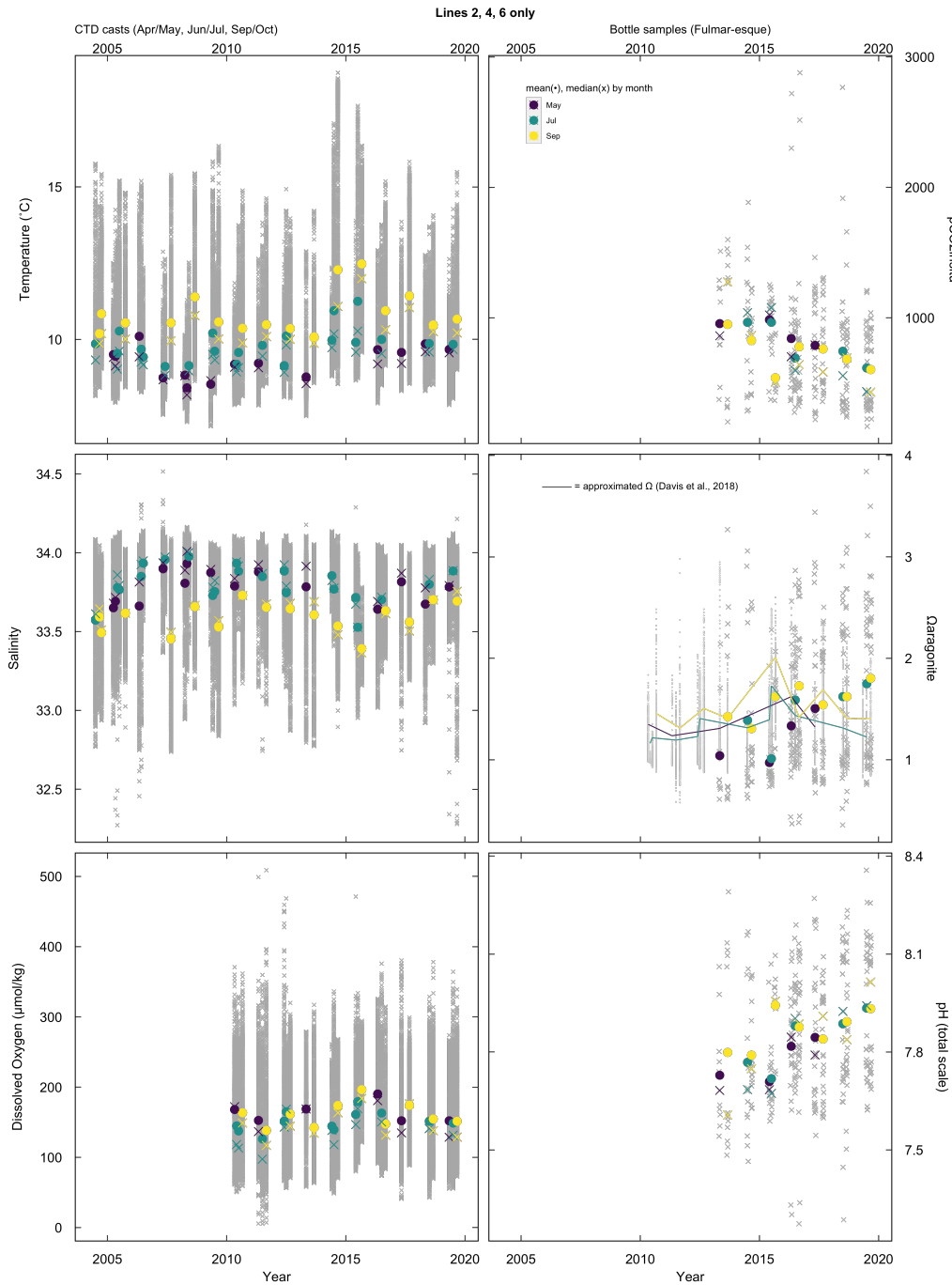rom 2013 onward, September DO trend is inverse of September salinity. Similarly, pH and pCO_2 trends are inverse of each other.

10. References

Alin, S.R., Feely, R.A., Dickson, A.G., Hernández-Ayón, J.M., Juranek, L.W., Ohman, M.D., Goericke, R., 2012. Robust empirical relationships for estimating the carbonate system in the southern California Current System and application to CalCOFI hydrographic cruise data (2005-2011): CCS pH and carbonate saturation models. J. Geophys. Res. Oceans 117, n/a-n/a. https://doi.org/10.1029/2011JC007511

Bakun, A., 1990. Coastal Ocean Upwelling. Science 247, 198–201. https://doi.org/10.1126/science.247.4939.198

Bakun, A., Black, B.A., Bograd, S.J., García-Reyes, M., Miller, A.J., Rykaczewski, R.R., Sydeman, W.J., 2015. Anticipated Effects of Climate Change on Coastal Upwelling Ecosystems. Curr. Clim. Change Rep. 1, 85–93. https://doi.org/10.1007/s40641-015-0008-4

Beardsley, R.C., Lentz, S.J., 1987. The Coastal Ocean Dynamics Experiment collection: An introduction. J. Geophys. Res. 92, 1455. https://doi.org/10.1029/JC092iC02p01455

Bond, N.A., Cronin, M.F., Freeland, H., Mantua, N., 2015. Causes and impacts of the 2014 warm anomaly in the NE Pacific: 2014 WARM ANOMALY IN THE NE PACIFIC. Geophys. Res. Lett. 42, 3414–3420. https://doi.org/10.1002/2015GL063306

Botsford, L.W., Lawrence, C.A., Dever, E.P., Hastings, A., Largier, J., 2006. Effects of variable winds on biological productivity on continental shelves in coastal upwelling systems. Deep Sea Res. Part II Top. Stud. Oceanogr. 53, 3116–3140. https://doi.org/10.1016/j.dsr2.2006.07.011

Caldeira, K., Wickett, M.E., 2003. Anthropogenic carbon and ocean pH. Nature 425, 365–365. https://doi.org/10.1038/425365a

Canadell, J.G., Le Quéré, C., Raupach, M.R., Field, C.B., Buitenhuis, E.T., Ciais, P., Conway, T.J., Gillett, N.P., Houghton, R.A., Marland, G., 2007. Contributions to accelerating atmospheric CO_2 growth from economic activity, carbon intensity, and efficiency of natural sinks. Proc. Natl. Acad. Sci. 104, 18866–18870. https://doi.org/10.1073/pnas.0702737104

Cavole, L., Demko, A., Diner, R., Giddings, A., Koester, I., Pagniello, C., Paulsen, M.-L., Ramirez-Valdez, A., Schwenck, S., Yen, N., Zill, M., Franks, P., 2016. Biological Impacts of the 2013–2015 Warm-Water Anomaly in the Northeast Pacific: Winners, Losers, and the Future. Oceanography 29. https://doi.org/10.5670/oceanog.2016.32

Chan, F., Barth, J.A., Blanchette, C.A., Byrne, R.H., Chavez, F., Cheriton, O., Feely, R.A., Friederich, G., Gaylord, B., Gouhier, T., Hacker, S., Hill, T., Hofmann, G., McManus, M.A., Menge, B.A.,

Nielsen, K.J., Russell, A., Sanford, E., Sevadjian, J., Washburn, L., 2017. Persistent spatial structuring of coastal ocean acidification in the California Current System. Sci. Rep. 7, 2526. https://doi.org/10.1038/s41598-017-02777-y

Chao, Y., Farrara, J.D., Bjorkstedt, E., Chai, F., Chavez, F., Rudnick, D.L., Enright, W., Fisher, J.L., Peterson, W.T., Welch, G.F., Davis, C.O., Dugdale, R.C., Wilkerson, F.P., Zhang, H., Zhang, Y., Ateljevich, E., 2017. The origins of the anomalous warming in the C alifornia coastal ocean and S an F rancisco B ay during 2014–2016. J. Geophys. Res. Oceans 122, 7537–7557. https://doi.org/10.1002/2017JC013120

Chavez, F.P., Pennington, J.T., Castro, C.G., Ryan, J.P., Michisaki, R.P., Schlining, B., Walz, P., Buck, K.R., McFadyen, A., Collins, C.A., 2002. Biological and chemical consequences of the 1997–1998 El Niño in central California waters. Prog. Oceanogr., Observations of the 1997-98 El Nino along the West Coast of North America 54, 205–232. https://doi.org/10.1016/S0079-6611(02)00050-2

Chhak, K., Di Lorenzo, E., 2007. Decadal variations in the California Current upwelling cells. Geophys. Res. Lett. 34, L14604. https://doi.org/10.1029/2007GL030203

Davis, C.V., Hewett, K., Hill, T.M., Largier, J.L., Gaylord, B., Jahncke, J., 2018. Reconstructing Aragonite Saturation State Based on an Empirical Relationship for Northern California. Estuaries Coasts 41, 2056–2069. https://doi.org/10.1007/s12237-018-0372-0

Dever, E.P., Lentz, S.J., 1994. Heat and salt balances over the northern California shelf in winter and spring. J. Geophys. Res. Oceans 99, 16001–16017. https://doi.org/10.1029/94JC01228

Di Lorenzo, E., Mantua, N., 2016. Multi-year persistence of the 2014/15 North Pacific marine heatwave. Nat. Clim. Change 6, 1042–1047. https://doi.org/10.1038/nclimate3082

Dickson, A.G., Sabine, C.L., Christian, J.R. (Eds.), 2007. SOP 6b Determination of the pH of sea water using the indicator dye m-cresol purple., in: Guide to Best Practices for Ocean CO2 Measurements, PICES Special Publication. North Pacific Marine Science Organization, Sidney, BC.

Dorman, C.E., Winant, C.D., 1995. Buoy observations of the atmosphere along the west coast of the United States, 1981–1990. J. Geophys. Res. 100, 16029. https://doi.org/10.1029/95JC00964

Feely, R., Doney, S., Cooley, S., 2009. Ocean Acidification: Present Conditions and Future Changes in a High-CO2 World. Oceanography 22, 36–47. https://doi.org/10.5670/oceanog.2009.95

Feely, R.A., Alin, S.R., Carter, B., Bednaršek, N., Hales, B., Chan, F., Hill, T.M., Gaylord, B., Sanford, E., Byrne, R.H., Sabine, C.L., Greeley, D., Juranek, L., 2016. Chemical and biological impacts of ocean acidification along the west coast of North America. Estuar. Coast. Shelf Sci. 183, 260–270. https://doi.org/10.1016/j.ecss.2016.08.043

Feely, R.A., Sabine, C.L., Hernandez-Ayon, J.M., Ianson, D., Hales, B., 2008. Evidence for Upwelling of Corrosive "Acidified" Water onto the Continental Shelf. Science 320, 1490–1492. https://doi.org/10.1126/science.1155676

Feely, R.A., Sabine, C.L., Lee, K., Berelson, W., Kleypas, J., Fabry, V.J., Millero, F.J., 2004. Impact of Anthropogenic CO$_2$ on the CaCO$_3$ System in the Oceans. Science 305, 362–366. https://doi.org/10.1126/science.1097329

Fumo, J.T., Carter, M.L., Flick, R.E., Rasmussen, L.L., Rudnick, D.L., Iacobellis, S.F., 2020. Contextualizing Marine Heatwaves in the Southern California Bight Under Anthropogenic Climate Change. J. Geophys. Res. Oceans 125. https://doi.org/10.1029/2019JC015674

García-Reyes, M., Largier, J., 2010. Observations of increased wind-driven coastal upwelling off central California. J. Geophys. Res. 115, C04011. https://doi.org/10.1029/2009JC005576

García-Reyes, M., Largier, J.L., 2012. Seasonality of coastal upwelling off central and northern California: New insights, including temporal and spatial variability: Upwelling Seasonality off California. J. Geophys. Res. Oceans 117, n/a-n/a. https://doi.org/10.1029/2011JC007629

García-Reyes, M., Sydeman, W.J., Schoeman, D.S., Rykaczewski, R.R., Black, B.A., Smit, A.J., Bograd, S.J., 2015. Under Pressure: Climate Change, Upwelling, and Eastern Boundary Upwelling Ecosystems. Front. Mar. Sci. 2. https://doi.org/10.3389/fmars.2015.00109

Gattuso, J.-P., Epitalon, J.-M., Lavigne, H., Orr, J., 2020. SeaCarb: seawater carbonate chemistry with R.

Gentemann, C.L., Fewings, M.R., García-Reyes, M., 2017. Satellite sea surface temperatures along the West Coast of the United States during the 2014-2016 northeast Pacific marine heat wave: Coastal SSTs During "the Blob." Geophys. Res. Lett. 44, 312–319. https://doi.org/10.1002/2016GL071039

Gruber, N., Hauri, C., Lachkar, Z., Loher, D., Frölicher, T.L., Plattner, G.-K., 2012. Rapid Progression of Ocean Acidification in the California Current System. Science 337, 220–223. https://doi.org/10.1126/science.1216773

Halle, C.M., Largier, J.L., 2011. Surface circulation downstream of the Point Arena upwelling center. Cont. Shelf Res. 31, 1260–1272. https://doi.org/10.1016/j.csr.2011.04.007

Halliwell Jr., G.R., Allen, J.S., 1987. The large-scale coastal wind field along the west coast of North America, 1981–1982. J. Geophys. Res. Oceans 92, 1861–1884. https://doi.org/10.1029/JC092iC02p01861

Harris, K.E., DeGrandpre, M.D., Hales, B., 2013. Aragonite saturation state dynamics in a coastal upwelling zone. Geophys. Res. Lett. 40, 2720–2725. https://doi.org/10.1002/grl.50460

Hartmann, D.L., 2015. Pacific sea surface temperature and the winter of 2014. Geophys. Res. Lett. 42, 1894–1902. https://doi.org/10.1002/2015GL063083

Hauri, C., Gruber, N., Vogt, M., Doney, S.C., Feely, R.A., Lachkar, Z., Leinweber, A., McDonnell, A.M.P., Munnich, M., Plattner, G.-K., 2013. Spatiotemporal variability and long-term trends of ocean acidification in the California Current System. Biogeosciences 10, 193–216. https://doi.org/10.5194/bg-10-193-2013

Huyer, A., 1983. Coastal upwelling in the California current system. Prog. Oceanogr. 12, 259–284. https://doi.org/10.1016/0079-6611(83)90010-1

Huyer, A., Barth, J.A., Kosro, P.M., Shearman, R.K., Smith, R.L., 1998. Upper-ocean water mass characteristics of the California current, Summer 1993. Deep Sea Res. Part II Top. Stud. Oceanogr. 45, 1411–1442. https://doi.org/10.1016/S0967-0645(98)80002-7

Huyer, A., Kosro, P.M., Fleischbein, J., Ramp, S.R., Stanton, T., Washburn, L., Chavez, F.P., Cowles, T.J., Pierce, S.D., Smith, R.L., 1991. Currents and water masses of the Coastal Transition Zone off northern California, June to August 1988. J. Geophys. Res. 96, 14809. https://doi.org/10.1029/91JC00641

Jacox, M.G., Edwards, C.A., Hazen, E.L., Bograd, S.J., 2018. Coastal Upwelling Revisited: Ekman, Bakun, and Improved Upwelling Indices for the U.S. West Coast. J. Geophys. Res. Oceans 123, 7332–7350. https://doi.org/10.1029/2018JC014187

Jacox, M.G., Hazen, E.L., Zaba, K.D., Rudnick, D.L., Edwards, C.A., Moore, A.M., Bograd, S.J., 2016. Impacts of the 2015-2016 El Niño on the California Current System: Early assessment and comparison to past events: 2015-2016 El Niño Impact in the CCS. Geophys. Res. Lett. 43, 7072–7080. https://doi.org/10.1002/2016GL069716

Jiang, L.-Q., Carter, B.R., Feely, R.A., Lauvset, S.K., Olsen, A., 2019. Surface ocean pH and buffer capacity: past, present and future. Sci. Rep. 9, 18624. https://doi.org/10.1038/s41598-019-55039-4

Juranek, L.W., Feely, R.A., Peterson, W.T., Alin, S.R., Hales, B., Lee, K., Sabine, C.L., Peterson, J., 2009. A novel method for determination of aragonite saturation state on the continental shelf of central Oregon using multi-parameter relationships with hydrographic data. Geophys. Res. Lett. 36, L24601. https://doi.org/10.1029/2009GL040778

Kaplan, D.M., Largier, J., 2006. HF radar-derived origin and destination of surface waters off Bodega Bay, California. Deep Sea Res. Part II Top. Stud. Oceanogr. 53, 2906–2930. https://doi.org/10.1016/j.dsr2.2006.07.012

Khatiwala, S., Tanhua, T., Mikaloff Fletcher, S., Gerber, M., Doney, S.C., Graven, H.D., Gruber, N., McKinley, G.A., Murata, A., Ríos, A.F., Sabine, C.L., 2013. Global ocean storage of anthropogenic carbon. Biogeosciences 10, 2169–2191. https://doi.org/10.5194/bg-10-2169-2013

Kim, T.-W., Lee, K., Feely, R.A., Sabine, C.L., Chen, C.-T.A., Jeong, H.J., Kim, K.Y., 2010. Prediction of Sea of Japan (East Sea) acidification over the past 40 years using a multiparameter regression model: SEA OF JAPAN (EAST SEA) ACIDIFICATION. Glob. Biogeochem. Cycles 24, n/a-n/a. https://doi.org/10.1029/2009GB003637

Kleypas, J.A., Buddemeier, R.W., Archer, D., Gattuso, J.-P., Langdon, C., Opdyke, B.N., 1999. Geochemical Consequences of Increased Atmospheric Carbon Dioxide on Coral Reefs. Science 284, 118–120. https://doi.org/10.1126/science.284.5411.118

Largier, J.L., Lawrence, C.A., Roughan, M., Kaplan, D.M., Dever, E.P., Dorman, C.E., Kudela, R.M., Bollens, S.M., Wilkerson, F.P., Dugdale, R.C., Botsford, L.W., Garfield, N., Kuebel Cervantes, B., Koračin, D., 2006. WEST: A northern California study of the role of wind-driven transport in the productivity of coastal plankton communities. Deep Sea Res. Part II Top. Stud. Oceanogr. 53, 2833–2849. https://doi.org/10.1016/j.dsr2.2006.08.018

Largier, J.L., Magnell, B.A., Winant, C.D., 1993. Subtidal circulation over the northern California shelf. J. Geophys. Res. 98, 18147. https://doi.org/10.1029/93JC01074

Le Quéré, C., Andrew, R.M., Friedlingstein, P., Sitch, S., Hauck, J., Pongratz, J., Pickers, P.A., Korsbakken, J.I., Peters, G.P., Canadell, J.G., Arneth, A., Arora, V.K., Barbero, L., Bastos, A., Bopp, L., Chevallier, F., Chini, L.P., Ciais, P., Doney, S.C., Gkritzalis, T., Goll, D.S., Harris, I.,

Haverd, V., Hoffman, F.M., Hoppema, M., Houghton, R.A., Hurtt, G., Ilyina, T., Jain, A.K., Johannessen, T., Jones, C.D., Kato, E., Keeling, R.F., Goldewijk, K.K., Landschützer, P., Lefèvre, N., Lienert, S., Liu, Z., Lombardozzi, D., Metzl, N., Munro, D.R., Nabel, J.E.M.S., Nakaoka, S., Neill, C., Olsen, A., Ono, T., Patra, P., Peregon, A., Peters, W., Peylin, P., Pfeil, B., Pierrot, D., Poulter, B., Rehder, G., Resplandy, L., Robertson, E., Rocher, M., Rödenbeck, C., Schuster, U., Schwinger, J., Séférian, R., Skjelvan, I., Steinhoff, T., Sutton, A., Tans, P.P., Tian, H., Tilbrook, B., Tubiello, F.N., van der Laan-Luijkx, I.T., van der Werf, G.R., Viovy, N., Walker, A.P., Wiltshire, A.J., Wright, R., Zaehle, S., Zheng, B., 2018. Global Carbon Budget 2018. Earth Syst. Sci. Data 10, 2141–2194. https://doi.org/10.5194/essd-10-2141-2018

Leising, A.W., Schroeder, I.D., Bograd, S.J., Abell, J., Durazo, R., Gaxiola-Castro, G., Bjorkstedt, E.P., Field, J., Sakuma, K., Robertson, R.R., Goericke, R., Peterson, W.T., Brodeur, R., Barceló, C., Auth, T.D., Daly, E.A., Suryan, R.M., Gladics, A.J., Porquez, J.M., McClatchie, S., Weber, E.D., Watson, W., Santora, J.A., Sydeman, W.J., Melin, S.R., Chavez, F.P., Golightly, R.T., Schneider, S.R., Fisher, J., Morgan, C., Bradley, R., Warybok, P., 2015. State of the California Current 2014-15: Impacts of the Warm-Water "Blob" (No. 56), California Cooperative Oceanic Fisheries Investigations Reports. Scripps Institution of Oceanography.

Lilly, L.E., Send, U., Lankhorst, M., Martz, T.R., Feely, R.A., Sutton, A.J., Ohman, M.D., 2019. Biogeochemical Anomalies at Two Southern California Current System Moorings During the 2014–2016 Warm Anomaly-El Niño Sequence. J. Geophys. Res. Oceans 124, 6886–6903. https://doi.org/10.1029/2019JC015255

Lima, F.P., Wethey, D.S., 2012. Three decades of high-resolution coastal sea surface temperatures reveal more than warming. Nat. Commun. 3, 704. https://doi.org/10.1038/ncomms1713

Lueker, T.J., Dickson, A.G., Keeling, C.D., 2000. Ocean pCO2 calculated from dissolved inorganic carbon, alkalinity, and equations for K1 and K2: validation based on laboratory measurements of CO2 in gas and seawater at equilibrium. Mar. Chem. 70, 105–119. https://doi.org/10.1016/S0304-4203(00)00022-0

Mantua, N.J., Hare, S.R., Zhang, Y., Wallace, J.M., Francis, R.C., 1997. A Pacific Interdecadal Climate Oscillation with Impacts on Salmon Production*. Bull. Am. Meteorol. Soc. 78, 1069–1080. https://doi.org/10.1175/1520-0477(1997)078<1069:APICOW>2.0.CO;2

McCabe, R.M., Hickey, B.M., Kudela, R.M., Lefebvre, K.A., Adams, N.G., Bill, B.D., Gulland, F.M.D., Thomson, R.E., Cochlan, W.P., Trainer, V.L., 2016. An unprecedented coastwide toxic algal bloom linked to anomalous ocean conditions. Geophys. Res. Lett. 43, 10,366-10,376. https://doi.org/10.1002/2016GL070023

Nelson, C.Scott., 1976. Wind stress and wind stress curl over the California current. Naval Postgraduate School, Monterey, California. https://doi.org/10.5962/bhl.title.60783

Norton, J.G., McLain, D.R., 1994. Diagnostic patterns of seasonal and interannual temperature variation off the west coast of the United States: Local and remote large-scale atmospheric forcing. J. Geophys. Res. 99, 16019. https://doi.org/10.1029/94JC01170

Orr, J.C., Fabry, V.J., Aumont, O., Bopp, L., Doney, S.C., Feely, R.A., Gnanadesikan, A., Gruber, N., Ishida, A., Joos, F., Key, R.M., Lindsay, K., Maier-Reimer, E., Matear, R., Monfray, P., Mouchet, A., Najjar, R.G., Plattner, G.-K., Rodgers, K.B., Sabine, C.L., Sarmiento, J.L., Schlitzer, R., Slater, R.D., Totterdell, I.J., Weirig, M.-F., Yamanaka, Y., Yool, A., 2005. Anthropogenic ocean

acidification over the twenty-first century and its impact on calcifying organisms. Nature 437, 681–686. https://doi.org/10.1038/nature04095

Papastephanou, K.M., Bollens, S.M., Slaughter, A.M., 2006. Cross-shelf distribution of copepods and the role of event-scale winds in a northern California upwelling zone. Deep Sea Res. Part II Top. Stud. Oceanogr. 53, 3078–3098. https://doi.org/10.1016/j.dsr2.2006.07.014

Pauly, D., Christensen, V., 1995. Primary production required to sustain global fisheries. Nature 374, 255–257. https://doi.org/10.1038/374255a0

Peterson, W.T., Fisher, J.L., Strub, P.T., Du, X., Risien, C., Peterson, J., Shaw, C.T., 2017. The pelagic ecosystem in the N orthern C alifornia C urrent off O regon during the 2014–2016 warm anomalies within the context of the past 20 years. J. Geophys. Res. Oceans 122, 7267–7290. https://doi.org/10.1002/2017JC012952

Peterson, W.T., Robert, M., Bond, N.A., 2015. The warm Blob continues to dominate the ecosystem of the northern California Current. PICES Press 23, 44–46.

Proye, A., Gattuso, J.-P., 2003. Seacarb, an R package to calculate parameters of the seawater carbonate system.

Sabine, C.L., Feely, R.A., Gruber, N., Key, R.M., Lee, K., Bullister, J.L., Wanninkhof, R., Wong, C.S., Wallace, D.W.R., Tilbrook, B., Millero, F.J., Peng, T.-H., Kozyr, A., Ono, T., Rios, A.F., 2004. The Oceanic Sink for Anthropogenic CO$_2$. Science 305, 367–371. https://doi.org/10.1126/science.1097403

Santora, J.A., Ralston, S., Sydeman, W.J., 2011. Spatial organization of krill and seabirds in the central California Current. ICES J. Mar. Sci. 68, 1391–1402. https://doi.org/10.1093/icesjms/fsr046

Seabra, R., Varela, R., Santos, A.M., Gómez-Gesteira, M., Meneghesso, C., Wethey, D.S., Lima, F.P., 2019. Reduced Nearshore Warming Associated With Eastern Boundary Upwelling Systems. Front. Mar. Sci. 6, 104. https://doi.org/10.3389/fmars.2019.00104

Snyder, M.A., Sloan, L.C., Diffenbaugh, N.S., Bell, J.L., 2003. Future climate change and upwelling in the California Current: FUTURE CLIMATE CHANGE AND UPWELLING IN THE CALIFORNIA CURRENT. Geophys. Res. Lett. 30. https://doi.org/10.1029/2003GL017647

Song, H., Miller, A.J., Cornuelle, B.D., Di Lorenzo, E., 2011. Changes in upwelling and its water sources in the California Current System driven by different wind forcing. Dyn. Atmospheres Oceans 52, 170–191. https://doi.org/10.1016/j.dynatmoce.2011.03.001

Sydeman, W.J., García-Reyes, M., Schoeman, D.S., Rykaczewski, R.R., Thompson, S.A., Black, B.A., Bograd, S.J., 2014. Climate change and wind intensification in coastal upwelling ecosystems. Science 345, 77–80. https://doi.org/10.1126/science.1251635

Thomson, R.E., Krassovski, M.V., 2010. Poleward reach of the California Undercurrent extension. J. Geophys. Res. 115, C09027. https://doi.org/10.1029/2010JC006280

Varela, R., Rodríguez-Díaz, L., de Castro, M., Gómez-Gesteira, M., 2021. Influence of Eastern Upwelling systems on marine heatwaves occurrence. Glob. Planet. Change 196, 103379. https://doi.org/10.1016/j.gloplacha.2020.103379

Wilkerson, F.P., Lassiter, A.M., Dugdale, R.C., Marchi, A., Hogue, V.E., 2006. The phytoplankton bloom response to wind events and upwelled nutrients during the CoOP WEST study. Deep Sea Res. Part II Top. Stud. Oceanogr. 53, 3023–3048. https://doi.org/10.1016/j.dsr2.2006.07.007

Wing, S.R., Botsford, L.W., Ralston, S.V., Largier, J.L., 1998. Meroplanktonic distribution and circulation in a coastal retention zone of the northern California upwelling system. Limnol. Oceanogr. 43, 1710–1721. https://doi.org/10.4319/lo.1998.43.7.1710

Yen, P.P.W., Sydeman, W.J., Hyrenbach, K.D., 2004. Marine bird and cetacean associations with bathymetric habitats and shallow-water topographies: implications for trophic transfer and conservation. J. Mar. Syst., The Role of Biophysical Coupling in Concentrating Marine Organisms Around Shallow Topographies 50, 79–99. https://doi.org/10.1016/j.jmarsys.2003.09.015

Chapter 3

Climate justice: the ethics of deep sea mining for green futures

Abstract

The demand for critical minerals is projected to surge given state leaders pushing for electric vehicles in an attempt to address the climate emergency. To meet demand, some commercial interests have turned to the deep sea, beyond national jurisdiction, where polymetallic nodules exist in abundance. While economic, scientific, and conservation perspectives have informed the discourse on deep sea mining, I argue that centering race is essential to accurately assess deep sea mining as a prospective solution to addressing the climate emergency. Using Nauru as a case study to understand the geopolitical economy of DSM from a Black feminist perspective highlights the racial and colonial logics present in DSM discourse, implicating DSM as a false solution due to erroneously centering green futures rather than climate justice. Despite the United Nations attempt to envision a more equitable extractive industry, racial capitalism undergirds the globalized political economies such that DSM is a manifestation of racial extractivism that cannot achieve climate justice..

1. Introduction

Previously prohibitive costs kept the deep sea largely unexplored. Now, through technological advancements, the deep sea is seemingly within reach for industrialization (Santos et al., 2018). Posed as Earth's last frontier (Kirkham et al., 2020; Ramirez-Llodra et al., 2011) and echoing America's Wild West gold rush, the ocean sparks unbridled interest due to loose high-sea international law and lucrative mining prospects.

Stakeholders, with divergent views and competing agendas from science to conservation and industry (e.g., Van Dover, 2011), create a complex challenge as they rush to explore the ocean's many unknowns. Mining advocates push an exploitative agenda to extract rare earth elements from nodules (for use in wind turbines, batteries, etc.), arguing that the minerals are necessary to enable a "green economy". Deep-sea mining (DSM) conversations currently engage science, conservation, and economics based upon a globalized political economy framework with capitalism underpinning the fate of the deep sea—however, other perspectives are absent.

Carver et al.(2020) articulated that complexities of DSM necessitated an interdisciplinary approach, and called for further engagement with feminist and decolonial approaches "to unpack the intersectional power dynamics that are implicit within practices of DSM". Striving for such a framework, Tilot et al. (2021) named social factors. For example, Tilot et al. (2021) shows the colonial logics in the idea that ocean mining is preferable over land mining. However, while Tilot et al. (2021) understand the constructs of indigeneity and colonialism as they relate to DSM, they omit the relationship between race and colonialism that is documented in the long history of exploitation that defines many aspects of how conservation and mining emerge as issues in the Pacific within globalized political economies.

In contrast, the field of Black Pacific studies has long recognized how race and colonialism have been coproduced and are factors relevant to what is happening in the Pacific (Asher, 2009; Feldman, 2012; Swan, 2018). For example, a 2021 symposium brought together scholars from Black studies and Native studies to consider "*the formation of Black diasporas in the Pacific as a legacy of global histories of racial capitalism and settler colonialism*" (Sharma et al., 2021), and conceptions of Blackness in Oceania, connecting Black liberation and Indigenous sovereignty within Oceania (Warren, 2019). Thus, here I ask how histories of racial

71

and imperial exploitation in the Pacific continue to shape who bears the burden of costs of deep sea mining including environmental damage and pollution, and who reaps the financial and technological benefits.

I propose a more robust DSM framework which foregrounds race and colonialism as factors that shape 1) the challenge of ensuring ocean justice amidst ongoing industrialization of the ocean and 2) the challenge of conservation centering green futures instead of justice. Such a framework furthering Carver et al. (2020) and Tilot et al. (2021) previous contextualizations of DSM necessitates understanding the social factors of DSM initiatives in the Pacific through a Black feminist lens. I argue that doing so connects the fate of the deep sea in its present contexts of environmental capitalism to the longer violent, colonial histories of mining and exploration from which it emerges. I hypothesize that such a framework, historicizing DSM and considering its social impacts, will help stakeholders 1) locate the colonial logics embedded in the exponential resource-use required for capitalistic futures that currently defines DSM and conservation practices, 2) understand the logics as manifestations of environmental racism and racial capitalism more broadly (Pulido, 2017; Robinson, 2000[1983]), and 3) see value in addressing the climate emergency by centering climate justice and not green futures.

1.1 Black feminist thought

Practices and approaches from disciplines in the social sciences and humanities, including Black feminism (Collins, 1989), facilitate analysis of complex relationships between the social impacts and politics of scientific practices (e.g., DSM, conservation, environmentalism) to assert that science and society are not separate (e.g., Agard-Jones, 2013; Roberts, 2003). Rather, science and society are coproduced and shaped by complex intersections

of social difference categories like race, gender, nation, and class (Crenshaw, 1989) within globalized political economies.

Black feminist thought is a canon of work that center the lived experiences of Black women. The idea that racism, sexism, and classism cannot be separated is a core throughline among the many expressions of Black feminist thought. Intersectionality as a theoretical framework has been articulated in various fractals over the centuries like Sojourner Truth's 1851 speech "Ain't I a Woman"; Frances Beal's (1969 [2008]) *Double Jeopardy* examining experiences of simultaneous racism and sexism; Audre Lorde's 1982 "We don't live single-issue lives" quote speaking to multidimensional threats people face; the term *intersectionality* itself coined by Kimberlé Crenshaw in 1989; Patricia Hill Collins' matrix of domination theory; and the term misogynoir coined largely by Moya Bailey and Trudy (2018). Such frameworks and theories are inclusive of other social categories of difference and enable more holistic understanding of issues by including both multiple perspectives and crucially missing histories that inform which assumptions are not questioned.

1.2 Intersectional critiques from marginalized voices

"Black feminist thought rearticulates a consciousness that already exists" (Collins, 1990). In *Undrowned: Black Feminist Lessons From Marine Mammals*, Alexis Pauline Gumbs writes that she was "confronted with the colonial, racist, sexist, heteropatriachalizing capitalist constructs"—constructs that she not only lived within but also that were evident in the scientific language used in the marine biology guidebooks she was reading (Gumbs, 2020). While Gumbs does not consider Undrowned a critique of the marine biology guidebooks that inspired it, the "objectivity that guidebook entries perform" and "the violent colonizing languages" of such western scientific texts do showcase standpoint theory (Harding, 1992; Roy, 2008) and the

importance of who is narrating/writing and how that informs the issues and topics addressed, including which lines of inquire pursued. For example, a Black/queer standpoint offered by Vanessa Agard-Jones opens lines of inquiry on endocrine-disrupting pesticide, chlordecone/kepone, showing how coloniality is made material. Agard-Jones (2012) draws from "feminist science studies and from [her] own fieldwork on sexual politics in Martinique [to] ask how the body [can inform] contemporary debates about power, politics, and the postcolonial". Further, intersectional critiques such as the anarcho-Indigenous feminist critique Macarena Gómez-Barris (2017) applies to Bolivia's extractive zone, which illuminates counterhistories like that of the Bolivian silver and tin mining industries "to see deeper into the workings of the mining industry, its demand for racialized and gendered labor within the extractive zone, and genealogies of resistance". It also "offers other models of anticolonial struggle often imperceptible to the official Marxist political narrative". Illustrating the importance of the intersectional critique, Gómez-Barris notes that critical Indigenous theory is a foundational analytical frame for critiquing extractivism while also highlighting Julieta Paredes' assertion that Indigenous cosmopolitics can be limited in achieving decolonial goals without feminisms that are critical to decolonial strategies. Furthermore, María Galindo's (2013) book title states the same idea, translated to: "It is impossible to decolonize without destroying patriarchy". Thus sites of kyriarchy, the social system built on interlocking forms of oppression and domination (Schüssler Fiorenza, 1992), like extractive zones of DSM are best unpacked using an intersectional critique like Black feminism.

1.3 Extractive capitalism, racial capitalism, and racial extractivism

Naomi Klein defines extractivism as "a nonreciprocoal, dominance-based relationship with the earth, one purely of taking. It is the opposite of stewardship, which involves taking but also taking care that regeneration and future life continue". She continues,

> Extractivism is the mentality of the mountaintop remover and the old-growth clear-cutter. It is the reduction of life into objects for use of others, giving them no integrity or value of their own—turning living complex ecosystems into "natural resources," mountains into "overburden" (as the mining industry terms the forests, rocks and streams that get in the way of its bulldozers). It is also the reduction of human beings either into labor to be brutally extracted, pushed beyond limits, or, alternatively, into social burden, problems to be locked out at borders and locked away in prisons or reservations. In an extractivist economy, the interconnection among these various objectified components of life are ignored; the consequences of severing them are of no concern.
> Extractivism is also directly connected to the notion of sacrifice zones—places that, to their extractors, somehow don't count and therefore can be poisoned, drained, or otherwise destroyed, for the supposed greater good of economic progress. This toxic idea has always been intimately tied to imperialism, with disposable peripheries being harnessed to feed a glittering center, and is bound up too with notions of racial superiority, because in order to have sacrifice zones, you need to have people and cultures who count so little that they are considered deserving of sacrifice. Extractivism ran rampant under colonialism because relating to the world as a frontier conquest—rather than as home—fosters this particular brand of irresponsibility. The colonial mind nurtures the belief that there is always somewhere else to go to and exploit once the current site of extraction has been exhausted. (Klein, 2014)

While Klein acknowledges sacrifice zones are bound to racial hierarchy, "notions of racial superiority" are but a passing reference rather than central to the critique like Gomez-Barris' work. The importance of choosing what is centered can be seen by Klein referencing writing by Ecuadorian ecologist Esperanza Martinez, "that fossil fuels, the energy sources of capitalism, destroy life—from the territories where they are extracted to the oceans and the atmosphere that absorb the waste" in a book where the main tenet is capitalism not carbon is the real culprit of climate change. Klein goes on to decenter fossil fuel and shows how in fact they are neutral or even beneficial, thus implicating capitalism. Extending Klein's critique, it stands to reason that by erroneously centering green futures we would not resolve the issue at hand supposedly presented by carbon, and that DSM-enabled green futures is a false solution pushed by DSM corporations and their allies as explored below. However, rather than centering capitalism like Klein, I argue race must be central to DSM discussions.

Scholar-activist Ruth Wilson Gilmore succinctly states "capitalism requires inequality and racism enshrines it" in her work on abolition and the prison industrial complex. By centering race,

the centuries of capitalism that Klein implicates as the driver of climate change is understood to be racial capitalism. From the Black radical tradition, Robinson (1983) coined racial capitalism "to correct the developmentalism and racism that led Marx and Engels to believe mistakenly that European bourgeois society would rationalize social relations" (Melamed, 2015). Understanding that racial capitalism is a relation, where capitalism depends on racial practice and racial hierarchy, makes visible how extractivism and sacrifice zones are racial extractivism. This is evident given "environmental racism is constituent of racial capitalism" (Pulido, 2017) and further that racial extractivism is a component of racial capitalism (Preston, 2017). "Racial extractivism positions race *and* colonialism as central to extractivist projects under neocolonialism and underpins how these epistemologies are written into the economic structure and social relation of production and consumption" [emphasis added] (Preston, 2017). Within this framework, the critique offered by Tilot et al. (2021) is incomplete as it does not engage race as a social factor that shapes DSM discourse. Drawing from Preston (2017) work on Canadian tar sands, "Racial extractivism acknowledges the multitude of ways in which colonial histories and reiterations of race-based epistemologies inform the discursive practices used by the oil and gas industry, for example, and by the Canadian white settler government in promoting and managing 'resource extraction'". Through examining the tar sands as a site of racial extractivism, Preston (2017) unpacks the "racial and colonial relations [that] are revealed as foundation and central…" and importantly, despite being beyond the scope of intervention, Preston still acknowledges that "these racial and colonial relations are also heteropatriarchal and necessarily intersect with the regulation of sex, gender, sexuality and kinship as many Indigenous, Black and women of colour scholars have argued (Maracle, 1996, Crenshaw, 1991, Collins, 2000, Razack, 2002)". The intersecting relations once again beckoning for a Black feminist perspective to contested sites of racial extractivism like DSM.

1.4 Different perspectives informing DSM conversations

The third volume of Perspectives on DSM: Sustainability, Technology, Environmental Policy and Management was published earlier this year (Sharma, 2022). In it, the chapters were divided into sections that led with the geosciences, followed by technology, ecology, economics, and closing with legal and socio-cultural frameworks. Despite 680 pages, none mentioned social factors that shape DSM conversations like imperialism, colonialism, or race. Standard DSM perspectives currently engaged are reviewed in Levin et al. (2020), primarily from science and conservation. The main environmental vulnerabilities are stated as 1) the loss of substrate, 2) changes to seafloor physical and geochemical properties, 3) sediment plumes, 4) contaminant release, and 5) sound, vibration, and noise pollution (Levin et al., 2020). Known repercussions include reduced and altered species composition persisting (Bluhm, 2001) beyond a quarter century after mining (Miljutin et al., 2011; Simon-Lledó et al., 2019). Given that "polymetallic nodules found on the abyssal plains of the oceans represent one of the slowest known geological processes" (Dutkiewicz et al., 2020) with average growth rates of 10-20 mm My-1 (Hein, 2016), the full recovery after disturbance would be on the order of millions of years. As for sediment plumes, while the majority of a plume may be limited to within only a few meters vertically from point of disturbance (Muñoz-Royo et al., 2022), the very low sedimentation environment in which nodules occur (<0.5 cm/ky; Dutkiewicz et al., 2020) would render mining sites and their associated disturbed areas (on the order of 10,000 sq km; Levin et al., 2020) inhospitable to both the growth of nodules and the surrounding fauna. Further, benthic megafauna likely facilitate the growth of nodules and keep them at the seabed surface through bioturbation, nodule lifting, detritus feeding, and foraging (Dutkiewicz et al., 2020) such that mining repercussions would render the very conditions that made the nodules possible altered for millions of years. Unknown

repercussions loom large due to scant knowledge of the deep sea, where the majority of species collected in the area of commercial interest, Clarion Clipperton Zone, are new to science (Amon et al., 2016; Gooday et al., 2017). As such, quantifying biodiversity lost to DSM is not possible presently (Le et al., 2017; Niner et al., 2018; Van Dover et al., 2017). Environmental repercussions from contaminate release include increased sedimentation rate and change in oxygenation due to fine tailing particles serving as nuclei for bacterial growth (Ellis, 2001). Given the many unknown DSM impacts, setting relevant thresholds to avoid significant adverse change is challenging (Levin et al., 2020).

Situating the problem of DSM in a much larger political and economic landscape, I argue, renders Figure 2 of Levin et al. (2020) map of countries engaged in DSM too narrow in scope to address the underlying drivers of DSM. While Levin et al. (2020) names "mining companies that have partnered with states on ISA exploration contracts" as stakeholders, the framing of such relationships as partnerships not only obscures the historical context from which they emerge but also neutralizes multiple axes of domination relevant to such private-public relationships. Conversely, Zalik (2018) understands how political economy and human geography inform such a map of players in DSM. For example, while the United States is not on the Levin et al. (2020) map, Zalik (2018) details how submarine geopolitics implicate the United States as central to the viability of DSM. First, "data-holders and finance capital in the global political economy of extraction", like defense contractor's Lockheed-Martin's commercially sensitive knowledge that serves as a "prerequisite for capital-intensive resource exploitation on ocean frontiers", wield power over contested sites beyond national jurisdiction (Zalik, 2018). Proprietary data leveraged with the United States non-ratification of United Nations Convention on the Law of the Sea (UNCLOS), which "partially protects data held by US-based firms from

the technology transfer requirement enshrined in UNCLOS", reveals "a manifestation of longer

ties between the US navy and ocean science through the twentieth century (Hamblin 2002):

Lockheed Martin has frequently ranked as the largest single contractor to the US military"

(Zalik, 2018).

Another set of countries missing from the Levin et al. (2020) are British commonwealth

countries Australia and to a lesser extent Canada and New Zealand. Applying the lens of political

economy of industrial extraction, Zalik (2018) briefly mentions the engagement of these

countries in DSM exploits through private firms sponsored by the Pacific states of Tonga, Nauru,

and Kiribati with ties to Canadian, New Zealand and Australian based capital. Zalik connects the

power of capital-state alliances to the UNCLOS corporate-friendly clauses, and posits the

ANZAC states caucus (i.e. Australia, New Zealand, and Canada) discourse surrounding private

DSM ventures headquartered or financed from their nationals reflect mercantilist dynamics.

Further, Zalik articulates the geopolitical tensions between the Global North and Global South as

"stemming from colonialism and decolonization in the twentieth century, as well as the twenty-

first century neo-mercantilist pursuit of market access" that "are expressed in the current

regulatory debate on the Area's exploitation regime", where the Area refers to the seabed beyond

national jurisdiction. Zalik specifies the tensions to be "negotiating access to, and control over,

the deep seabed's spatial, regulatory, and technological frontier, a zone for which scientific

knowledge is limited". Drawing from cultural and historical geographers who demonstrate the

deep seabed's social constitution, Zalik links the constitution to the coupled "interests of global

extractive and financial capital which relied on extraction from humans or nature (Arrigihi and

Silver 1999; Braudel 1992; Moore 2015; Rodney 1972)". Zalik counters the narratives private

firms espouse about the deep seabed being external to social contestation "by centering social

histories that document resistance to oppressive domination under mercantile, imperial, and colonial dispossession (Gilroy, 1993; Lehman 2018; Linebaugh and Rediker 2000)", "the direct involvement of branches of global arms and oil industries in technological development and data gathering, and covert activities involving state militaries, navies, and public and private intelligence agencies (Doel 2003; Farish 2006; Hamblin 2002; Mackenzie and Spinardi 1988a, b; Oreskes 2003; Reidy and Rozwadowski 2014)", and recalling that "the oceans were indeed central to world historical racialization".

2. Case study

In centering ocean justice and climate justice more broadly as the challenge of DSM in the Pacific, a Black feminist framework can be crucial to reconsidering what is currently transpiring between the Micronesian island-state Nauru and Canadian The Metals Company (TMC, formerly DeepGreen; Shabahat, 2021). Nauru is the smallest island nation in the world with just 21 sq-km. Western colonization of Nauru began in 1886 first by Germany and then by the British and later Australia through the United Nations. At the turn of the 20th century, British entrepreneurs began ravaging Nauru for phosphate with the help of Germany and later Australia, Britain, and New Zealand (Williams and Macdonald, 1985). Nauru gained independence in 1968 and subsequently brought Australia before the International Court of Justice over the environmental damage due to mining. By the end of the 20th century, phosphate on Nauru was exhausted (Shenon, 1995).

2.1 Historicizing racial extractivism in Nauru

The lucrative phosphate mining began with white prospectors, illustrating the intimate connection between exploration, colonialism, and extraction. Albert Ellis, the son of a chemist, determined in 1899 that a rock from Nauru was phosphate-rich (see Ellis' own 1936 book). He

subsequently left Australia for Nauru and led the mining effort that in less than a decade extracted

two million tons of phosphate from nearly one sixth of the island (240 acres; Wright, 1986). On

Nauru and neighboring Banaba/Ocean Island (now part of Kiribati), Canadian Ronald Wright

writes "The imperial government decided to exploit the two islands for the greatest benefit of

Britain and her colonies by transforming the phosphate company into a Crown corporation under

joint British, Australian, and New Zealand control. The British Phosphate Commission (BPC), as

it now became, was to be run on a "non-profit" basis, selling fertilizer at cost to subsidize the

empire's farmers." Wright continues "While the BPC subsidized millions of white imperial

subjects around the world, it could not bring itself to give fair, let alone generous terms to the

owners of the few acres in the Pacific that made all this possible." While Wright focuses on Banaba

we can learn the type of character Albert Ellis is through his interactions/transactions with

Banabans. "…the chief of Tabwewa greeted Ellis; and Ellis, like other Europeans before him,

imagined that this man was the King of Banaba. The white men strode about the place, drilling

holes and analyzing the results on the spot. Ellis was good at his job: he concluded that Ocean

Island was almost pure phosphate, that the whole island could be mined away, and that this might

take eighty years. In all three things he was absolutely right". Ellis secured "the sole right to raise

and ship all the rock and alluvial Phosphate on Ocean Island… for 999 years in exchange for £50

per annum in trade goods." Ellis "had got the Banabans to give him a licence to destroy their

country in return for a pittance in overpriced trinkets and third-rate tinned food. Not satisfied with

this, he made so bold as to hoist the Union Jack (without authorization from Britain) and inform

the Banabans that they were now kain Engram, people of England" (Wright, 1986). "The company

failed to keep even the minimal obligations to the Banabans that it had allowed itself in the original

agreement: food trees disappeared with the land; natives were charged far higher prices than whites

at the company store; and distilled water, which Ellis had promised the Banabans in return for the firewood to make it, was sold at such a price that the inhabitants had to continue drinking from *bangabanga* increasingly polluted by the mining" (Wright, 1986). What began as an entrepreneurial economic venture grew into full fledge colonization through relations predicated on othering and categories of social difference and harnessing the state apparatus. Thus we can understand the plundering of Nauru to be a manifestation of racial capitalism. As Jodi Melamed (2015) argues, capital "can only accumulate by producing and moving through relations of severe inequality among human groups… antinomies of accumulation require loss, disposability, and the unequal differentiation of human value, and racism enshrines the inequalities that capitalism requires".

2.2 Insatiable appetite for resources and capital

The accumulation of wealth during the 20th century in Nauru and neighboring Banaba/Ocean Island was staggering. Just over a decade into BPC mining on Banaba, Indigenous resistance (supported by British resident commissioners) to the BPC demanding new land leases resulted in consecutive dismissals of commissioners until the BPC got more land in 1913. "Too many powerful people were making too much money. The company could not be touched. Meanwhile the company's shareholders were reaping unheard-of profits: annual dividends of 50 and 60 percent at a time when a tenth of that was considered a good return" (Wright, 1986). Just over another decade, the BPC again wanted more land. While the BPC offered double the 1913 price per acreage (i.e. £100/acre) and 1.5x the 1913 royalty fee of £0.025 per ton of raw phosphate, the offer paled in comparison to the Banabans valuation of their land at "£5000 per acre—a figure which…the High Commissioner for the Western Pacific considered 'not unreasonable' in light of the fact that an acre yielded £40,000 worth of phosphate, even at the BPC's artificially low prices."

(Wright, p.140). Yet Grimble, the resident commissioner (and subordinate of the High Commissioner) recommended a price just 3% of the Banabans' valuation without consulting the Banabans and "then tried to use his knowledge of the Banabans' culture to break their solidarity and win over a faction to these terms" (Wright, 1986). Despite this localized divide-and-conquer imperialist strategy, Banabans remained united and their counteroffer of £5 per carload infuriated the resident commissioner, who then retaliated against "the landowners for exercising the right to keep their property" (ibid). Ironically, Sir Arthur Grimble portrayed himself in his two 1950s books and radio broadcasts "as a benign, paternalistic figure ruling his simple native 'children' for their own good in the best of all possible worlds, the British Empire" (ibid). In the 1976 London court case, Grimble's 1928 letter showed that he as "a resident commissioner had threatened the people under his care with the destruction of their village and lands if they did not sell their birthright to a Crown corporation for a song…. He was not the only one to blame…. He was the instrument… used by ruthless financial and political interests to achieve their ends" (ibid).

2.3 Contemporary resource extraction

Echoes of the 20th century racial extractivism are evident in the present contexts of Nauru and the new resource extraction ventures with legacy British empire financing structures. A century later, Nauru enters into a relationship with Australian-led, Canadian incorporated Nautilus Minerals Inc. that had merged just two years prior with Canadian Orca Petroleum Inc. in 2006. David Heydon, an Australian prospector and then Nautilus' CEO and president, established Nauru Offshore Resources Inc. (NORI) in March 2008 as a wholly-owned subsidiary. Sponsored by Nauru, NORI submitted an exploration license application less than a month later to the United Nations' International Seabed Authority (ISA) for the Clarion-Clipperton Zone where Heydon is listed as the chairman of NORI. The ISA was established under section 4, article 156 of the 1982

United Nations Convention on the Law of the Sea (UNCLOS), and charged not only with administering the seabed and its resources beyond national jurisdiction for the common heritage of mankind under part XI, section 2, article 136, but importantly reserving half of all explored sites prospective value for developing nations (annex III, article 8). The exploration of the prior decade (see Kang and Liu, 2021; Wertenbaker, 1977 for a review) inspired the 1982 UNCLOS article so that access to seabed minerals was not exclusive to wealthy nations with capital and expertise (i.e. American, British, French, Belgian, German, Dutch, Australian, Canadian, and Japanese). Importantly, the subsequent article, i.e. article 9(4), stipulated that "Any State Party which is a developing State or any natural or juridical person sponsored by it and *effectively controlled by it* or by other developing State which is qualified applicant, or any group of the foregoing, may notify the Authority that it wishes to submit a plan of work pursuant to article 6 of this Annex with respect to a reserved area" [emphasis added]. However, not only was NORI a wholly-owned subsidiary, but its leadership only temporarily reflected Nauruan leadership during its 2008 and its updated 2011 ISA exploration applications (ISBA/17/C/9, 2011; ISBA/17/C/14, 2011).

Shortly after establishing NORI, Heydon left Nautilus in 2008 and later establishes DeepGreen Resources in 2010. While CEO of DeepGreen, Heydon was simultaneously also director and chairman of NORI (see NORI application to the Legal and Technical Commission in 2008) and signed a 15-year exploration contract in his NORI director capacity. Similarly, his son, Robert Heydon, was simultaneously both COO of DeepGreen and vice president of NORI. During this time, NORI became a wholly-owned subsidiary of DeepGreen and remains as such under the The Metals Company (DeepGreen rebranded as TMC in 2021). The nature of how this private-public relationship arose is of import given ISA regulations are to promote developing nations negotiating power in determining agreements with private industry.

ISA data confidentiality regulations, meant to ensure developing nations held negotiating power when seeking partners with financial capital and foreign investors in general, were breached in 2007 and again in 2011 and 2012 by ISA staff communicating directly with Nautilus and later DeepGreen executives, all greenlighted and facilitated by the now ISA Secretary General (Lipton, 2022). Such disclosures compromised the nature of the private-public relationship between Nauru and DeepGreen, as confidential data was no longer a key bargaining chip and DeepGreen merely needed on paper a developing state party to UNCLOS to proceed. The weight that confidential data holds can be seen through ISA debates over what should be considered "commercially sensitive" data and can be likened to treasure maps. The skewed power balance from its inception is especially true in light of the fact that Nauru questioned its ability to fulfill an agreement where its financial and regulatory liabilities were outside its capacity. Specifically, Nauru raised its own concerns in fulfilling sponsor responsibilities regulating extractive industries and sought advisory opinion from the International Tribunal for the Law of the Sea in March 2010, "in reality no amount of measures taken by a sponsoring State could ever fully 'secure compliance' of a contractor when the contractor is a separate entity from the State" (ISBA/16/C/6). Namely the burden of regulating commercial exploits in the developing nation's piece of the ISA reserved area would be shouldered by a small island nation with no capacity to effectively regulate, and already infamous for its lack of oversight and financial deregulation in the 1990s that prioritized access to foreign currency through Nauru-registered shell banks. Yet, under UNCLOS, liability for a contractor like TMC breaking ISA rules would fall to the sponsoring nation unless the state proved that they 1) enforced strict national laws, and 2) they effectively controlled the foreign-owned subsidiary.

Even if small island nations were able to enforce regulations, the legislation itself is developed with external influence. For example, the Deep Sea Minerals Project, launched in 2011 by the Pacific Community (formerly the South Pacific Commission) to develop national policies and legislation to govern DSM in the South Pacific, was funded by the European Union. The Pacific Community itself was established by colonial powers as a regional technical agency and five of the six colonial powers remain in the organization today, all with DSM stakes in the Pacific including Australia, New Zealand, the United Kingdom, and the United States. Further, the Pacific Community contracted out a knowledge assessment of Pacific marine minerals to the UN Environment Programme and GRID-Arendal where the technical steering committee—established to guide and support the project deliverable of helping Pacific islands states enact national legislation that in part secures equitable financial arrangements for their people—included Robert Heydon. The resulting national DSM legislation adopted by Pacific island states including Nauru, Kiribati, and Tonga "share similar legislative structures and mechanisms" (ISA, 2021). Such external influence enables the regulated community to essentially self-regulate and echo the 20th century where official apparatuses were merely instruments of financial and political interests that began with private exploits.

Under UNCLOS, the other interpretation of *effective control* if not regulatory is economic control (Rojas and Phillips, 2019). However, TMC "has maintained nearly complete financial control" in its DSM projects with Nauru and Tonga (Lipton, 2022). The exploitative nature of the relationship is further implicated when the mirage of wealth that lured small Pacific island nation states on the promise of DSM being its economic panacea is revealed. While the terms of agreement between The Metals Company and Nauru or Kiribati (which includes Banaba/Ocean Island) are not public, Tonga, the third island nation The Metals Company has "partnered" with,

reportedly would receive less than 0.5% of the profits at just \$2/ton (Lipton, 2022) while the average 2019 valuation of nodules was \$484/ton and as high as \$1,100/ton (CRU consulting, 2020). The paltry rates echo the deals and plunder from less than a century earlier in the region. Additionally, a former member of the Tonga parliament said he was given less than an hour to review new national regulations in 2014, urgency that severely undermined the clause mandating effective regulatory control by sponsoring states. Further, the agreements signed heavily favor TMC legally where subsequent new national legislation and regulations or changes must grandfather TMC subsidiaries.

Without viable alternatives to sustain their economies given past exploits, island nation states fall prey to foreign investors' promises of access to wealth that seldom translates to material wealth for the nations. While UNCLOS stipulates an alternative for developing nations to getting involved in DSM through private-public partnerships, i.e. the ISA's own in-house mining operation called the Enterprise, the body has yet to be established despite calls from the Global South to do so. The operationalization of the Enterprise would facilitate mining done under the redistributive principle of common heritage. Yet, the tension between ISA's two mandates, where articles 136-145 promote the equality of all countries and the common heritage principle while articles 150-152 promote exploitation, production, and profits, gave way to industry capture of the ISA (e.g., the ISA secretary-general Michael Lodge facilitated the release of confidential data to Nautilus). Thus, the Enterprise as a pathway for land-locked states and states lacking access to financial capital remains elusive.

3. *Green futures for whom?*

The inequitable financial terms of private-public agreements and slow-walk of operationalizing the redistribution of profit implicates the green futures narrative of mining

executives and the ISA secretary general alike as greenwashing extractivism, and a manifestation of racial capitalism. The report commissioned by the Deep Sea Minerals Project itself defines the metric for achieving a green economy with respect to DSM being "if an equitable portion of the economic proceeds of deep sea mining are reinvested into other forms of economic, social, and natural capital…" (Baker and Beaudoin, 2013). While TMC has met contractual obligations by offering a $1000 scholarship to nationals of the Pacific island states their subsidiaries are incorporated in, the returns on sponsorship pale in comparison to the prospective profits offshoring and onshoring liability. The classic paradigm of the Global North benefiting from exploits while saddling the Global South with burdens of said exploits is also visible at the heart of the green futures narrative, electric vehicles.

Reduction of tailpipe emissions will likely disproportionately occur in developed states while adverse impacts are externalized elsewhere, including DSM disproportionately affecting Pacific states. With pollution occurring farther from the place of use (including the energy needed to charge EVs which is disproportionately produced in Black and brown neighborhoods, Klein's message that "Nauru's fate tells us that there is no middle of nowhere, nowhere that doesn't 'count'" resonates. Further, our culture of disavowing pollution "we cannot easily see… is a big part of what makes carbon pollution such a stubborn problem: we can't see it, so we don't really believe it exists" (Klein, 2014). Thus, the same logics that created the climate emergency are also employed by the false solution meant to address it, conveniently disappearing the issue of racial extractivism. Addressing racial extractivism would mean reckoning with racial capitalism and that would disrupt current world systems. As the United Nations Department of Social and Economic Affairs asserted in 1951, "ancient philosophies have to be scrapped; old social institutions have to disintegrate; bonds of caste, creed and race

have to burst; and large numbers of persons who cannot keep up with progress have to have their expectations of a comfortable life frustrated". Simply put, a just transition is a cultural revolution, which is why we must center climate justice in the discussions of DSM. By doing so, solutions that balance the narrative of individualism with radical dependency and community (i.e. Muhammad Ali's "Me, We" ethos) like reduction of energy use by developed countries actualized in the form of mass transit. Ultimately, an intersectional lens like that offered by Black feminisms allows for a multitude of perspectives to be in dialogue, for example, by exhuming submerged perspectives of resistance against structures rooted in slavery, imperialism, and capitalism to holistically grapple with climate change in all its context for more accurate assessments of drivers and potential solutions like DSM. Such an approach enables interrogation of assumptions underpinning theoretical benefits of DSM through, for example, decentering the goal of development itself (Escobar, 2012) and ushering in imaginative futures outside of racial capitalism and toward climate justice.

4. Acknowledgments

5. References

Agard-Jones, V., 2013. Bodies in the System. Small Axe 17, 182–192.

Agard-Jones, V., 2012. What the Sands Remember. GLQ J. Lesbian Gay Stud. 18, 325–346. https://doi.org/10.1215/10642684-1472917

Amon, D.J., Ziegler, A.F., Dahlgren, T.G., Glover, A.G., Goineau, A., Gooday, A.J., Wiklund, H., Smith, C.R., 2016. Insights into the abundance and diversity of abyssal megafauna in a polymetallic-nodule region in the eastern Clarion-Clipperton Zone. Sci. Rep. 6, 30492. https://doi.org/10.1038/srep30492

Asher, K., 2009. Black and green: Afro-Colombians, development, and nature in the Pacific lowlands. Duke University Press, Durham.

Bailey, M., Trudy, 2018. On misogynoir: citation, erasure, and plagiarism. Fem. Media Stud. 18, 762–768. https://doi.org/10.1080/14680777.2018.1447395

Baker, E., Beaudoin, Y., 2013 Deep Sea Minerals and the Green Economy.

Beal, F.M., 2008. Double Jeopardy: To Be Black and Female. Meridians 8, 166–176.

Bluhm, H., 2001. Re-establishment of an abyssal megabenthic community after experimental physical disturbance of the seafloor. Deep Sea Res. Part II Top. Stud. Oceanogr. 48, 3841–3868. https://doi.org/10.1016/S0967-0645(01)00070-4

Carver, R., Childs, J., Steinberg, P., Mabon, L., Matsuda, H., Squire, R., McLellan, B., Esteban, M., 2020. A critical social perspective on deep sea mining: Lessons from the emergent industry in Japan. Ocean Coast. Manag. 193, 105242. https://doi.org/10.1016/j.ocecoaman.2020.105242

Collins, P.H., 1990. Black Feminist Thought: Knowledge, Consciousness, and the Politics of Empowerment, 2nd ed. Routledge, New York. https://doi.org/10.4324/9780203900055

Collins, P.H., 1989. The Social Construction of Black Feminist Thought. Signs 14, 745–773.

Crenshaw, K., 1989. Demarginalizing the Intersection of Race and Sex: A Black Feminist Critique of Antidiscrimination Doctrine, Feminist Theory and Antiracist Politics. Univ. Chic. Leg. Forum 1989, 31.

CRU consulting, 2020. Polymetallic nodule valuation report.

Dutkiewicz, A., Judge, A., Müller, R.D., 2020. Environmental predictors of deep-sea polymetallic nodule occurrence in the global ocean. Geology 48, 293–297. https://doi.org/10.1130/G46836.1

Ellis, D.V., 2001. A Review of Some Environmental Issues Affecting Marine Mining. Mar. Georesources Geotechnol. 19, 51–63. https://doi.org/10.1080/10641190109353804

Escobar, A., 2012. Encountering development: the making and unmaking of the third world. Princeton University Press, Princeton, N.J.

Feldman, H.C., 2012. Strategies of the Black Pacific: Music and Diasporic Identity in Peru, in: Dixon, K., Burdick, J. (Eds.), Comparative Perspectives on Afro-Latin America. University Press of Florida, pp. 42–71. https://doi.org/10.5744/florida/9780813037561.003.0003

Fiorenza, E.S., 1992. But She Said: Feminist Practices of Biblical Interpretation. Beacon Press (Ma).

Galindo, M., 2013. No se puede descolonizar sin despatriarcalizar: teoría y propuesta de la despatriarcalización. Mujeres Creando, La Paz, Bolivia.

Gómez-Barris, M., 2017. The Extractive Zone: Social Ecologies and Decolonial Perspectives. Duke University Press. https://doi.org/10.1215/9780822372561

Gooday, A.J., Holzmann, M., Caulle, C., Goineau, A., Kamenskaya, O., Weber, A.A.-T., Pawlowski, J., 2017. Giant protists (xenophyophores, Foraminifera) are exceptionally diverse in parts of the abyssal eastern Pacific licensed for polymetallic nodule exploration. Biol. Conserv. 207, 106–116. https://doi.org/10.1016/j.biocon.2017.01.006

Gumbs, A.P., 2020. Undrowned: black feminist lessons from marine mammals, Emergent strategy series. AK Press, Chico.

Harding, S., 1992. Rethinking Standpoint Epistemology: What Is "Strong Objectivity?" Centen. Rev. 36, 437–470.

Hein, J.R., 2016. Manganese Nodules, in: Harff, J., Meschede, M., Petersen, S., Thiede, Jö. (Eds.), Encyclopedia of Marine Geosciences, Encyclopedia of Earth Sciences Series. Springer Netherlands, Dordrecht, pp. 408–412. https://doi.org/10.1007/978-94-007-6238-1_26

ISA, 2021. Comparative Study of the Existing National Legislation on Deep Seabed Mining.

Kang, Y., Liu, S., 2021. The Development History and Latest Progress of Deep-Sea Polymetallic Nodule Mining Technology. Minerals 11, 1132. https://doi.org/10.3390/min11101132

Kirkham, N.R., Gjerde, K.M., Wilson, A.M.W., 2020. DEEP-SEA mining: Policy options to preserve the last frontier - Lessons from Antarctica's mineral resource convention. Mar. Policy 115, 103859. https://doi.org/10.1016/j.marpol.2020.103859

Le, J.T., Levin, L.A., Carson, R.T., 2017. Incorporating ecosystem services into environmental management of deep-seabed mining. Deep Sea Res. Part II Top. Stud. Oceanogr., Advances in deep-sea biology: biodiversity, ecosystem functioning and conservation 137, 486–503. https://doi.org/10.1016/j.dsr2.2016.08.007

Levin, L.A., Amon, D.J., Lily, H., 2020. Challenges to the sustainability of deep-seabed mining. Nat. Sustain. 3, 784–794. https://doi.org/10.1038/s41893-020-0558-x

Lipton, E., 2022. Secret Data, Tiny Islands and a Quest for Treasure on the Ocean Floor - The New York Times [WWW Document]. URL https://www.nytimes.com/2022/08/29/world/deep-sea-mining.html (accessed 11.8.22).

Melamed, J., 2015. Racial Capitalism. Crit. Ethn. Stud. 1, 76–85. https://doi.org/10.5749/jcritethnstud.1.1.0076

Miljutin, D.M., Miljutina, M.A., Arbizu, P.M., Galéron, J., 2011. Deep-sea nematode assemblage has not recovered 26 years after experimental mining of polymetallic nodules (Clarion-Clipperton Fracture Zone, Tropical Eastern Pacific). Deep Sea Res. Part Oceanogr. Res. Pap. 58, 885–897. https://doi.org/10.1016/j.dsr.2011.06.003

Muñoz-Royo, C., Ouillon, R., El Mousadik, S., Alford, M.H., Peacock, T., n.d. An in situ study of abyssal turbidity-current sediment plumes generated by a deep seabed polymetallic nodule mining preprototype collector vehicle. Sci. Adv. 8, eabn1219. https://doi.org/10.1126/sciadv.abn1219

Naomi Klein, 2014. This Changes Everything : Capitalism Vs. The Climate. Simon & Schuster, [Place of publication not identified].

Niner, H.J., Ardron, J.A., Escobar, E.G., Gianni, M., Jaeckel, A., Jones, D.O.B., Levin, L.A., Smith, C.R., Thiele, T., Turner, P.J., Van Dover, C.L., Watling, L., Gjerde, K.M., 2018. Deep-Sea Mining With No Net Loss of Biodiversity—An Impossible Aim. Front. Mar. Sci. 5, 53. https://doi.org/10.3389/fmars.2018.00053

Preston, J., 2017. Racial extractivism and white settler colonialism: An examination of the Canadian Tar Sands mega-projects. Cult. Stud. 31, 353–375. https://doi.org/10.1080/09502386.2017.1303432

Pulido, L., 2017. Geographies of race and ethnicity II: Environmental racism, racial capitalism and state-sanctioned violence. Prog. Hum. Geogr. 41, 524–533. https://doi.org/10.1177/0309132516646495

Ramirez-Llodra, E., Tyler, P.A., Baker, M.C., Bergstad, O.A., Clark, M.R., Escobar, E., Levin, L.A., Menot, L., Rowden, A.A., Smith, C.R., Van Dover, C.L., 2011. Man and the Last Great Wilderness: Human Impact on the Deep Sea. PLoS ONE 6, e22588. https://doi.org/10.1371/journal.pone.0022588

Roberts, C., 2003. Drowning in a Sea of Estrogens: Sex Hormones, Sexual Reproduction and Sex. Sexualities 6, 195–213. https://doi.org/10.1177/1363460703006002003

Robinson, C.J., 2000. Black marxism: the making of the Black radical tradition. University of North Carolina Press, Chapel Hill, N.C.

Rojas, A., Phillips, F.-K., 2019. Effective Control and Deep Seabed Mining: Toward a Definition [WWW Document]. Cent. Int. Gov. Innov. URL https://www.cigionline.org/publications/effective-control-and-deep-seabed-mining-toward-definition-1/ (accessed 11.9.22).

Roy, D., 2008. Asking Different Questions: Feminist Practices for the Natural Sciences. Hypatia 23, 134–157.

Santos, M.M., Jorge, P.A.S., Coimbra, J., Vale, C., Caetano, M., Bastos, L., Iglesias, I., Guimarães, L., Reis-Henriques, M.A., Teles, L.O., Vieira, M.N., Raimundo, J., Pinheiro, M., Nogueira, V., Pereira, R., Neuparth, T., Ribeiro, M.C., Silva, E., Castro, L.F.C., 2018. The last frontier: Coupling technological developments with scientific challenges to improve hazard assessment of deep-sea mining. Sci. Total Environ. 627, 1505–1514. https://doi.org/10.1016/j.scitotenv.2018.01.221

Shabahat, E., 2021. Why Nauru Is Pushing the World Toward Deep-Sea Mining. Hakai Mag.

Sharma, N., Swan, Q., Tzu-Chun Wu, J., Man, S., Widener, D., 2021. Black Trans-Pacific Mobility.

Sharma, R. (Ed.), 2022. Perspectives on Deep-Sea Mining: Sustainability, Technology, Environmental Policy and Management. Springer International Publishing, Cham. https://doi.org/10.1007/978-3-030-87982-2

Shenon, P., 1995. A Pacific Island Nation Is Stripped of Everything. N. Y. Times.

Simon-Lledó, E., Bett, B.J., Huvenne, V.A.I., Köser, K., Schoening, T., Greinert, J., Jones, D.O.B., 2019. Biological effects 26 years after simulated deep-sea mining. Sci. Rep. 9, 8040. https://doi.org/10.1038/s41598-019-44492-w

Swan, Q., 2018. Blinded by Bandung?: Illumining West Papua, Senegal, and the Black Pacific. Radic. Hist. Rev. 2018, 58–81. https://doi.org/10.1215/01636545-4355133

Tilot, V., Willaert, K., Guilloux, B., Chen, W., Mulalap, C.Y., Gaulme, F., Bambridge, T., Peters, K., Dahl, A., 2021. Traditional Dimensions of Seabed Resource Management in the Context of Deep Sea Mining in the Pacific: Learning From the Socio-Ecological Interconnectivity Between Island Communities and the Ocean Realm. Front. Mar. Sci. 8, 637938. https://doi.org/10.3389/fmars.2021.637938

Van Dover, C.L., 2011. Tighten regulations on deep-sea mining. Nature 470, 31–33. https://doi.org/10.1038/470031a

Van Dover, C.L., Ardron, J.A., Escobar, E., Gianni, M., Gjerde, K.M., Jaeckel, A., Jones, D.O.B., Levin, L.A., Niner, H.J., Pendleton, L., Smith, C.R., Thiele, T., Turner, P.J., Watling, L., Weaver, P.P.E., 2017. Biodiversity loss from deep-sea mining. Nat. Geosci. 10, 464–465. https://doi.org/10.1038/ngeo2983

Warren, J.P., 2019. Reading Bodies, Writing Blackness: Anti-/Blackness and Nineteenth-Century Kanaka Maoli Literary Nationalism. Am. Indian Cult. Res. J. 43, 49–72. https://doi.org/10.17953/aicrj.43.2.warren

Wertenbaker, W., 1977. MINING THE WEALTH OF THE OCEAN DEEP. N. Y. Times.

Williams, M., Macdonald, B., 1985. The phosphateers: a history of the British Phosphate Commissioners and the Christmas Island Phosphate Commission. Melbourne University Press ; International Scholarly Book Services [distributor], Carlton, Vic. : Beaverton, OR.

Wright, R., 1986. On Fiji Islands. Viking, New York, N.Y., U.S.A.

Zalik, A., 2018. Mining the seabed, enclosing the Area: ocean grabbing, proprietary knowledge and the geopolitics of the extractive frontier beyond national jurisdiction. Int. Soc. Sci. J. 68, 343–359. https://doi.org/10.1111/issj.12159